

**INVESTIGATION OF  
8-YEAR-LONG COMPOSITION RECORD IN THE EASTERN  
MEDITERRANEAN PRECIPITATION**

**A THESIS SUBMITTED TO  
THE GRADUATE SCHOOL OF NATURAL AND APPLIED SCIENCES  
OF  
MIDDLE EAST TECHNICAL UNIVERSITY**

**BY**

**ÖZLEM IŞIKDEMİR**

**IN PARTIAL FULFILLMENT OF THE REQUIREMENTS  
FOR  
THE DEGREE OF MASTER OF SCIENCE  
IN  
ENVIRONMENTAL ENGINEERING**

**JANUARY 2006**

Approval of the Graduate School of Natural and Applied Sciences

---

Prof. Dr. Canan Özgen  
Director

I certify that this thesis satisfies all the requirements as a thesis for the degree of Master of Science.

---

Prof. Dr. Filiz B. Dilek  
Head of Department

This is to certify that we have read this thesis and that in our opinion it is fully adequate, in scope and quality, as a thesis for the degree of Master of Science.

---

Asst. Prof. Dr. Hakan Pekey  
Co-Supervisor

---

Prof. Dr. Gürdal Tuncel  
Supervisor

**Examining Committee Members**

Prof. Dr. Kahraman Ünlü (METU, ENVE) \_\_\_\_\_

Prof. Dr. Gürdal Tuncel (METU, ENVE) \_\_\_\_\_

Asst. Prof. Dr. Hakan Pekey (DOSAP Researcher, METU) \_\_\_\_\_

Asst. Prof. Dr. İpek İmamoğlu (METU, ENVE) \_\_\_\_\_

Asst. Prof. Dr. Eftade O. Gaga (Anadolu Unv., ENVE) \_\_\_\_\_

I hereby declare that all information in this document has been obtained and presented in accordance with academic rules and ethical conduct. I also declare that, as required by these rules and conduct, I have fully cited and referenced all material and results that are not original to this work.

Name, Last name: Özlem IŞIKDEMİR

Signature :

## **ABSTRACT**

### **INVESTIGATION OF 8-YEAR-LONG COMPOSITION RECORD IN THE EASTERN MEDITERRANEAN PRECIPITATION**

**Işıkdemir, Özlem**

**M.S., Department of Environmental Engineering**

**Supervisor: Prof. Dr. Gürdal Tuncel**

**Co-Supervisor: Asst. Prof. Dr. Hakan Pekey**

**January 2006,128 pages**

Measurement of chemical composition of precipitation is important both to understand acidification of terrestrial and aquatic ecosystems and neutralization process in the atmosphere. Such data are scarce in the Mediterranean region. In this study, chemical composition of daily, wet-only, 387 number of rain water samples collected between 1991 and 1999 were investigated to determine levels, temporal variation and long-term trends in concentrations of major ions and trace elements between 1991 and 1999. Samples had already been collected and some of the analysis had been completed. The anions  $\text{SO}_4^{2-}$ ,  $\text{NO}_3^-$  and  $\text{Cl}^-$  were analyzed by HPLC coupled with UV-VIS detector,  $\text{NH}_4^+$  was analyzed by colorimetry and  $\text{H}^+$  ion was analyzed by pH meter. The major ions and trace metals were analyzed by using Atomic Absorption Spectrometry (AAS) and Graphite Furnace Atomic Absorption

Spectrometry (GFAAS). In this study complete data set were generated by analyzing samples that had not been previously analyzed for major ions and trace elements with Inductively Coupled Plasma with Optical Emission Spectrometry (ICP-OES).

Statistical tools were used to determine the distribution of the pollutants. The rain water data tends to be log-normally distributed since data show large variations due to meteorological conditions, physical and chemical transformations and air mass transport patterns. The median pH of the rain water was found to be 5.29, which indicates that the rain water is not strongly acidic. This case is not a result of lacking of acidic compounds but rather indicates extended neutralization process in rain water. Eastern Mediterranean atmosphere is under the influence of three general source types: (1) anthropogenic sources, which are located to the north and northwest of the basin brings low pH values to the region ( $\text{SO}_4^{2-}$ ,  $\text{NO}_3^-$  ions); (2) a strong crustal source, which is dried and suspended local soil and air masses transported from North Africa transport which have high pH values ( $\text{Ca}^{2+}$ , Al, Fe ions) and (3) a marine source, which is the Mediterranean Sea itself ( $\text{Na}^+$ ,  $\text{Cl}^-$  ions). In the region, the main acid forming compounds are  $\text{H}_2\text{SO}_4$  and  $\text{HNO}_3$  whereas;  $\text{CaCO}_3$  and  $\text{NH}_3$  are responsible for the neutralization process.

To describe the level of pollutant concentrations and the factors that affect their variations in rain water; ion compositions, neutralization of acidity, short and long-term variability of ions and elements, their time trend analysis and wet deposition fluxes were investigated briefly. Positive matrix factorization (PMF) was used to determine components of ionic mass in the precipitation. In Antalya Station the rain water has five factors: free acidity factor, crustal factor, marine factor,  $\text{NO}_3^-$  factor and  $\text{SO}_4^{2-}$  factor. Potential Source Contribution Function (PSCF) and trajectory statistics were used to determine source regions generating these components.  $\text{NO}_3^-$  has potential source regions of Western Mediterranean countries and North Africa, whereas  $\text{SO}_4^{2-}$  has additional southeasterly trajectory components of Israel and south east of Turkey.

**Key Words:** Eastern Mediterranean, wet deposition, neutralization of acidity, time trend analysis, potential source contribution function, positive matrix factorization.

## ÖZ

### DOĞU AKDENİZ BÖLGESİ YAĞIŞLARININ 8 YILLIK KOMPOZİSYON VERİLERİNİN İNCELENMESİ

**Işıkdemir, Özlem**

**Y.Lisans, Çevre Mühendisliği Bölümü**

**Tez Yöneticisi: Prof. Dr. Gürdal Tuncel**

**Yardımcı Tez Yöneticisi: Yrd. Doç. Dr. Hakan Pekey**

**Ocak 2006, 128 sayfa**

Yağmur suyu kimyasal kompozisyonunun incelenmesi, karasal ve sucul ekosistemlerde asitlenmeyi ve atmosferde nötralizasyon prosesini anlamak açısından oldukça önemlidir. Akdeniz bölgesinde bu tür veri sınırlıdır. Bu çalışmada, 1991-1999 yılları arasında toplanan günlük, 387 tane yağmur suyu örneğinin kimyasal kompozisyonu ana iyonlar ve eser elementler için incelenmiş, zamanla değişimleri ve uzun dönem eğilimi incelenmiştir. Örnekler önceden toplanmış ve bir kısmı analiz edilmiştir.  $SO_4^{2-}$ ,  $NO_3^-$  ve  $Cl^-$  anyonları UV-VIS detektörü ile eşlendirilmiş HPLC ile,  $NH_4^+$  kolorimetri metodu ile ve  $H^+$  iyonu pH metre ile analiz edilmiştir. Ana iyonlar ve eser elementler Atomik Absorpsiyon Spektrometrisi (AAS) ve Grafit Fırın Atomik Absorpsiyon Spektrometrisi (GFAAS) ile ölçülmüştür. Bu çalışmada, daha önce analiz edilmeyen örnekler ana iyonlar ve eser elementler Inductively Coupled

Plasma-Optik Emisyon Spektrometrisi (ICP-OES) ile analiz edilmiş ve veri seti tamamlanmıştır

Kirletici konsantrasyon dağılımı istatistiksel yöntemler kullanılarak araştırılmıştır. Yağmur suyu veri seti meteorolojik özellikler, fiziksel ve kimyasal değişimler ve hava kütle taşınımlarındaki farklılıklar nedeniyle büyük varyasyonlar gösterir ve bu nedenle log-normal dağılım göstermeye eğilimlidir. Yağmur suyu içerisindeki medyan pH 5.29 olarak bulunmuştur, bu yağmur suyunun asidik olmadığını gösterir. Bu durum asit bileşenlerinin yağmur suyu içerisinde az olmasından değil, daha çok nötralizasyonun yoğun ve etkili olmasından kaynaklanır. Doğu Akdeniz atmosferi üç genel kaynağın etkisi altındadır: (1) antropojen kaynaklar, yoğunlukla bölgenin kuzey ve kuzey batısından düşük pH'lı hava kütlesi taşır ( $\text{SO}_4^{2-}$ ,  $\text{NO}_3^-$  iyonları); (2) yoğun toprak kaynağı, bölgede kuruyan ve kalkan yerel toprak ve Kuzey Afrika'dan taşınan yüksek pH'lı kaynak ( $\text{Ca}^{2+}$ , Al, Fe iyonları) ve (3) deniz kaynağı, Akdeniz'den taşınır ( $\text{Na}^+$ ,  $\text{Cl}^-$  iyonları). Bölgede başlıca asit bileşenleri  $\text{H}_2\text{SO}_4$  ve  $\text{HNO}_3$ 'dir, bununla birlikte,  $\text{CaCO}_3$  ve  $\text{NH}_3$  nötralizasyondan sorumludur.

Yağmur suyunda kirletici konsantrasyonlarının düzeyini belirlemek ve değişimlerini etkileyen faktörleri tanımlayabilmek için; iyon kompozisyonu, asiditenin nötralizasyonu, kısa ve uzun dönem değişimleri, zaman trend analizleri ve yaş çökme akıları detaylı olarak incelenmiştir. Yağmur suyu iyon yükü Pozitif Matris Faktörizasyonu (PMF) kullanılarak yapılmıştır. Antalya istasyonunda yağmur suyu kompozisyonundaki beş faktör bulunmuştur. Bu faktörler: Serbest asidite faktörü, toprak faktörü, deniz faktörü,  $\text{NO}_3^-$  faktörü,  $\text{SO}_4^{2-}$  faktörü'dür. Bu faktörleri üreten kaynak bölgeleri Potansiyel Kaynak Katkı Fonksiyonu (PSCF) ve trajektori istatistikleri kullanılarak bulunmuştur.  $\text{NO}_3^-$  potansiyel kaynak bölgeleri Batı Akdeniz ülkeleri ve Kuzey Afrika'dır.  $\text{SO}_4^{2-}$  buna ek olarak İsrail ve Türkiye'nin güney doğusu gibi güney doğu trajektörlerini de içermektedir.

Anahtar Kelimeler: Doğu Akdeniz, yaş çökme, asiditenin nötralizasyonu, zaman trend analizi, potansiyel kaynak katkı fonksiyonu, pozitif matris faktörizasyonu.

*To my family...*

## ACKNOWLEDGEMENTS

I would like to express my sincere appreciation to my supervisor Prof. Dr. Gürdal Tuncel for his guidance, advice, criticism, encouragements and insight throughout the research. I would like to thank my co-supervisor Asst. Prof. Dr. Hakan Pekey, for his directions, helpful comments and encouragement throughout my research.

Sincere acknowledgement is to Central Laboratory of the METU for providing data. I wish to express my appreciation to Dr.Feyime Şahin and Ms. Serap Tekin in Central Laboratory of METU for their assistance and companionship throughout the study.

I am thankful to Fatma Öztürk, Güray Doğan and D.Deniz Genç for their assistance, helpful insights and friendship during the study.

I wish to express my appreciation to Asst. Prof. Dr. Beyhan Pekey and Dr. Öznur Oğuz Kuntasal for their endless support and assistance throughout the study.

I extend my sincere thank to Elif Bulut, Selin Akyol, Sertaç Tezcan Öncü, Mihriban Civan, Funda Yetgin, Firdes Yenilmez and Burcu Uyuşur for their friendship during my hard working days.

Finally, I would like to express my deepest appreciation to my family for their love, understanding, encouragement, patience and for their endless support throughout my life.

## TABLE OF CONTENTS

PLAGIARISM .....	III
ABSTRACT.....	IV
OZ.....	VI
ACKNOWLEDGMENT.....	IX
TABLE OF CONTENTS .....	X
LIST OF TABLES .....	XIII
LIST OF FIGURES.....	XV
LIST OF ABBREVIATIONS.....	XVII
CHAPTER	
INTRODUCTION.....	1
1.1. Framework .....	1
1.2. Objectives of the Study .....	3
1.3. Study Overview (Outline of the Study) .....	4
1.4. Previous Work.....	5
BACKGROUND.....	6
2.1. Atmospheric Removal Mechanisms .....	6
2.2. Acid Deposition .....	7
2.2.1. Chemical Composition .....	7
2.2.1.1. Principal Precursors of Acidification.....	8
2.2.1.2. Principal Agents of Neutralization.....	9
2.2.2. Studies of Acid Precipitation .....	10
2.2.2.1. Studies of Chemical Composition.....	10
2.2.2.2. Studies of Time Trend.....	13
2.3. Receptor Oriented Models .....	15
2.3.1. Enrichment Factors .....	15
2.3.2. Positive Matrix Factorization.....	16
2.3.3. Trajectory Statistics.....	19
2.4.1. Flow climatology .....	20

2.4.2. Potential Source Contribution Function Analysis.....	20
2.5. Backtrajectory Analysis .....	23
2.4. Geography and Climatology of Mediterranean Region .....	24
MATERIALS AND METHODS.....	26
3.1. Sampling Site .....	26
3.2. Sampling Procedures.....	27
3.2.1. Preparation of Sampling Bottles .....	27
3.2.2. Collection of Wet Deposition Samples .....	28
3.3. Sample Handling .....	30
3.3.1. Determination of Volume and pH.....	30
3.3.2. Preparation of samples for Ion Chromatography and AAS Analysis .....	30
3.4. Analysis of Samples .....	32
3.4.1. Determination of Anions by Ion Chromatography .....	32
3.4.2. Determination of $\text{NH}_4^+$ by Spectrophotometer .....	33
3.4.3. Determination of Trace Elements by AAS .....	33
3.4.3.1. Flame Atomic Absorption Spectroscopy .....	33
3.4.3.2. Graphite Furnace Atomic Absorption Spectroscopy .....	34
3.4.4. Determination of Trace Elements by ICP-OES .....	35
3.5. Data Quality Assurance (QA) .....	36
3.5.1. Field and Laboratory Blanks.....	36
3.5.2. Calculation of Detection Limits .....	37
3.5.3. Analysis of Standard Reference Materials.....	38
RESULTS AND DISCUSSIONS.....	39
4.1. General Characteristics of the Data.....	39
4.1.1. Distribution Characteristics of the Data.....	40
4.1.2. Comparison of the Precipitation Data with the Literature and the EMEP Network.....	44
4.2. Ionic Composition of Wet Deposition .....	52
4.2.1. Ion Balance.....	52
4.2.2. Contributions of Ions to Total Ion Mass .....	53
4.3. Acidity of Wet Deposition .....	60
4.3.1. Rainwater pH .....	60
4.3.2. Neutralization of Acidity.....	63
4.4 Temporal Variability of Wet Deposition .....	68

4.4.1. Short Term (Daily) Variation.....	69
4.4.1.1 Baseline concentrations of measured parameters .....	74
4.4.2 Long Term (Seasonal) Variations .....	77
4.5. Time Trend Analysis.....	83
4.6. Wet Deposition Fluxes.....	87
4.6.1. Seasonality of Wet Deposition Fluxes .....	89
4.6.2. Comparison of the Wet Deposition Fluxes with the EMEP Network .....	93
4.7. Sources of Measured Species.....	94
4.7.1. Correlation Matrix.....	94
4.7.2. Enrichment Factors .....	99
4.7.2.1. Crustal Enrichment Factors (EF <sub>c</sub> ) .....	100
4.7.3. Positive Matrix Factorization.....	101
4.7.4. Potential Source Contribution Function.....	112
CONCLUSION.....	115
5.1. Recommendations for Future Research .....	119
REFERENCES.....	120

## LIST OF TABLES

Table 1.1. Monthly average temperature and total precipitation amounts observed during the years 1992 and 1993 and long term averages for the Antalya Meteorological Station. (Güllü, G., 1996a) .....	25
Table 3.1. Analytical techniques and devices used in the determination of rain water composition .....	32
Table 3.2. Parameters used in FAAS and FAES analysis.....	34
Table 3.3. Parameters used in GFAAS analysis. ....	35
Table 3.4. The wavelengths of ions and elements were analysed by ICP-OES.....	35
Table 3.5 Sample to blank ratios of elements .....	37
Table 3.6 Detection limits of elements and ions (ppm) .....	38
Table 4.1 Summary Statistics of Measured Species .....	42
Table 4.2 Parameters indicating distribution characteristics of the variables.....	43
Table 4.3 The location of the EMEP stations used for the comparison.....	47
Table 4.4 Comparison of observed volume weighted average concentrations of trace elements with literature values ( $\mu\text{g/l}$ ).....	51
Table 4.5 Contributions of ions to total ion, total cation and total anion mass in each year, in wet and dry season and during the period November 1991 and August 1999.....	54
Table 4.6 Sources contributing to observed concentrations of ions and elements in the Eastern Mediterranean.....	59
Table 4.7 Concentrations of ions for $\text{pH}<5$ , $\text{pH}\geq 5$ and whole data set.....	62
Table 4.8 Median ( $\text{H/nss-SO}_4^{2-}+\text{NO}_3^-$ ) and ( $\text{SO}_4^{2-}/\text{NO}_3^-$ ) ratios calculated for the whole dataset and for all months.....	64
Table 4.9 Regional background concentrations. ....	75
Table 4.10 Linear Regression analysis to determine time trends.....	85
Table 4.11 Results of regression analysis of wet deposition fluxes with precipitation. ....	88
Table 4.12 Annual and seasonal average wet deposition fluxes corresponding to the measured ions ( $\text{mg/m}^2$ ). ....	90
Table 4.13 Total and seasonal average wet deposition fluxes corresponding to the measured ions.....	91

Table 4.14 Correlation coefficients between ions and elements in whole data set...	95
Table 4.15 Correlation coefficients between ions and elements in wet season data set. .....	96
Table 4.16 Correlation coefficients between ions and elements in dry season data set. .....	97
Table 4.17 Percent contribution of each factor on calculated concentrations of elements and ions. ....	106

## LIST OF FIGURES

Figure 3.1. Standard and modified Andersen precipitation sampler (Al-Momani, 1995c).....	29
Figure 4.1 Frequency distributions and best fit curves for Al, Pb, Na <sup>+</sup> and SO <sub>4</sub> <sup>2-</sup> .....	45
Figure 4.2 Comparison of volume weighted average concentrations of major ions of Antalya station with the results of other EMEP stations. ....	50
Figure 4.3. Comparison of concentrations of elements measured in this study with those reported for the EMEP stations.....	50
Figure 4.4 The plot of the equivalent sum of anions to equivalent sum of cations. ..	52
Figure 4.5 Contribution of ions to total ion mass.....	55
Figure 4.6 Contribution of anions to total anion mass and contribution of cations to total cation mass.....	56
Figure 4.7 Seasonal variations in the contributions of ions to total ion mass.....	57
Figure 4.8 Plot of equivalent Na concentration to equivalent Cl concentration .....	57
Figure 4.9 Frequency distribution of pH.....	61
Figure 4.10 Trajectory plots of pH a) greater than 5 b) lower than 5. ....	63
Figure 4.11 Monthly variations for the equivalent ratio of SO <sub>4</sub> <sup>2-</sup> /NO <sub>3</sub> <sup>-</sup> in rainwater. 65	65
Figure 4.12 Monthly variations for the equivalent ratio of H <sup>+</sup> /(nss-SO <sub>4</sub> <sup>2-</sup> +NO <sub>3</sub> <sup>-</sup> ) in rain water.....	66
Figure 4.13 The relation between H <sup>+</sup> /(nss-SO <sub>4</sub> <sup>2-</sup> +NO <sub>3</sub> <sup>-</sup> ) ratio and the precipitation amount.....	67
Figure 4.14 The plot of (H <sup>+</sup> +Ca <sup>2+</sup> +NH <sub>4</sub> <sup>+</sup> ) versus (SO <sub>4</sub> <sup>2-</sup> +NO <sub>3</sub> <sup>-</sup> ) (µeq/l).....	68
Figure 4.15 The time trend plot of SO <sub>4</sub> <sup>2-</sup> , NO <sub>3</sub> <sup>-</sup> and H <sup>+</sup> and corresponding backtrajectories. ....	70
Figure 4.16 The time trend plot of NH <sub>4</sub> <sup>+</sup> .....	72
Figure 4.17 The time trend plot of Mg <sup>2+</sup> , Ca <sup>2+</sup> and K <sup>+</sup> . ....	72
Figure 4.18 The time trend plot of Al and Fe. ....	72
Figure 4.19 The time trend plot of Na <sup>+</sup> and Cl <sup>-</sup> .....	73
Figure 4.20 The time trend plot of Ni and Cr. ....	74
Figure 4.21 The time trend plot of Pb.....	74
Figure 4.22 Monthly median concentrations of H <sup>+</sup> .....	78
Figure 4.23 Monthly median concentrations of SO <sub>4</sub> <sup>2-</sup> and NO <sub>3</sub> <sup>-</sup> .....	78

Figure 4.24 Monthly median concentrations $\text{NH}_4^+$ .....	79
Figure 4.25 Monthly median concentrations of $\text{Na}^+$ and $\text{Cl}^-$ .....	80
Figure 4.26 Monthly median concentrations of Al, Fe, Ni, Cr and $\text{Ca}^{2+}$ .....	81
Figure 4.27 Monthly median concentrations of $\text{Mg}^{2+}$ and $\text{K}^+$ .....	81
Figure 4.28 Monthly median concentrations of Cd, Cu, Pb and Zn. ....	83
Figure 4.29 The time trend distribution of $\text{H}^+$ , $\text{SO}_4^{2-}$ , $\text{NO}_3^-$ and $\text{NH}_4^+$ among the EMEP Stations between the years 1991-1999. ....	86
Figure 4.30 Plot of wet deposition flux of $\text{H}^+$ , $\text{SO}_4^{2-}$ , $\text{NO}_3^-$ , $\text{NH}_4^+$ , $\text{Ca}^{2+}$ , $\text{Cl}^-$ , Cu and Al with precipitation amount. ....	92
Figure 4.31 Comparison of wet deposition fluxes of EMEP Stations and Turkey Antalya Station between the years 1991 and 1999. ....	93
Figure 4.32 Crustal Enrichment Factor (EFc) of rainwater composition .....	100
Figure 4.33 Seasonal differences of crustal enrichment factor of rain water composition .....	101
Figure 4.34 Calculated total ionic mass concentrations vs. measured total ionic mass concentrations. ....	105
Figure 4.35 Median values of the observed-to-predicted ratios of elements. ....	105
Figure 4.36 Factor loadings (F-loading), Enrichment factors (EFc) of elements, Explained variances (EV) and monthly average values of G factor scores. ....	107
Figure 4.37 Top and side views of the backtrajectories that correspond to highest 20% of the G scores. ....	108
Figure 4.38 The spatial distribution of PSCF values of Factor 1, 4, 5 scores and $\text{SO}_4^{2-}$ ion concentrations. ....	114

## LIST OF ABBREVIATIONS

<b>D</b>	Deposition flux
<b>ECMWF</b>	European Center for Medium Range weather Forecast
<b>EFc</b>	Crustal Enrichment Factor
<b>EMEP</b>	European Monitoring and Evaluation Programme
<b>FA</b>	Factor Analysis
<b>FAAS</b>	Flame Atomic Absorption Spectrometry
<b>FAES</b>	Flame Atomic Emission Spectrometry
<b>GFAAS</b>	Graphite Furnace Atomic Absorption Spectrometry
<b>HPLC</b>	High Performance Liquid Chromatography
<b>L<sub>d</sub></b>	Detection limit
<b>P</b>	Precipitation amount
<b>PCF</b>	Principal Component Factor
<b>PMF</b>	Positive Matrix Factorization
<b>E</b>	Residual matrix
<b>e<sub>ij</sub>/s<sub>ij</sub></b>	Scaled residual
<b>EV</b>	Explained variation
<b>F</b>	Matrix of source composition
<b>G</b>	Matrix of contribution
<b>Q</b>	Sum of squares of weighted residuals “Chi-square”
<b>s<sub>ij</sub></b>	Uncertainty estimate
<b>α</b>	Outlier threshold distance
<b>PSCF</b>	Potential Source Contribution Factor
<b>P(A<sub>ij</sub>)</b>	Residence time of randomly selected air parcel
<b>P(B<sub>ij</sub>)</b>	Residence time of contaminated air parcel
<b>S<sub>b</sub></b>	Standard deviation
<b>SRM</b>	Standard Reference Material

## CHAPTER 1

### INTRODUCTION

#### 1.1. Framework

Acid deposition, more commonly known as acid rain, is one of the major air pollution problems, which may impair air quality and damage public health, acidify lakes and streams, harm sensitive forest and coastal ecosystems, degrade visibility and accelerate the decay of building materials. The emissions of sulfur dioxide and nitrogen oxides are the key pollutants in the formation of acid rain that reacts with water, oxygen and other oxidants in the atmosphere and generate various acidic compounds, which finally turn to atmosphere as acid deposition.

Researches have denoted that the major reason of acid rain is the combustion of fossil fuels. For instance, in the US, electric power generation is by far the largest single source of SO<sub>2</sub> emissions accounting for approximately 67 percent of total SO<sub>2</sub> emissions and 22 percent of total annual NO<sub>x</sub> emissions nationwide in 2002 (EPA, 2004).

Precipitation chemistry is an important research area since; the chemical composition of rain water is a useful index for the determination of pollution level at a site and the cycling of materials through the atmosphere by different processes that is involved in element scavenging by rain water and cloud water (Alagha and Tuncel, 2003; Baez et al., 1997; Pio et al., 1991). Furthermore, contributions of organics compounds, heavy metals and major ions to pollution problems and their contents can be identified by the investigation of wet deposition samples in industrialized countries (Jaradat et al., 1999).

The evaluation of precipitation chemistry is an indicator for chemical climate, overall air quality (Lehmann et al., 2005) and of the related sources of the gases and particulate matter (Tuncel and Ungör, 1996). Indeed, the local and regional dispersions and the impacts of pollutants on ecosystems are identified by precipitation chemistry (Mouli et al., 2005; Lee et al., 2000; Tuncel and Ungör, 1996). In other words, the chemistry of precipitation is influenced by the strength of emission sources, chemical reactions that are held in atmosphere and the scavenging mechanism of moving air masses (Alagha, 2000; Avila and Alarcon, 1999; Beverland et al., 1998).

The recognition of the transboundary nature of the problem has led to take international actions; therefore, the United Nations Conference on the Human Environment held in Stockholm, has indicated the acid rain problem in Europe and has initiated the Long-range transport of air pollutants study in 1972. In 1979, Convention on Long-Range Transboundary Air Pollution is signed by 32 European countries, the Eastern European nations, the US and the Canada. In 1985, the Protocol on the Reduction of Sulphur Emissions or their Transboundary Fluxes is signed by the 21 Parties and intended to reduce 1980 sulphur emissions by more than 50% by 1993. All the parties to that Protocol have reached the target of reducing emissions by at least 30%. In 1988, Protocol concerning the Control of Emissions of Nitrogen Oxides or their Transboundary Fluxes, signed by 25 parties, have targeted a reduction of 9% compared to year 1987. Furthermore, NO<sub>x</sub> Protocol requires the application of an effects-based approach by applying the multi-pollutant, multi-effect critical load approach, a new instrument being prepared at present should provide for further reduction of emissions of nitrogen compounds. In 1994 the Oslo Protocol on Further Reduction of Sulphur Emissions that signed by 26 Parties is aimed to set long term targets to reduce sulfur emissions by effects-based approach, the critical load concept, best available technology, energy savings, the application of economic instruments and other considerations. In 1999, Convention on long-range transboundary air pollution has been signed to set emission levels for sulphur, NO<sub>x</sub>, VOCs and ammonia for the year 2010. The protocol implements the Europe's sulfur emissions should be cut by at least 63% and NO<sub>x</sub> emissions by 41%, its VOC

emissions by 40% and its ammonia emissions by 17% compared to 1990. (UNECE, 2005)

The achieved emission reductions are compared between European Union (Austria, Belgium, Germany, Denmark, Spain, Finland, France, United Kingdom, Greece, Ireland, Italy, Luxembourg, Netherlands, Portugal, and Sweden) and USA for the years 1980 and 1998. SO<sub>2</sub> and NO<sub>2</sub> emission reductions for US and EU are 26.9%, 70% and 10.1%, 20.8%, respectively. On the other hand, per capita reductions of SO<sub>2</sub> and NO<sub>2</sub> for US and EU are 67.6%, 31.4% and 22.4%, 21.4%, respectively. (Hayward, 2004) Furthermore, EPA (2004) compared the sulfate and inorganic nitrogen wet deposition reductions from the years between 1989-1991 to the years between 2001 and 2003. Deposition reductions between these years are calculated by taking the averages of the areas of Mid-Atlantic, Midwest, Northeast and Southeast, 30.35% for wet sulfate deposition and 8% for wet inorganic nitrogen deposition.

Furthermore, between the years 1990 and 2000, the decreases in Europe primarily due to large reductions of primary emissions of NO<sub>x</sub>, SO<sub>2</sub> and NMVOCs, 27 %, 60% and 29 %, respectively, have been achieved through improved flue gas treatments, fuel switching, use of low sulfur fuels in power stations and the introduction of catalytic converters for cars. Reductions in emissions of acidifying gases in the main emitting sectors were: energy industries, 48%; industry (energy and processes), 51%; other (energy and non-energy), 54%; transport, 25%; and agriculture, 17%. (EEA, 2003)

## **1.2. Objectives of the Study**

It is fairly well established that Mediterranean Region is under strong influence of pollutants transported over industrialized European countries (Güllü et al., 1997; Al-Momani et al., 1995a). Consequently the data generated in this region has a vital importance to understand the levels and source regions of pollutants. The transport and deposition of pollutants from various source regions are well defined for western Mediterranean (Deboudt et al., 2004; Avila ve Alarcon, 2003; Charron et al., 2000; Avila ve Alarcon, 1999; Draaijers et al., 1997; Avila, 1996; Sanusi et al., 1996; Van Leeuwen et al., 1996; Erisman et al., 1995; Guerzoni et al., 1995; Hedin et al., 1994; Losno et al., 1991, Pio et al., 1991 ), however for eastern Mediterranean little data

are available (Güllü et al., 2004; Güllü et al., 2003; Güllü et al., 2001; Al-Momani et al., 1999; Al-Momani et al., 1998; Güllü et al., 1998; Al-Momani et al., 1997; Güllü et al., 1997; Güllü, 1996a; Al-Momani et al., 1995a; Al-Momani, 1995c; Kubilay and Saydam, 1995).

In this study, concentrations of major ions and trace elements in rain water and their long term trends are investigated for the years between 1992 and 1999 in Eastern Mediterranean region. The objectives of the study are as follows:

- (1) To determine the long term chemical composition of atmospheric deposition by the investigation of the concentrations of major ions and trace elements, being powerful markers to identify source areas affecting the deposition in Eastern Mediterranean region,
- (2) To study the factors affecting the long term acidity of rain water and to explain the neutralization processes and acid-base chemistry,
- (3) To understand the long term variations of the pollutants by applying time series analysis,
- (4) To identify the source regions that long range transport patterns of pollutants to the Eastern Mediterranean region by applying multivariate statistical techniques with back trajectory information.

### **1.3. Study Overview (Outline of the Study)**

In the following chapter, wet deposition and its chemical characteristics are discussed with highlighting the acid deposition phenomena and literature survey studies conducted in Mediterranean region are given. Furthermore, time trend analysis is reviewed by the information regarding the geography and climatology of the area.

Location of the sampling station, sampling techniques, instrumentation, analytical techniques used and the computation of back trajectory are given in the third chapter. Furthermore, data quality assurance, field blanks, detection limits, data handling and checking are included.

The obtained results are extensively discussed in the fourth chapter. The characteristics of the measured ions, neutralization of rain water acidity, long term variations, time trend analysis, wet deposition fluxes of pollutants and the determination of source regions of pollutants are discussed in this chapter.

In the last chapter, concluding remarks, some suggestions for further research are presented.

#### **1.4. Previous Work**

In Eastern Mediterranean aerosol composition and their temporal variability is studied by Güllü et al. (2003); Güllü et al. (1998), Al-Momani et al. (1997), Güllü, (1996a); Güllü et al. (1996b); Al-Momani et al. (1995a), Kubilay and Saydam (1995), wet deposition is studied by Al-Momani et al. (1998), Al-Momani et al. (1997), Güllü et al. (1997), Al-Momani et al. (1995a), Al-Momani (1995c). Potential source regions and transportation of air masses to the area is studied by Güllü et al. (2004), Güllü et al., 2003; Güllü et al. (2001); Al-Momani et al. (1999); Güllü (1996a); Al-Momani, I.F. (1995c).

Previously, chemical composition and variations of wet deposition were investigated in short term bases in Eastern Mediterranean region. By this study, the chemical composition, its variation and acid-base chemistry is redefined with a wide range data set. Furthermore, time trend analysis is applied for 8-years long to observe the long range variation of species. Positive matrix factorization and potential source contribution function were applied to redefine the source contributions and their corresponding source regions.

## **CHAPTER 2**

### **BACKGROUND**

#### **2.1. Atmospheric Removal Mechanisms**

Precipitation which is a major pathway of natural and anthropogenic species from atmosphere to oceanic and terrestrial ecosystems (Alagha et al., 2003; Lee et al., 2000 and Losno et al., 1991), is a crucial mechanism for the removal of air borne gases and particles, whose concentrations varies with amount of emissions, atmospheric transformations and weather, from the atmosphere (Lehmann et al., 2005; Tuncel and Ungör, 1996).

Acidic substances in the atmosphere are deposited and transported through soils into lakes, streams, and groundwater on the earth's surface by two mechanisms. The first mechanism, wet deposition, involves the dissolution of acidic substances into cloud water, and the subsequent fallout of acidified precipitation to the earth's surface named as acid rain and includes two main process rainout and washout. Where the former refers to in-cloud scavenging by precipitation of cloud droplets or ice crystals and the latter refers to below-cloud scavenging by precipitation. The second mechanism is dry deposition, where the acidic particles and their precursors can also settle directly to the earth's surface through gravitational settling.

Wet and dry depositions of chemical species provide as well as a natural source for atmospheric trace substances and also a source of nutrients for the biological systems at the Earth surface. Various sources for atmospheric chemistry is identified by the chemical characteristics, the space and time evolution of these depositions (Al-Momani et al., 1998). Furthermore, the evaluation of atmospheric deposition in qualitative and quantitative terms is significant for the evaluation of regional

diversity, the determination of critical loads, the demonstration of pluri-annual trends analysis and the setting of emission reduction policies on regional scale could be performed (Alagha et al., 2003).

The type of deposition is crucial since the elimination of particulate matter occurs seasonally from the atmosphere by the local rain events (Mouli et al., 2005; Deboudt et al., 2004). Furthermore, the major removal mechanism for most of the heavy metals is wet deposition that is as large as three or four times of dry deposition (Deboudt et al., 2004).

## **2.2. Acid Deposition**

Acid deposition is defined as the dispersion of acid forming compounds into atmosphere and absorbing into liquid drops in cloud and fogs and removing by rain or snow, that are rainout and washout. In other words, acid deposition occurs as a consequence of acidic absorbing media reach to Earth surface by cleaning the atmosphere (Chen, W.H., 2001).

The compounds of  $\text{SO}_4^{2-}$  and aerosols of NO,  $\text{NO}_2$ ,  $\text{HNO}_2$ ,  $\text{HNO}_3$  and aerosols of  $\text{NO}_3^-$  and  $\text{NH}_3$  and  $\text{NH}_4^+$  are responsible from the acidification and eutrophication processes (Erisman et al., 1995).

Wet and dry acid deposition is responsible from the acidification of lakes and damaging of forests and metal structures (Charron et al., 2000; Al-Momani et al., 1995a; Losno et al., 1991).

### **2.2.1. Chemical Composition of Acid Precipitation**

The formation and transport of acid precipitation is a complicated process (Zeng and Hopke, 1989). The acidity in precipitation mainly depends on the acid precursors and neutralizing species in the precipitation. The acidity of precipitation is determined dynamically by the acid-base reactions which can occur between acidic species ( $\text{CO}_2$ ,  $\text{H}_2\text{SO}_4$ ,  $\text{HNO}_3$ ,  $\text{HCOOH}$ ) and basic species ( $\text{NH}_3$ ,  $\text{CaCO}_3$ ) forming material in air or liquid water (Al-Momani, 1995c).

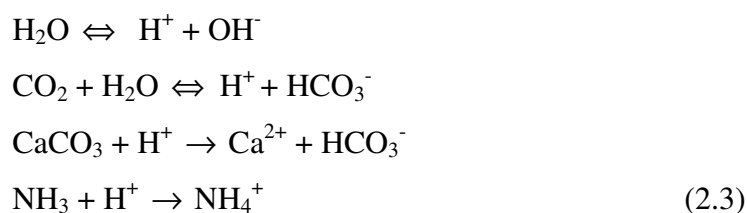
While nitric and sulfuric acids or their precursors so as  $\text{NO}_x$  and  $\text{SO}_2$  dissolves in water to give hydrogen ions, they ultimately turn to nitrate ions ( $\text{NO}_3^-$ ) and sulfate ions ( $\text{SO}_4^{2-}$ ).  $\text{CO}_2$  dissolves in water and forms a weak acid of  $\text{HCO}_3^-$  with an acidity constant of  $\text{pK}_a$  6.8. (Losno et al., 1991) The formula is given as follows:



If the  $\text{CO}_2$  concentration is assumed to be equal to 350 ppm in the atmosphere, we obtain as (Granat, 1972):

$$\text{p}[\text{HCO}_3^-] = -\ln([\text{HCO}_3^-]) = 11.24 - \text{pH} \quad (2.2)$$

For rural or urban areas in which the contributions of organic acids is small, acid-base budget is computed by the following reactions: (Losno et al., 1991)



The presence of  $\text{NO}_3^-$  and  $\text{NH}_4^+$  can directly be attributed to an input of  $\text{HNO}_3$  and  $\text{NH}_3$ . Since the acidity in precipitation mainly depends on the acid precursors and neutralizing species in the precipitation, it can not be clearly explained by pH alone (Avila et al., 2003; Al-Momani et al., 1997, Al-Momani et al., 1995a).

### 2.2.1.1. Principal Precursors of Acidification

Acid rain precursors include both anthropogenic emissions such as from fossil fuel combustion and mobile sources and natural emissions such as volcanoes. Wet deposition of sulfur and nitrogen oxides is the precursors of major acids of  $\text{H}_2\text{SO}_4$  and  $\text{HNO}_3$  that are resulted from mainly fossil fuel combustion (Mouli et al., 2005; Alagha and Tuncel, 2003; Chen, W.H., 2001; Al-Momani et al., 2000; Charron et al., 2000; Jaradat et al., 1999). The formation of acids, in cloud or rain droplets which is known as acid deposition, has detrimental effects on the ecosystem and the

complexity of source- receptor relationship (Al-Momani et al., 1998). As an example, in poorly buffered watersheds, the acid deposition results in the modifications and changes of species composition and amounts in ecosystem (Mouli et al., 2005; Al-Momani et al., 2000).

Areas under strong influence of SO<sub>2</sub> and NO<sub>x</sub> gases have lower pH values (Losno et al., 1991). Additionally, these precursor gases cause acid precipitation which has an impact on aquatic and terrestrial ecosystems (Lehmann et al., 2005; Seto et al., 2000). Moreover, to decrease the acidity of precipitation, it is necessary to understand the chemical characteristics of the sources of the acid precipitation, and also their geographical positions (Zeng and Hopke, 1989).

In urban areas, the produced sulfur and nitrogen oxides that are emitted from space heating and motor vehicles are removed by wet precipitation since the integrity of these gases in rain droplets is fast (Kaya and Tuncel, 1997; NRC, 1983). Having dissolved in droplets, HSO<sub>3</sub><sup>-</sup> is oxidized to SO<sub>4</sub><sup>2-</sup> by the species, namely H<sub>2</sub>O<sub>2</sub> and O<sub>3</sub>. Oxidation by O<sub>3</sub> is effective in heavily polluted urban atmosphere, whereas oxidation by H<sub>2</sub>O<sub>2</sub> is effective in rural atmosphere. Furthermore, presence of trace metals such as Fe<sup>3+</sup> and Mn<sup>2+</sup> in cloud and fog droplets increases the level of oxidation in the atmosphere. Additionally, the oxidation of these gases occurs in the existence of photochemical mechanisms. (Tunçer, 2000)

Acidifying compounds can remain in the atmosphere for several days which implies that their transport takes place over several thousand kilometers (Charron et al., 2000) meaning that contribution from long range transport of these compounds has higher probability.

#### **2.2.1.2. Principal Agents of Neutralization**

The acid-base status of precipitation is a result of a balance between acidifying compounds, mainly oxides of sulfur and nitrogen and alkaline compounds, mainly ammonia and alkaline material in windblown soil dust (Rodhe et al., 2002). The chemical composition and solubility of alkaline particles such as oxides, hydroxides, carbonates or silicates affects the acid neutralizing capacity (Draaijers et al., 1997).

Quantification of base cations of wet deposition such as Ca, Mg, K and Na is significant for chemical processes of acid deposition, since the acidity is a function of both acidic and basic content (Leeuwen et al., 1996).

Neutralization process and extend of the precipitation acidity can be influenced by the emissions of gaseous  $\text{NH}_3$  that is released from the agricultural, industrial and natural activities (Losno et al., 1991) and alkaline dusts that are generated through wind erosion (Mouli et al., 2005; Al-Momani et al., 2000; Saxena et al., 1996). Furthermore, Saharan dust consists of calcite ( $\text{CaCO}_3$ ), dolomite ( $\text{CaCO}_3 \cdot \text{MgCO}_3$ ) and gypsum ( $\text{CaSO}_4 \cdot 2\text{H}_2\text{O}$ ) in the dust soil has major role in the neutralization of precipitation (Al-Momani et al., 2000). In the same manner, neutralization by  $\text{CaCO}_3$  is mainly reported in the areas where the composition of rain water contains high amounts of Saharan dust having high  $\text{CaCO}_3$  content (Al-Momani et al., 2000; Losno et al., 1991).

### **2.2.2. Studies of Acid Precipitation**

Precipitation chemistry is a significant research area since, sulfur and nitrate species contributes to acidic deposition leading to adverse impacts on acid sensitive ecosystems and major ions responsible from neutralization and indication of processes occur in the atmosphere. Therefore, the monitoring of these pollutants, investigate the contribution of the acidity and neutralization and their long term trends makes us to understand the nature of processes and their effects. Furthermore, bring into force us to implement policies to reduce the emissions.

#### **2.2.2.1. Studies of Chemical Composition**

Deposition of potential acid has been mapped on a small scale over Europe by Erisman et al. (1995) indicated that largest potential acid deposition is found in the border area between Germany, Poland and the Czech Republic which is known as Black Triangle. Furthermore, in northern Scandinavia and part of Scotland, Portugal and Spain the potential acid deposition is very low.

In addition to the acidifying components, wet deposition of the base cations  $\text{Ca}^{2+}$ ,  $\text{Mg}^{2+}$ ,  $\text{K}^+$  (and  $\text{Na}^+$ ) also needs to be quantified, because they too play an integral role in the chemical processes of acid deposition, since the acidity of any material is a function of both its acidic and basic content (Leeuwen et al., 1996).

In Scandinavia, Denmark, northern and western Germany, The Netherlands and the southeast of the United Kingdom, the percentage of neutralization by base cations is less than 25% whereas in large parts of southern Europe it is more than 50%. Furthermore, in southern Portugal, southern Spain, Sardinia and the west coast of Ireland and Scotland the amount of neutralization exceeds 100% by counteraction of non-sea-salt deposition of magnesium, calcium and potassium ions. (Draaijers et al., 1997) Total base cation deposition shows the highest fluxes in Ireland, Scotland, Italy, former Yugoslavia, Ukraine and the Black Triangle (Leeuwen et al., 1996).

Wet depositions of alkaline particles were studied in relation to the issue of acidification through their ability to neutralize acidity (Draaijers et al., 1997; Leeuwen et al., 1996; Hedin et al., 1994). In this respect, Saharan dust is a significant source of base cation containing particles in the atmosphere of Southern Europe (Draaijers et al., 1997). Studies conducted in the southern Mediterranean point out that the neutralization of strong acids occurs by the incorporation of suspended nature alkaline dust and soil long-range transported from African desert areas (Avila and Alarcon 2003; Avila and Alarcon, 1999; Losno et al., 1991).

Western Mediterranean has an extensive database about wet deposition and acidifying and neutralization processes take place in region. The backtrajectory analyses made in region have distinguished the source regions as African, European, oceanic and local (Avila and Alarcon, 2003; Avila and Alarcon, 1999; Al-Momani et al., 1997; Guerzoni et al., 1995; Losno et al., 1991). Furthermore, in southern Sardinia Guerzoni et al., (1995) showed that the influence of Saharan dust is apparent since neutralization occurs due to the enrichment of Ca, Mg and  $\text{SO}_4$  ions. Sanusi et al., (1996) indicated that in eastern France major ion concentrations are higher in urban areas and precipitation acidity is lower in rural areas. Moreover, in the region, the main neutralization agent that is originated from the mountains is  $\text{CaCO}_3$ . Furthermore, Charron et al. (2000) pointed out that  $\text{SO}_2$  and  $\text{NO}_x$  emissions from

Eastern Europe responsible from the high acidity of Morvan, France rain water and acid-buffering effect of largely emitted  $\text{NH}_3$  and neutralizing effect of Saharan dust from Mediterranean basin and northern Africa explain the acid-base chemistry in the region.

Among the numerous influences, the Saharan dusts originated from North West Africa has a distinctive neutralization capacity that is transported to the Mediterranean region (Al-Momani et al., 2003; Güllü et al., 2003; Al-Momani et al., 2000; Avila and Alarcon, 1999; Jaradat et al., 1999; Guerzoni et al., 1995; Kubilay and Saydam, 1995; Losno et al., 1991).

Although similar results are observed for Eastern Mediterranean region, where is under the influence of three general source types of anthropogenic sources located in North and Northwest of the basin, strong crustal source transported from North Africa and suspended from local soil and marine source from Mediterranean region, few studies have been conducted (Güllü et al., 2004; Güllü et al., 1998; Al-Momani et al., 1998; Al-Momani et al., 1997). Back trajectories have correspond that low pH is due to the industrial regions where the main wind sector is from west, northwest and north. In the region  $\text{CaCO}_3$  is the main neutralizing agent of 70%, while the neutralization by  $\text{NH}_3$  is small (Al-Momani et al., 1997; Al-Momani et al., 1995a).

In Turkey, numerous studies have been conducted to explain the chemical composition of wet deposition, acidifying compounds and neutralization process. In the Coast of Aegean Sea, Al-Momani et al. (1995b), in Black Sea, Alagha and Tuncel (2003) and in Ankara Kaya and Tuncel (1997) and Tuncel and Ungör (1996) recorded the similar pH values compared with the Eastern Mediterranean region. Furthermore, acidity is explained as not due to the lack of anthropogenic contribution but explained as more neutralization process that is mainly from calcareous soil containing high  $\text{CaCO}_3$  and fertilizers containing high amounts of  $\text{NH}_3$  and  $\text{NH}_4^+$  occurs.

Precipitation chemistry in Northern Jordan is similar to that of other areas of the Mediterranean basin. Although, concentrations of  $\text{NO}_3^-$  and  $\text{SO}_4^{2-}$  were high, neutralization by the alkaline soil dust allows the precipitation to be neutral (Al-

Momani et al., 2003). In the same manner, Al-Momani et al. (2000) and Jaradat et al. (1999) indicated that the neutralization mainly occurs by the dissolution of Saharan dust containing large fractions of calcite ( $\text{CaCO}_3$ ), dolomite ( $\text{CaCO}_3 \cdot \text{MgCO}_3$ ) and gypsum ( $\text{CaSO}_4 \cdot 2\text{H}_2\text{O}$ ) into rain water.

In East Asia, Fujita et al. (2000) has indicated that the mean pH is 4.9 with the maximum annual average observed at Jinan (pH: 6.1) and minimum value at Tokyo (pH: 4.5) and the contribution to acidity is resulted from sulfuric acid in China and nitric acid in Japan. Although, higher anthropogenic emissions occur in China, higher pH values are observed due to the sufficient neutralization by airborne calcium and ammonia produced by natural and anthropogenic activities. Since the neutralization capacity is moderate in Japan, pH values are lower.

#### **2.2.2.2. Studies of Time Trend**

Numerous studies have been recorded to explain the long term trend analysis of wet precipitation samples and their contribution to acidity in Europe (Avila and Alarcon., 2003; Puxbaum et al., 1998; Draaijers et al., 1997; Leeuwen et al., 1996; Sanusi et al., 1996; Guerzoni et al., 1995; Hedin et al., 1994; Losno et al., 1991; Erisman et al., 1989), in the United States (Lehmann et al., 2005; Lynch et al., 1995) in Mexico (Baez et al., 1997; ), in Japan (Seto et al., 2004). Decreasing sulfate concentrations and slight increase in nitrate concentrations and pH has been observed for the studies which have continued since 1965 in Europe.

Puxbaum et al., (1998), have showed the relationship between  $\text{SO}_4^{2-}$ ,  $\text{Ca}^{2+}$ ,  $\text{NH}_4^+$  and  $\text{H}^+$  ions in Central Austria for the years from 1984 to 1993. The 65% decrease of hydrogen concentration can be explained not only the 33% decline in sulfate concentrations but also the significant decline in Ca concentrations (39%) and slight increase in ammonium concentration (14%). In Netherlands, Erisman et al., (1989) showed long term trend as the reduction of 19% of the total acid deposition between 1980 and 1986 is due to mainly sulfate deposition. While 6% increase in  $\text{NH}_x$  deposition is observed,  $\text{NO}_y$  deposition remained constant during 1980 and 1986. In Netherlands, between 1978 and 1989, 34% reduction in  $\text{SO}_4^{2-}$  and in Sweden, between 1971 and 1989, 54-68% reduction in  $\text{SO}_4^{2-}$  is recorded by Hedin et al.

(1994). In the same manner, in Northeastern US, Hedin et al. (1994) has indicated the approximate long term trend as 38% reduction for  $\text{SO}_4^{2-}$  between 1965 and 1990.

Weekly rain water samples are collected and analyzed from the Montseny Mountains in the Northwest of Spain during 1983 to 2000. Significant increase in alkalinity, median pH and  $\text{NO}_3^-$  is observed while nss- $\text{SO}_4$  has decreased from 1983. Decreasing exc $\text{SO}_4^{2-}$  concentrations in local rains coincides with reduction in  $\text{SO}_2$  emissions of about 47%. (Avila and Alarcon, 2003)

Lynch et al., (1995) has carried out a study in the United States to investigate 13 years precipitation chemistry data is collected from 58 stations. For sulfate concentration, at 42 of the 58 sites an average decrease of 28% and for hydrogen concentration at 17 sites an average 40% decrease is observed. The  $\text{NO}_3^-$  concentrations exhibit a decreasing pattern through the country except for the west sites. The strong positive relationships between  $\text{H}^+$  concentrations and  $\text{SO}_4^{2-}$  and  $\text{NO}_3^-$  concentrations and negative correlation with Ca and  $\text{NH}_4^+$  are observed. Furthermore, a long term trend study conducted in the United States from 1985 to 2002 has indicated that ammonium concentrations increased about 10% while, sulfate concentrations decreased about 25%. Nitrate concentrations decreased approximately 25% and earth crustal cations are decreased significantly. (Lehmann et al., 2005)

Baez et al, (1997) has studied in Mexico City for 7 years of daily bulk and wet deposition samples. Long term analysis of the data show high variability therefore the data could not be able to evaluate. The variations can be due to the meteorological factors such as wind direction, rainfall rate, total amount of rainfall and height of cloud base.

Seto et al., (2004) has conducted a study in Japan to a data set from 1989 to 1998. The non-seasalt deposition decreased on a national scale with a mean change rate of 3.5% annually. In contrast,  $\text{NO}_3^-$  and  $\text{NH}_4^+$  deposition for the Japan Sea area showed increasing mean change rates of 3.4% and 3.7% annually, respectively. For  $\text{H}^+$  deposition, negative change rates (4-6%) annually were estimated for the Pacific Ocean, East China Sea and Seto Inland Sea. Zhang et al. (2003) represents that in

Tibet Lhasa region, measurements are compared for the period of 1987-1988 and 1997-1999. Although the soil is highly alkaline, the mean pH is decreased from 8.36 to 7.5. Sulfate is increased from 2.47 to 5.2 and nitrate is increased from 1.96 to 6.9 due to the extreme increase in anthropogenic emissions. Furthermore, the sharp increase in acidic substances is responsible from the decrease in pH. Inversely, ammonium is decreased from 21.92 to 14.3.

### 2.3. Receptor Oriented Models

Receptor models proceed on the idea of observing the ambient airborne particle concentration at a receptor and seek to apportion the observed concentrations between several source types based on knowledge of the compositions of the source and receptor materials. The methodologies fall into two categories (1) Chemical Mass Balance (CMB), (2) multivariate models such as Principal Component Analysis, factor analysis/multiple regression and target transformation factor analysis (Cheng et al., 1993). Since CMB have limited abilities to locate regional sources air pollutants because only chemical information is used and the regional pollutants are often secondary in their chemical and these chemical receptor models can not determine the specific location of the sources. Furthermore, receptor models have limited success in modeling long-range transport of secondary species and it is difficult to construct relationship for the secondary species using traditional receptor models with only chemical data (Cheng et al., 1993). To overcome these shortcomings, meteorological information needs to be incorporated into the receptor model. Receptor models and applications have been reviewed by Watson et al. (2002), Polissar et al. (1999), Hopke et al., 1995; Gao et al. (1994), Cheng et al., 1993; Zeng and Hopke, (1989), Ashbaugh, et al. (1985), Henry et al. (1984).

#### 2.3.1. Enrichment Factors

Enrichment factor is described as the double normalization technique used for quantification of non-crustal contribution by using a reference element of Al.

$$EF_c = \frac{(C_x / C_{Al})_{rain}}{(C_x / C_{Al})_{crust}} \quad (2.4)$$

Where  $C_x$  and  $C_{Al}$  are the concentrations of a trace metal  $x$  and Al, in the rain and  $C_{Al}$  is Al concentrations in average crustal material.

The metals with EF ratio close to 1 originates from weathering of the Earth's crust, and EF ratio between 1 and 10 might indicate the influence of the chemical composition of local soil. EF ratio between 10 and 500 denote moderate enrichment, indicating other sources in addition to crustal materials, and those greater than 500 are clear evidence of extreme enrichment, indicating severe contamination due to human activities (Hou et al., 2005; Alagha, 2000; Al-Momani, 1995c).

### **2.3.2. Positive Matrix Factorization**

Positive Matrix Factorization (PMF) has been developed by Paatero and Tapper (1994) and Paatero (1997) as an alternative to conventional receptor modeling approaches such as factor analysis (FA) and principal component analysis (PCA). PMF is a factor analytic technique that uses non-negativity constraints and allows non-orthogonal factors. Every data point can be individually weighed, in order to increase the importance of strong variables and decrease the effect of weak variables in the model. (Paatero and Hopke, 2003; Paatero, 1997).

The distinctive advantage of PMF over factor analysis (FA) or principal component analysis (PCA) is explained as the following: (1) In PMF, the chemical components coming from various sources can be apportioned among the factors and mass profiles of source structure are described in a more reasonable manner in PMF than the PCA model. (Qin et al., 2002) (2) In PMF, negative loadings of factors are not included. (3) PMF utilizes a point-by-point least-squares minimization scheme which provides the usage of input matrix without transformation (Lee et al., 1999). Therefore, in PMF, auto scaling, which tends to scale weak variables too high, as a pretreatment of the data set is not required (Paatero and Hopke, 2003; Paatero, 1997). (4) PMF separates sources with better resolution than FA. (5) By using error estimate, PMF can handle elements more effectively and by using enforced rotation techniques and can feed subjective information into factor analysis (Qin et al., 2002). (6) Handling of missing and below detection limit values have been achieved in PMF much better than FA. Besides these advantages, PMF has a disadvantage that the choice of the

number of factors is a compromise. Using too few factors will combine sources of different nature together. Using too many factors will make a real factor further dissociate into two or more non-existing sources. (Lee et al., 1999)

PMF uses a weighted least-squares fit with the known error estimates of the elements of the data matrix used to derive the weights. It produces quantitative non-negative solutions which can be written as:

$$X = GF + E \quad (2.5)$$

Where  $X$  is the known  $i \times j$  matrix of the  $j$  measured chemical species in  $i$  samples.  $G$  is an  $i \times h$  matrix of source contributions to the samples (time variations).  $F$  is a  $h \times j$  matrix of source compositions (source profiles). Both  $G$  and  $F$  are factor matrices to be determined.  $E$  is defined as a residual matrix, which is the difference between the measurement  $X$  and the model as a function of factors  $G$  and  $F$ .

The objective of PMF is to minimize the sum of the squares of the residuals weighted inversely with error estimates of the data points. Furthermore, PMF constrains all of the elements of  $G$  and  $F$  to be non-negative; meaning that sources cannot have negative species concentration and sample cannot have a negative source contribution. The task of PMF analysis can thus be described as to minimize  $Q(E)$ , where  $Q$  is the sum of squares of weighted residuals, often called “chi-square” (Paatero, 1997; Polissar et al., 1998).  $Q(E)$  is defined as the following equation:

$$Q(E) = \sum_{i=1}^m \sum_{j=1}^n (E_{ij} / \sigma_{ij})^2 \quad (2.5)$$

$\sigma_{ij}$  is the standard deviation of the observed values  $X_{ij}$ , which will be defined in the subsequent sections in detail.

$$Q(E) = \sum_{i=1}^n \sum_{j=1}^m \left( \frac{e_{ij}}{h_{ij} s_{ij}} \right)^2 \quad (2.7)$$

Where  $s_{ij}$  is an uncertainty estimate in the  $j$  th element measured in the  $i$  th sample and  $h_{ij}^2 = 1$  if  $|e_{ij}/s_{ij}| \leq \alpha$ ; otherwise  $h_{ij}^2 = |e_{ij}/s_{ij}|/\alpha$ . ( $e_{ij}/s_{ij}$ ) is defined as scaled residual.

To handle outlier values in the data, the robust mode can be selected by taking the value of outlier threshold distance,  $\alpha$ , as 2.0, 4.0, or 8.0.  $\alpha$  is a user selectable parameter that is analogous to cutting limits of the winsorized mean (Paatero, 1997).

If the standard deviations for the data array are theoretically known, then it is possible to judge the quality of fit based on the Q value. The value of Q should be approximately equal to the number of points in the data matrix minus the total number of elements in the factor matrices (Paatero, 2000). Since, in the presence of outliers the observation of the value of Q is difficult, it may be more helpful to investigate the distribution of scaled residuals,  $(e_{ij} / s_{ij})$  which should have a random pattern of positive and negative values between -2.0 and 2.0 (Paatero, 2000).

An important parameter resulting from the PMF analysis is the explained variation (EV) value, which is a measure of the contribution of each chemical species in each source.

$$EV_j = 1 - \frac{\sum_{i=1}^n E_{ij}^2 / \sigma_{ij}^2}{\sum_{i=1}^n X_{ij}^2 / \sigma_{ij}^2} \quad (2.8)$$

$EV_j$  is defined the quantity “total explained weighted variation” of compound j. EV is less than or equal to 1.  $E_{ij}$  is the matrix of random errors, the difference between the model and the measured data.

$$\sigma_{ij} = \sqrt{e_j^2 + (d_j X_{ij})^2} \quad (2.9)$$

where,  $e_j$  is the detection limit for compound j,  $X_{ij}$  is error estimates for low concentrations of compound j.  $d_j$  is proportional uncertainty of  $X_{ij}$  or the percent error of high concentrations of compound j.

PMF has been applied in different research efforts, to derive information about pollution sources influencing the data, for wet deposition at Finland (Anttila et al., 1995); for sources of aerosols at Atlanta (Kim et al., 2004), at Thailand ( Chueinta et

al., 2000), at Hong Kong (Qin et al., 2002; Lee et al., 1999); for sulfate and nitrate species at Georgia and Alabama (Liu et al., 2005) and for major ions at city of Coruna, Spain (Prendes et al., 1999).

In this study, for the calculation of Positive Matrix Factorization, the version of PMF2 that is developed by Paatero is used. The program is downloaded from the ftp address of University of Helsinki (<ftp://rock.helsinki.fi/pub/misc/pmf/>) and further the license is taken from the University of Helsinki.

### **2.3.3. Trajectory Statistics**

Application of atmospheric trajectory model is one of the most commonly used techniques for interpreting measurements and evaluating the transport of chemical constituents in the atmosphere by describing the paths of the air parcels followed in the atmosphere, before they are intercepted at the station.

There are several methods that have been developed to compute the trajectories. In most of the trajectory models, observed or analyzed winds are used to compute horizontal advection component. The vertical components of the trajectories are computed as the isobaric, in which trajectory is assumed to follow a constant pressure surface, isentropic, in which trajectory is assumed to follow a constant temperature potential, and kinematic, in which trajectory is assumed to move with the vertical velocity wind fields generated by diagnostic or prognostic model.

The isobaric trajectory modes were used extensively in the past. Currently, isentropic trajectory models are widely used in trajectory calculations. Isentropic models are advantageous due to not requiring vertical motion data (Fuelberg et al., 1996).

In this study two different trajectory statistics methods, flow climatology (FC) and potential source contribution function (PSCF), are used to compare the source regions affecting chemical compositions of depositions.

### **2.4.1. Flow climatology**

Flow climatology is the earliest statistical method for the identification of the sources of air pollutants. It is often used to understand air flow patterns and to determine the pollution input from distant sources to the area. Furthermore, the approach involves computing several years of trajectories ending at a selected receptor site and their classification according to their transport speed and direction.

In this study for flow climatology, each trajectory was separated into 1-hr long segments and coordinates of the end points of these segments. Number of segments in each of the 16 wind sectors, which gives the residence time of air masses in each wind sector, and which is a measure of the air mass transport frequency is computed for each station. The countries falling into the sectors associated with high pollutant concentrations at the receptor site are pronounced as the source regions of air pollutants.

### **2.4.2. Potential Source Contribution Function Analysis**

The Potential Source Contribution Function (PSCF) is a new receptor-oriented model which is able to incorporate the meteorological and geographic information into an analysis. PSCF identifies the source areas that have a potential to contribute to the high concentrations of contaminants observed at the receptor site. (Gao et al., 1994) The concept of PSCF has been developed by Ashbaugh et al., (1985) for performing the apportionment of secondary species, for combining air parcel back trajectories from a receptor site with chemical data at the site to infer possible source locations. Gao et al. (1993) has extended the PSCF analysis to provide an apportionment of secondary species along with emissions estimates.

The PSCF is an estimate of the conditional probability that a trajectory which passed through a given cell in the emissions grid ( $g$ ) contributed a concentration greater than some threshold  $ij$  value to ambient concentrations at the receptor site. Suppose  $N$  represents the total number of trajectory segment endpoints during the whole study period.  $P(A_{ij})$  represents the residence time of a randomly selected air parcel on the  $ij^{\text{th}}$  cell relative to time period  $T$ .  $n_{ij}$  endpoints fall into the  $ij^{\text{th}}$  cell.

$$P(A_{ij}) = \frac{n_{ij}}{N} \quad (2.10)$$

$P(B_{ij})$  refers to the residence time for these contaminated air parcels.  $m_{ij}$  is the endpoints that correspond to the trajectories that arrived at a receptor site with pollutant concentrations higher or lower than some pre-specified value.

$$P(B_{ij}) = \frac{m_{ij}}{N} \quad (2.11)$$

PSCF is the conditional probability that an air mass with specified pollutant concentrations arrives at a receptor site after having been observed to reside in a specific geographical cell. It is defined as a conditional probability:

$$PSCF = \frac{P(B_{ij})}{P(A_{ij})} = \frac{m_{ij}}{n_{ij}} \quad (2.12)$$

Cells related to the high values of potential source contribution function are the potential source areas. The grid size chosen for the potential source contribution function computations should be sufficiently large to assimilate the uncertainty of a trajectory endpoint. PSCF is calculated every one hour trajectory segment end point for each single grid cell of 1° longitude and 1° latitude terminates within that grid cell. In previous studies, 5° longitude and 5° latitude applied by Alagha, (2000) and Tunçer, (2000), whereas, single grid cell (1° longitude and 1° latitude) is applied by Doğan, (2005).

The value of PSCF ranges between 0 and 1. Any grid cell having PSCF of 0 is unlikely to be the source region, while the value of 1 is the source region. For large values of  $n_{ij}$ , the results are statistically stable. Therefore it is necessary to reduce the effect of small values of  $n_{ij}$  by developing a weight function.

The use of non-parametric bootstrap method shows the statistical significance of the spatial distribution of the PSCF values (Wehrens et al., 2000). The method assumes

that the concentration values are independent and identically distributed (Lupu and Maenhaut, 2002). Randomly picked trajectory is checked to determine if it is associated with a sample whose concentration for the species of interest is above the criterion level. In this case, both the contaminated and total point counters ( $m_{ij}$  and  $n_{ij}$ ) for the grid cells in which this trajectory's end point fall are incremented. The samples below the criterion level, only the total point counters ( $n_{ij}$ ) for the trajectory's grid cells are incremented (Hopke et al., 1995). Then the PSCF values calculated for each of the grid cells are sorted. The number of iterations is denoted as  $\beta$  and the significance level as  $\alpha$ .

$$P_{ij} \geq P_{((\beta+1)(1-\alpha/2))ij}^* \quad (2.13)$$

If the null hypothesis is rejected at  $(1-\alpha)100\%$  confidence level, then, for the further analysis only PSCF values satisfying the above relation are retained (Lupu and Maenhaut, 2002).

The uncertainties are related to unidentified sources, background sources, emissions estimates at the time of calculation, the differential loss of species (e.g., by deposition), and mixing of air parcels from different cells during transit from source to receptor (Polissar et al., 1999).

PSCF has been applied in numerous studies to examine the long range transport and location of sources of precipitation constituents at Eastern United States (Lucey et al., 2001), at Blacksea, Turkey (Alagha, O., 2000), at Ontario, Canada (Zeng and Hopke, 1989), at Eastern Mediterranean (Güllü et al., 1997), transport of pollutants to Arctic Basin (Hopke et al., 1995), sulfate and nitrate species at Rubidoux, California (Gao et al., 1994), atmospheric sulfate at Dorset, Ontario (Cheng et al., 1993) atmospheric pollution aerosols at Blacksea, Turkey (Doğan, 2005; Alagha, O., 2000), at Eastern Mediterranean (Güllü et al., 2001; Güllü et al., 1997; Güllü, G., 1996a).

## 2.5. Backtrajectory Analysis

Application of atmospheric trajectory model is one of the most commonly used techniques for interpreting measurements and evaluating the transport of chemical constituents in the atmosphere. The model can calculate transport pathways of air parcels forward in time from a source region or backward in time from a receptor. Trajectories ending at low altitude are generally sufficient to have a good description of the origins of the air masses influencing the composition of rain water (Deboudt et al., 2004; Beverland et al., 1998; Colin et al., 1990).

In this study, a publicly available model (TL511L60) on the CRAY C90/UNICOS computer at the European Center for Medium Range Weather Forecast Center (ECMWF, Reading, UK) were used to obtain three dimensional (3-D), five and a half day back-trajectories arriving at the receptor site at four barometric levels (900, 850, 700 and 500 hPa). The TL511L60, general circulation model of ECMWF, consists of a dynamical component and a coupled ocean wave component. The model calculates the position of the air mass at every 15 minutes. The atmosphere is separated into 60 layers up to 0.1 hPa (about 64 km). The model uses a regular latitude-longitude grid system with a resolution of 1.5\*1.5 degrees to produce data at every 6 hours (00, 06, 12 and 18 UTC) per day.

Back-trajectory analysis has been applied in numerous studies to examine the long range transport and location of sources of precipitation constituents at Black sea, Turkey (Güllü et al., 2001; Alagha, O., 2000), at Eastern Mediterranean (Güllü et al., 2003; Güllü et al., 2001; Al-Momani et al., 1999; Al-Momani et al., 1997), atmospheric pollution aerosols at Black sea, Turkey (Alagha, O., 2000; Güllü et al., 1998), at Eastern Mediterranean (Güllü et al., 2003; Güllü et al., 2001; Al-Momani et al., 1999; Al-Momani et al., 1997; Güllü, G., 1996a; Kubilay and Saydam, 1995). The trajectories ending at 850 hPa, have been a good approximation to the mean transport since this pressure level frequently lies near the centre of the transport layer have been applied for wet precipitation samples at Spain (Avila and Alarcon, 1999), at Japan (Seto et al., 2000) at Western Europe (Deboudt et al., 2004).

## **2.4. Geography and Climatology of Mediterranean Region**

The Mediterranean can be regarded as a transitional zone between the continental influences of Europe and Asia, the desert climate of North Africa and the oceanic effects from the Atlantic (Maheras et al., 1999). The Mediterranean Sea lies between 30° N and 46°N and between 5.5° W and 36° E. Its east-west extent is approximately 4000 km and its average north-south extent is about 800 km. The sea is enclosed by mountains except along the North African Coast east of Tunisia. Although the whole coastline is very irregular, it is mainly divided into two major geographical areas: (1) the western basin which is from Gibraltar to Italy, (2) the eastern basin which is from Italy to Syrian coast. (UNEP/WMO, 1989)

The topography behind the coastline of the Mediterranean is complex and provides barriers and channels for air flow that brings extremely different air masses to the region. Strong winds, which are tunneled through gaps in the mountain ranges that surround the Mediterranean Basin, are among the best known meteorological features of the region: (1) the north-westerly mistral through the Alp-Pyrenees gap; (2) the northeasterly bora through the Trieste gap; (3) the easterly lavender and the westerly vendaval through the Strait of Gibraltar; and (4) the warm southwesterly sirocco, ghibli, or khamsin from Africa. (UNEP/ WMO, 1989) The surface pressure field is influenced by the oceanic Azores High, the Siberian winter anticyclone, the northwestern extension of the South Asian summer thermal low, as well as more transient anticyclones and traveling depressions (Maheras et al., 1999).

Eastern Mediterranean atmosphere is under the influence of three general source types: (1) anthropogenic sources, which are located to the north and northwest of the basin; (2) a strong crustal source located in North Africa; and (3) a marine source, which is the Mediterranean Sea itself. (Güllü et al., 2003; Güllü et al., 1998; Güllü, 1996a; Al-Momani, 1995c) For the years 1992 and 1993 and long term monthly average temperature and total precipitation amount for the Antalya station are given in Table 1.1.

Table 1.1. Monthly average temperature and total precipitation amounts observed during the years 1992 and 1993 and long term averages for the Antalya Meteorological Station. (Güllü, G., 1996a)

	1992		1993		Long term average	
	Temp. ( C )	Tot. Prec. (mm)	Temp. ( C )	Tot. Prec. (mm)	Temp. ( C )	Tot. Prec. (mm)
<b>January</b>	8.29	-	7.6	264.7	9.8	255.8
<b>February</b>	7.06	81.5	8.5	116	10.2	164.56
<b>March</b>	10.96	182.1	10.9	129.3	12.6	89.35
<b>April</b>	15.19	34	15	29.6	15.9	43.72
<b>May</b>	19.13	19.6	18.3	120.5	19.7	29.79
<b>June</b>	24	3	24.9	20	24.4	6.65
<b>July</b>	27.06	1	28.3	-	28.1	3.97
<b>August</b>	28.22	0.1	28.1	-	27.9	4.27
<b>September</b>	24.24	2.2	23.7	-	24.7	13.77
<b>October</b>	20.77	0.6	21.2	74.8	19.7	62.22
<b>November</b>	13.9	194.4	12.9	100.9	15.3	111.47
<b>December</b>	8.1	176	11.6	80	11.8	269.76

In Eastern Mediterranean region, the most frequent air mass transport to the Mediterranean basin is from the north and northwest (Güllü et al., 2003; Güllü et al., 1998; Kubilay and Saydam, 1995) and surface winds blow for only 2% of the time from the direction of the city, indicating that transport of pollutants from the city is not significant. (Güllü et al., 2003; Güllü et al., 1998) Approximately 80% of the precipitation falls during winter season. (Güllü et al., 2003; Al-Momani et al., 1998; Güllü et al., 1998)

## **CHAPTER 3**

### **MATERIALS AND METHODS**

#### **3.1. Sampling Site**

Wet deposition samples was collected from Antalya Station that is established in the Mediterranean coast of Turkey approximately 20 km's from the town of Antalya (31.0 longitude east of Greenwich and 36.8 latitude north of Equator).

Site selection was performed in 1991 using available selection criteria for regional monitoring networks, such as EMEP, GAW, and MPAP etc. Criteria used in different networks are not substantially different from each other. They all include precautions for the proposed station not to be close to point, area and line sources. In addition to universal criteria to be a regionally representative sampling point, the sampling site should also satisfy the following three requirements; (1) Station must be located at a site where power is available; (2) Station must be located on a government property in order to prevent potential vandalism from occurring and (3) there must be capable people to change samples.

The station was provided by the given requirements that it was under protection throughout the year and power was available. The station was established 20 km away from the city of Antalya and no point sources were affecting the site.

The station contains 2 components, namely the platform and the field laboratory. The Platform, which is built approximately 20 m above the sea level on a rock structure, consists of 4m x 4m concrete base that is surrounded by 2 m high fence. The wiring of the fence was covered by polyethylene to avoid contamination of collected samples by metal particles that can result from the corrosion of the metal.

The equipments on the platform include wet only precipitation sampler, a wet and dry deposition sampler, a Hi-Vol sampler and a Hi-Vol impactor. The field laboratory is a container with dimensions of 3m x 2m x 2m. The field laboratory includes a storage area, a refrigerator to store samples until they are shipped to Ankara, housing for the spare parts of the sampling equipment and a sample change area. The power is supplied from the field laboratory to the required equipments on the platform and field laboratory.

The sampling station has been operating since December 1991 without any long term interruption. In this study, wet deposition samples collected between December 1991 and August 1999. A total of 387 wet-only samples were collected and analyzed during this period. Samples collected for the years 1996 and 1997 for metal analysis were first filtered for insoluble part and the soluble part were freeze-dried and stored for the analysis. These freeze dried samples and filters containing insoluble fractions of the samples (those collected in 1996 and 1997) were analyzed for elements in 2004 – 2005 using inductively coupled plasma emission spectrometry at the Central Laboratory of the METU. During the calculations of the daily concentrations of metals that analyzed by Central Laboratory of METU, both soluble and insoluble parts are added to each other. The remaining parts of the data were previously analyzed for ions and trace elements by the analysis techniques that will be discussed in the subsequent sections in detail.

## **3.2. Sampling Procedures**

### **3.2.1. Preparation of Sampling Bottles**

Polyethylene bottles that are used to collect wet deposition samples for the metal and major ions analysis were soaked in 30% HNO<sub>3</sub> for about 24 hours and are washed several times with deionized water. During the whole procedure of cleaning of sampling equipments, extraction and analysis, deionized water which is first double distilled and then deionized using Bernstead Nanopure 550 deionization system, was used. 10 mL 10% suprapure HNO<sub>3</sub> was added to each bottle before they were sent to the station. Bottles used for ion analysis is sent without adding any acid. All bottles

were dried in the clean area and heat sealed in a polyethylene bags before they were shipped to the field.

### **3.2.2. Collection of Wet Deposition Samples**

On the platform two rain samplers were installed that one of them was used for the analysis of major ions and trace metals and the other was used for the analysis of  $\text{Cl}^-$ ,  $\text{NO}_3^-$ ,  $\text{SO}_4^{2-}$  and  $\text{NH}_4^+$ . Both of the rain samplers contain rain sensor which provides opening of the lid when rain start and closing tightly when rain stops.

The sampler used for metal analysis which is manufactured by the Karble Co. contains a 27 cm diameter of polyethylene funnel that is exposed to rain with an activated rain-sensor. Rain water is collected by the funnel that is passed through the all polyethylene gravity filtration unit and filtered through 0.45  $\mu\text{m}$  pore size cellulose acetate membrane filter. This filtration unit is installed into standard equipment to separate insoluble part of the rain water. The filtration of rain water is achieved before rain water enters the bottles with a capacity of 500 mL and was acidified by adding 10 mL of 10% sub-boiled  $\text{HNO}_3$  solution to prevent insoluble part from decomposing. Since in rain water the trace metal concentrations are very low, all the reagents used during the experimental part should have the highest purity. In order to purify the commercial suprapure  $\text{HNO}_3$  grade (MERCK), the sub-boiling system in the laboratory is used. Before, loading the collection bottle to the cap and the membrane filter over the filter holder, the collection funnel and filtration unit were rinsed by 100 mL double distilled deionized water. For each sampling, the polyethylene tubing is replaced with the new precleaned ones.

The second sampler used for ion analysis is a standard Andersen “acid precipitation sampler”. The sampler contains two 30 cm diameter of buckets having an activated rain sensor that closes the bucket when the rain stops and opens when the rain starts and collects wet and dry deposition samples. For ion analysis, the same procedure is applied for the collection except the bottles does not contain acid.

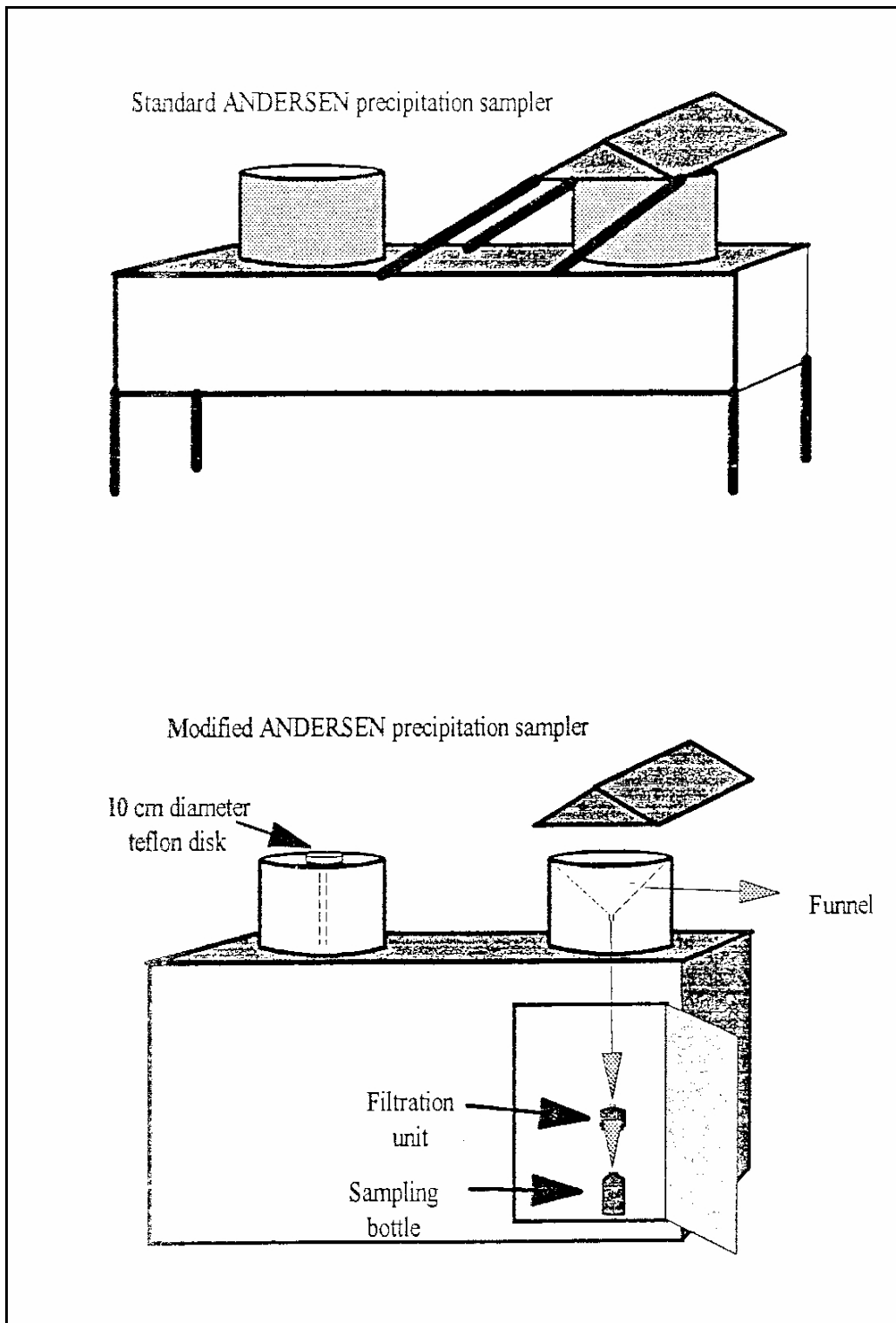


Figure 3.1. Standard and modified Andersen precipitation sampler (Al-Momani, 1995c).

Al-Momani (1995c) has conducted some modifications to standard Andersen “acid rain sampler” to reduce the blank characteristics and improve the chemical integrity of the collected sample. A funnel is placed in the rain bucket and it is connected to a polyethylene filtration unit which has a reservoir capacity of 250 mL. Further, the filtration unit is connected to a 250 mL capacity of high density polyethylene bottle. The schematic diagram of the modified sampler is given in Figure 3.1. Modified sampler provides; direct sampling to bottles, eliminates the possibility of composition change due to storage since filtration take place before sample collection and metal analysis can be made precisely since sampler equipments are made of polyethylene.

### **3.3. Sample Handling**

#### **3.3.1. Determination of Volume and pH**

At the laboratory, the sampling bottles were opened and its volume and pH are measured. To measure the volume, calibrated sampling bottles are used from volume of water at 25 °C. The volume of the samples is determined by comparing the height of the rain water with the calibrated bottle. The pH is measured using a Radiometer PHM 80 portable pH meter equipped with a combination glass electrode. pH meter is calibrated before measurements using standard buffer solutions at pH 4.00 and 7.00.

#### **3.3.2. Preparation of samples for Ion Chromatography and AAS Analysis**

Since major ions are water soluble, they can be analyzed without significant sample preparation. However, fine particulate matter can clog the IC column and they should be removed by filtration before analysis. The 0.45 µm pore size filtered rain water samples are further filtered through 0.2 µm pore size of filter in the laboratory. The filtration through 0.2 µm pore size cellulose acetate or cellulose nitrate filters were resumed in the first two years of sampling. Later, such filtration proved to be very slow for the analysis of large number of samples and a guard column, filled with the same packing material with the analytical column, but which is only 1 cm long was placed in front of the analytical column to avoid clogging of the analytical column. Guard column was repacked at certain intervals.

The filtered samples for the AAS (Atomic Absorption Spectrometry) are stabilized by 0.5% HNO<sub>3</sub> solution. The blank samples are treated in the same way. The soluble portion of the filtered rain water is preserved for long times by freeze-drying technique in the laboratory.

Soluble fractions of the metals which were acidified in the field laboratory were directly analyzed by flame Atomic Absorption Spectrometry (FAAS) and Graphite Furnace Atomic Absorption Spectrometry (GFAAS).

The insoluble part of the rain water samples were extracted through the digestion of filters. In digestion procedure, each filter was put into Teflon bottles and 6 mL of suprapure HNO<sub>3</sub> and 1 mL of HF were added then the Teflon bottles' taps were closed and were put into ETHOS 900 Microwave Labstation. Program 9, were used to extract the samples and continued for 30 minutes, contains 4 steps such that step 1 continues for 6 minutes at 250W, step 2 continues for 6 min at 400W, step 3 continues for 6 minutes at 650W and step 4 continues for 6 minutes at 250W. After 6 minutes of cooling time, the samples are taken and waited into steady state cooling container for 30 minutes to cool down the samples. The samples in teflon bottles were taken out from the digester and were put into hot plate for 1.5 hours at 75-80 °C to volatile the remaining HF in the samples. HF should be carefully removed from the samples to reduce the damaging effects occur in glass lens of ICP-OES during the analysis. After HF was removed from the samples, the remaining samples were completed into 50 ml with deionized water and stored for the ICP-OES analysis.

Standard reference materials are digested with the same procedure used for insoluble part except for program used. Program 7 is used for where the first step continues for 5 minutes at 600W, second step continues for 5 minutes at 400W, third step continues for 5 minutes for 600W and last step continues for 3 minutes at 350W. 0.1 gram of SRM is mixed with 6 ml HNO<sub>3</sub> and 1 ml of HF and the same procedure is applied for the digestion procedure.

### 3.4. Analysis of Samples

Analytical techniques and devices used in the determination of rain water composition are given in Table 2.1. The measurement procedures for the corresponding species are explained in the subsequent sections briefly. Only the measurements by ICP-OES, was conducted in the year 2005 for metal analysis for the samples of 1996 and 1997 and the remaining part was conducted during the year the samples have been collected.

Table 3.1. Analytical techniques and devices used in the determination of rain water composition

Measured species	Analysis techniques
SO <sub>4</sub> <sup>2-</sup> , NO <sub>3</sub> <sup>-</sup> , Cl <sup>-</sup>	HPLC (2010) coupled with Vydac column with Jasco 875 UV-VIS detector
Mg, Fe, Al and Zn	FAAS (Perkin Elmer 1100B spectrophotometer)
Ca, Na, K	FAES (Perkin Elmer 1100B spectrophotometer)
Cu, Zn, Cd, Ni, Pb, Cr and Al	GFAAS (Perkin Elmer 1100B spectrophotometer coupled with HGA700)
Ca, Na, K, Mg, Al, Cd, Cu, Fe, Cr, Ni, Pb and Zn	ICP-OES (Inductively Coupled Plasma Optical Emission Spectrometry)
NH <sub>4</sub> <sup>+</sup>	Colorimetric (Nessler's method)
pH	Radiometer PHM 80 portable pH meter

#### 3.4.1. Determination of Anions by Ion Chromatography

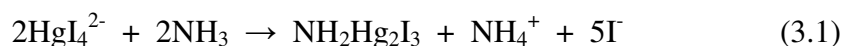
Rain water samples were analyzed for ions Cl<sup>-</sup>, NO<sub>3</sub><sup>-</sup> and SO<sub>4</sub><sup>2-</sup> by using a Varian Model 2010 HPLC coupled with a VYDAC 302 IC anion exchange column. The system is connected to a computer with software that can calculate the peak areas. Detector was JASCO model 875 UV-VIS detector with a 100 µL volume flow cell. The sample is filtered through 0.2 µm pore size filter and 100 µL portion of the filtrate were directly injected to the IC.

Mobile phase used was 1 mM of phthalic acid adjusted to pH 4.94 by sodium borate.

In order to not to damage the column, the mobile phase was degassed in an ultrasonic shaker for 15 minutes. Calibration curves for  $\text{Cl}^-$ ,  $\text{NO}_3^-$  and  $\text{SO}_4^{2-}$  were prepared by injecting series of standard solution for these ions prepared from  $\text{NaCl}$ ,  $\text{NaNO}_3$  and  $\text{K}_2\text{SO}_4$  respectively.

### 3.4.2. Determination of $\text{NH}_4^+$ by Spectrophotometer

Ammonium was determined spectrophotometrically by Unicam 8625 UV-VIS spectrometer. The Nessler's reagent which is an alkaline solution of mercuric iodide ( $\text{K}_2\text{HgI}_4$ ) is combined with  $\text{NH}_3$  to form a yellow to brown color according to the following reaction;



The absorbance of the colored solution was measured at 425 nm in a glass cell with an optical path length of 1 cm. Standard ammonium solutions were prepared by using ammonium sulfate after drying it at  $100^\circ\text{C}$  for about 1 hour. For each time that Nessler's reagent was changed, a new calibration curve was prepared.

### 3.4.3. Determination of Trace Elements by AAS

#### 3.4.3.1. Flame Atomic Absorption Spectroscopy

Trace elements and major ions are determined Na and K are with flame photometry (Jenway PFP7); Fe, Al, Mg, Zn are determined through Flame Atomic Absorption Spectrometry (FAAS); Ca, Na and K with Flame Atomic Emission Spectrometry (FAES) by Perkin Elmer Model 1100B Atomic Absorption Spectrometer. All elements are analyzed by using Air- $\text{C}_2\text{H}_2$  flame except for Al that  $\text{N}_2\text{O}-\text{C}_2\text{H}_2$  is used. Except for Al and Fe, concentrations of the most trace elements were too low to be detected in the flame mode in both soluble and insoluble fractions of the collected rain water samples. Al and Fe are analyzed by FAAS for only insoluble fraction and insoluble fractions are determined by GFAAS. Zn was the only elements analyzed by FAAS in both soluble and insoluble fractions. Working instrumental settings are summarized for each element of FAAS and FAES analysis in Table 2.2.

Before starting the analysis, the instrument was warmed up for about 20 minutes. In FAAS analysis, light from a hollow cathode lamp is adjusted to enter into the flame by overlapping the lights of both hollow cathode lamp and deuterium lamp. In order to read the highest absorbance, both the flame and lamp positions are carefully adjusted and multi-element solution is used. In FAES analysis only flame is used and absorbance is adjusted by using multi element solution. Analysis was done by direct aspiration of sample to the flame. The nebulizer uptake rate was in the range of 7-8 mL/min. The standards used for the calibration were analytical grade from Aldrich for Ca and Na and Fluka Chemica for the other elements. To prepare the calibration curves, linear method was used.

Table 3.2. Parameters used in FAAS and FAES analysis.

Element	Na	K	Ca	Mg	Fe	Zn	Al
<b>Technique</b>	A	A	A	B	B	B	C
<b>Wavelength, nm</b>	589.1	766.1	422.7	285.2	248.2	213.9	309.2
<b>Slit width, nm</b>	0.2	0.7	0.7	0.7	0.2	0.7	0.7
<b>Air, mL/min</b>	8.7	8.5	7.7	8.0	9.8	10.1	-
<b>Acetylene, mL/min</b>	1.4	1.6	2.1	2.0	2.2	2.2	7.0
<b>N.Oxide, mL/min</b>	-	-	-	-	-	-	5.0

A: FAES (Air-C<sub>2</sub>H<sub>2</sub>), B: FAAS (Air-C<sub>2</sub>H<sub>2</sub>), C: FAAS (N<sub>2</sub>O- C<sub>2</sub>H<sub>2</sub>)

### 3.4.3.2. Graphite Furnace Atomic Absorption Spectroscopy

Trace elements that concentrations are lower to detect with flame AAS are detected by using graphite furnace AAS. Concentrations of Cu, Zn, Cd, V, Ni, Pb, Cr, Al, Sb and Se in the soluble and Zn, Cu, Cd, Pb, Ni and Cr in the insoluble fractions of rain water samples are determined by graphite furnace atomic absorption spectrometry, using a Perkin Elmer 1100B spectrometer coupled to a Perkin Elmer HGA 700 electrothermal atomization system. In conjunction with hollow cathode lamps for each element, deuterium lamp was used to correct for nonspecific background absorption. As a purge gas Argon was used with a flow of 300 mL/min in all steps except for the atomization step, during which gas flow interrupted. Instrumental settings used for each element are listed in Table 2.3.

Table 3.3. Parameters used in GFAAS analysis.

	<b>Cd</b>	<b>Cu</b>	<b>Pb</b>	<b>Ni</b>	<b>Cr</b>	<b>Al</b>
<b>Tube</b>	U	P	U	P	P	P
<b>Wavelength, nm</b>	228.7	324.8	283.3	232	357.8	309.2
<b>Slit width, nm</b>	0.7	0.7	0.7	0.2	0.7	0.7
<b>Sample volume, <math>\mu</math>L</b>	50	20	20	20	20	10
<b>Lamp current, mA</b>	3	10	7	30		15

U: Uncoated tube, P: Pyrocoated

#### 3.4.4. Determination of Trace Elements by ICP-OES

The non analyzed portion of the rain water data set were measured by Inductively Coupled Plasma Optical Emission Spectrometry (ICP-OES). The ions Ca, Na, K, Mg and elements Al, Cd, Cr, Cu, Fe, Ni, Pb and Zn were detected by two solid state detector of Perkin Elmer Optima 4300 DV Model. Plasma, which is formed by the in reaction of RF (Radio-frequency) power and ionized argon gas, is the complete atomization unit with high temperatures of 5500-8000 °K. Automatic dual view plasma provides both lowest detection limit by axial view and high working range by radial view with high accuracy and speed. The samples were introduced by the 1.5 ml/min velocity. The standart material of Merck 4 ICP Multi Element Solution was used for the all ions and elements except for the V element Inorganic Ventures 1000 ppm stock solution were used. The wave lengths of all ions and elements were presented in the Table 3.4.

Table 3.4. The wavelengths of ions and elements were analysed by ICP-OES

<b>Elements &amp; ions</b>	<b>Ca</b>	<b>Na</b>	<b>K</b>	<b>Mg</b>	<b>Al</b>	<b>Cd</b>
<b>Wavelength, nm</b>	315.887	588.995	766.490	279.077	396.153	228.802
<b>Elements &amp; ions</b>	<b>Cr</b>	<b>Cu</b>	<b>Fe</b>	<b>Ni</b>	<b>Pb</b>	<b>Zn</b>
<b>Wavelength, nm</b>	267.716	327.393	238.204	231.604	220.353	206.200

The accuracy of analytical measurements in FAAS, FAES, GFAAS and ICP-OES were checked by routine analysis of National Institute of Standards (NIST) standard reference materials GSP-1 and GSP-2 (US Geological Survey Silver Plume Granodiorite), SRM 1646 (Estuarine Sediment), STM-1 (Syenite), 1633-b (trace

element in coal fly ash), IAEA-336 (International Atomic Energy Agency trace elements in lichen), PCC-1 (U.S. Geological Survey analysed Peridotite).

### **3.5. Data Quality Assurance (QA)**

#### **3.5.1. Field and Laboratory Blanks**

Contamination of precipitation samples by ions and metals has a strong possibility since their concentrations are very low in precipitation. Therefore, in precipitation samples blank measurements plays an important role.

Field blanks have the same procedure of sampling, sample handling and analysis with procedures used for precipitation samples. Field blanks contain the filter and filtrate fractions referring insoluble and soluble part respectively. For the metal analysis, the sides of the funnel were rinsed by 200 mL double distilled deionized water. After passing through the filtration unit which is equipped with 0.45  $\mu\text{m}$  pore size filter paper, the water was collected in the polyethylene bottle. From field blanks, the detection limits were calculated. The procedure is given in the following sections.

Laboratory blanks estimate the contribution of each reagent and laboratory process to contamination. For the preparation of laboratory blanks, the same procedure were applied for the soluble and insoluble portion except the sample was added.

The ratio between average concentrations in samples to average concentrations of blanks of elements and cations are represented in Table 3.5. The values below 15% blank correction means that most of the measured species could be determined reliably by the used sampling procedure and contribution of field blank values on the uncertainties are negligible.

Table 3.5 Sample to blank ratios of elements

	Sample (ppm)	Field Blank (ppm)	Sample/ Blank	% Blank
<b>Mg</b>	0.3512	0.0123	28.57	3.50
<b>Ca</b>	0.5937	0.0472	12.59	7.94
<b>K</b>	0.2757	0.0145	19.07	5.24
<b>Na</b>	2.6476	0.0131	202.36	0.49
<b>Cu</b>	0.0061	0.0003	24.40	4.10
<b>Al</b>	0.8930	0.0319	27.98	3.57
<b>Ni</b>	5.5369	0.0000		
<b>Fe</b>	0.6310	0.0322	19.62	5.10

### 3.5.2. Calculation of Detection Limits

The detection limits for rain water constituents are calculated from 10 replicates of the field blank samples. It is accepted that below this value data has significant limitations. Furthermore, limit of quantification is calculated, which is about 10 folds greater than detection limits. The data points below this value imply questionable results.

The detection limit ( $L_d$ ) for soluble and insoluble part is taken to be three times the standard deviation of the blank results. The detection limit is calculated by the following equation:

$$L_d = 3.0 \times S_b \quad (3.2)$$

The Standard deviation is defined as:

$$S_b = \left( \left( \frac{1}{N-1} \right) \sum_{i=1}^N (C_i - \bar{C})^2 \right)^{1/2} \quad (3.3)$$

Where N is the number of field blanks,  $C_i$  is the concentration of the relevant substance in the  $i$  th field and  $\bar{C}$  is the field blank average after elimination of “extreme” blank values. Too high values are eliminated due to the contamination of the blank samples.

The detection limits of elements and ions for ICP-OES, FAAS, GFAAS, HPLC and average sample concentrations are introduced in Table 3.6. The detection limit shows small changes between ICP-OES and AAS. FAAS has higher detection limit than ICP-OES. Conversely, GFAAS has slightly lower detection limits than ICP-OES except for Zn. In all cases, the samples have significantly higher concentrations compared to all analysis techniques. Therefore, with the suggested methods, the corresponding ions and elements could be detected accurately.

Table 3.6 Detection limits of elements and ions (ppm)

	<b>ICP-OES (ppm)</b>	<b>FAAS (ppm)</b>	<b>GFAAS (ppm)</b>	<b>HPLC (ppm)</b>	<b>Sample concentration (ppm)</b>
<b>SO<sub>4</sub><sup>2-</sup></b>				0.06	6.105
<b>NO<sub>3</sub><sup>-</sup></b>				0.05	3.442
<b>Cl<sup>-</sup></b>				0.05	21.537
<b>Na</b>	0.009	0.11			2.648
<b>Mg</b>	0.010	0.08			0.351
<b>K</b>	0.003	0.03			0.276
<b>Ca</b>	0.012	0.12			0.594
<b>Cr</b>	0.003		0.0007		12.204
<b>Fe</b>	0.006	0.2			0.631
<b>Ni</b>	0.004		0.0043		5.537
<b>Cu</b>	0.001		0.0007		0.006
<b>Zn</b>	0.004		0.02		0.013
<b>Cd</b>	0.002		0.00006		5.277
<b>Al</b>	0.012		0.0001		0.893
<b>Pb</b>	0.016		0.0008		0.004

### 3.5.3. Analysis of Standard Reference Materials

The accuracy of AAS analysis is routinely checked by the analysis of standard reference materials. NIST standard reference materials of GSP1, GSP2, SRM 1646, 1633-b, IAEA-336, PCC-1 were reanalyzed with the samples before starting the analysis and after each 10 samples were analyzed. The found values and certified values were compared and the difference of two values should be less than 10%. As soon as the difference is greater than the pre-specified value, the calibration of the device was made again and the calculations were done considering the new calibration curve.

## CHAPTER 4

### RESULTS AND DISCUSSIONS

#### 4.1. General Characteristics of the Data

A brief summary of statistics of the 387 of daily rain water samples of major ions, trace elements and pH those are collected in Eastern Mediterranean Sea coast of Turkey, during the time period between November 1991 and August 1999, is presented in Table 4.1. Concentrations of 17 species ( $H^+$ ,  $SO_4^{2-}$ ,  $NO_3^-$ ,  $NH_4^+$ ,  $Cl^-$ ,  $Mg^{2+}$ ,  $Ca^{2+}$ ,  $K^+$ ,  $Na^+$ ,  $Cd$ ,  $Cu$ ,  $Pb$ ,  $Al$ ,  $Ni$ ,  $Cr$ ,  $Zn$  and  $Fe$ ) were determined and their volume weighted arithmetic average, arithmetic mean, associated standard deviation, geometric mean, median, minimum and maximum values are reported in the table.

Since concentrations of elements and ions in rain water depend on the rainfall, through dilution and processes such as limb scavenging (Tuncel and Ungör, 1996; Al-Momani et al., 1995b; Seto et al., 1992) volume weighted arithmetic average is frequently used to avoid the influence of precipitation amounts on concentrations of elements (Alagha and Tuncel, 2003; Seto, et al., 2000; Al-Momani et al., 1998; Kaya and Tuncel, 1997; Saxena et al., 1996; Baez et al., 1996).

Volume weighted arithmetic average is described by the following equation:

$$C_p = \frac{1}{\sum_x p_x} * \sum_x (C_x * p_x) \quad (4.1)$$

Where  $C_p$  is the volume weighted concentration,  $p_x$  is the precipitation amount of day  $x$  and  $C_x$  is the concentration of an element or ion in that particular day.

In atmospheric data, high standard deviations do not imply poor analysis or sampling. High scatter in the data are expected due to dependence of concentrations on meteorology and transport both of which are highly variable. In addition to

variations in meteorological conditions, physical and chemical transformations in the atmosphere, changes in the air mass transport patterns and the variations in the source strengths can also be reasons of the variations in atmospheric data. (Alagha, 2000; Kaya and Tuncel 1997; Al-Momani, 1995c) Due to the large variations in the concentrations of species, atmospheric data tend to be log-normally distributed, which can be better described by geometric mean or median. (Güllü et al., 1998)

In the data set, the highest concentrations were observed for the species predominantly originate from anthropogenic ( $\text{SO}_4^{2-}$ ,  $\text{NO}_3^-$ ), crustal ( $\text{Ca}^{2+}$ , Al, Fe) and marine sources ( $\text{Na}^+$ , Cl<sup>-</sup>). These are typically observed in most precipitation studies (Avila and Alarcon, 2003; Charron et al., 2000; Güllü et al., 1998a; Al-Momani et al. 1995a; Kubilay and Saydam, 1995).

#### **4.1.1. Distribution Characteristics of the Data**

The distribution of the data is described by the measures of ratio arithmetic mean to geometric mean, skewness, Kolmogrov Smirnov test, alpha value and p value, which are presented in Table 4.2. The type of distribution is initially described by the ratio arithmetic mean to geometric mean and skewness coefficients.

Skewness is a value to measure the symmetry or shape of the data. In a frequency histogram, polygon and density trace, the right end of the plot has a longer tail, the distribution extends toward larger values and the mean is greater than the median, the data is called as right skewed (positively skewed). If the data has a longer tail on the left end of the plot and the median is greater than the mean, the data is called as left skewed (negatively skewed). In environmental research right skewed data is more common. The ratio of arithmetic mean to geometric mean is also a measure of skewness. As the ratio deviates from the unity, the distribution type approaches to log-normal distribution.

Both the ratio of arithmetic to geometric mean and skewness is an indicator of the symmetry of the data. To determine the distribution type of the data further statistic tests should be applied. The Kolmogrov Simirnov (K-S-DN) statistics is used to test the “goodness of the fit” of the data to log-normal distribution. Statgraphics Statistics

Software was used for the statistical analysis. Assuming that log-normal distribution is valid, Statgraphics performs Chi-Square test by dividing the range of variable into non-overlapping intervals and compares the number of observations in each class to the number of expected based on the fitted distribution. Kolmogrov Simirnov test computes the maximum distance between the cumulative distribution of the variable and the cumulative distribution of the fitted log-normal distribution. The computed maximum distance is referred to as Kolmogrov-Simirnov (K-S-DN) statistic.

The observed significance level for the Kolmogrov – Simirnov DN statistics is represented by a value of “alpha”. As a disproof of the null hypothesis that distribution is log-normal, alpha value can be approximately computed from the below given equation:

$$Alpha = \left( 0,12 + \sqrt{N} + \frac{0.11}{\sqrt{N}} \right) * DN \quad (4.2)$$

High number of samples (N) increases the reliability of the assessment by supplying adequate degrees of freedom. Therefore, K-S DN statistics can be used and alpha-value less than 1.358 indicates that one can reject the idea that the variable comes from a log-normal distribution with 95% confidence level. Furthermore, p-value of performed test can also be used as a quantitative proof for the assumed distribution. If the P-value of the Kolmogrov- Simirnov is greater than 0.1, we can accept the idea that variable comes from a log-normal distribution with 90% or higher confidence level. Geometric mean and median values are close and significantly higher than arithmetic mean for the elements having log-normal distribution. Therefore, reporting arithmetic averages is not a proper way of representing the log-normally distributed data.

Frequency histograms are prepared and Kolmogrov-Simirnov test was applied for all the elements measured in this study. The frequency histograms and associated distribution curves  $SO_4^{2-}$ ,  $Na^+$ , Al and Pb are given in Figure 4.1. All of the elements shown in the figure have right-skewed distributions. However, Kolmogrov-Simirnov test indicated that distributions of elements  $H^+$ , Cu, Pb, Al, Ni, Zn and Fe are log normal with 95% confidence.

Table 4.1 Summary Statistics of Measured Species

Units	Number of samples(N)	Volume Weighted		Arithmetic		Standard Deviation	Geometric		Median	Minimum		Maximum Value
		Arithmetic Mean	Mean	Mean	Mean		Value	Value				
pH unit	302	5.29	5.299	5.23	0.816	5.29	2.96	6.93				
H <sup>+</sup> mgL <sup>-1</sup>	302	0.024	0.027	0.005	0.086	0.0051	0.00012	1.096				
SO <sub>4</sub> <sup>2-</sup> mgL <sup>-1</sup>	336	6.2	6.105	3.43	10.36	3.22	0.3	96.38				
NO <sub>3</sub> <sup>-</sup> mgL <sup>-1</sup>	297	2.74	3.44	1.47	7.77	1.54	0.01	86.38				
NH <sub>4</sub> <sup>+</sup> mgL <sup>-1</sup>	223	0.94	1.41	0.66	1.97	0.78	0.0057	14.35				
Cl <sup>-</sup> mgL <sup>-1</sup>	341	21.95	21.54	7.99	52.06	7.29	0.08	664.0				
Mg <sup>2+</sup> mgL <sup>-1</sup>	218	1.27	1.23	0.597	2.11	0.54	0.01	20.4635				
Ca <sup>2+</sup> mgL <sup>-1</sup>	217	4.46	3.91	2.08	7.25	2.16	0.098	65.9				
K <sup>+</sup> mgL <sup>-1</sup>	217	1.23	0.92	0.39	1.98	0.34	0.025	15.83				
Na <sup>+</sup> mgL <sup>-1</sup>	218	10.16	8.50	3.35	22.91	2.81	0.067	272.8				
Cd µgL <sup>-1</sup>	87	0.75	0.71	0.36	0.86	0.29	0.040	3.30				
Cu µgL <sup>-1</sup>	139	4.97	5.24	3.28	7.54	3.14	0.65	58.74				
Pb µgL <sup>-1</sup>	130	8.17	9.51	5.31	12.06	5.51	0.125	67.57				
Al µgL <sup>-1</sup>	164	762.04	679.60	264.44	1327.86	242.57	8.67	11004.6				
Ni µgL <sup>-1</sup>	120	21.12	22.16	13.38	24.78	12.84	1.31	165.05				
Cr µgL <sup>-1</sup>	114	8.28	9.18	5.39	10.40	5.34	0.42	66.03				
Zn µgL <sup>-1</sup>	125	46.62	83.56	18.38	381.16	18.75	0.63	3397.02				
Fe µgL <sup>-1</sup>	121	645.17	574.33	241.93	919.92	245.63	2.33	6384.87				

Table 4.2 Parameters indicating distribution characteristics of the variables.

	Arithmetic mean/ Geometric mean	Skewness	K-S-DN	Alpha value	p-value	Log-normal Distribution Type
<b>pH</b>	1.01	-0.187	0.0677	1.185	0.008	No
<b>H<sup>+</sup></b>	5.40	8.697	0.059	1.033	0.106	Yes
<b>SO<sub>4</sub><sup>2-</sup></b>	0.18	5.275	0.0513	0.947	0.095	No
<b>NO<sub>3</sub><sup>-</sup></b>	2.34	6.98	0.0574	0.996	0.078	No
<b>NH<sub>4</sub><sup>+</sup></b>	2.14	3.98	0.0615	0.926	0.070	No
<b>Cl</b>	2.70	7.47	0.0624	1.160	0.002	No
<b>Mg<sup>2+</sup></b>	2.06	5.41	0.051	0.760	0.058	No
<b>Ca<sup>2+</sup></b>	1.88	6.21	0.046	0.683	0.0031	No
<b>K<sup>+</sup></b>	2.36	4.93	0.068	1.010	0.0003	No
<b>Na<sup>+</sup></b>	2.54	8.13	0.091	1.355	0	No
<b>Cd</b>	1.97	1.65	0.087	0.823	0.54	No
<b>Cu</b>	1.60	4.76	0.063	0.751	0.63	Yes
<b>Pb</b>	1.79	2.76	0.053	0.611	0.86	Yes
<b>Al</b>	2.57	5.10	0.037	0.479	0.98	Yes
<b>Ni</b>	1.66	2.58	0.051	0.565	0.92	Yes
<b>Cr</b>	1.70	2.50	0.046	0.497	0.97	No
<b>Zn</b>	4.55	7.41	0.082	0.927	0.37	Yes
<b>Fe</b>	2.37	3.95	0.055	0.612	0.86	Yes

However, although distributions of,  $\text{SO}_4^{2-}$  and  $\text{Na}^+$  are also right-skewed, these distributions are not log-normal with 95% confidence. Other elements which are not shown in the figure show distribution characteristics either like Pb, Ni and Zn or like  $\text{SO}_4^{2-}$  and Na. Distribution characteristics of all elements and ions measured in this study are depicted in Table 4.2.

Most of the elements behave like  $\text{SO}_4^{2-}$  and Na, which means they have right skewed distributions, but these distributions can not be explained by a pure log-normal curve. Only the  $\text{H}^+$  ion and elements Cu Pb, Al, Ni, Zn and Fe have purely log-normal distributions. For all other elements histograms are right skewed, but distributions are not log-normal.

It should be noted that, the uncertainty in Kolmogorov-Smirnov test depends on the number of data points. The assessments should be fairly reliable for ions and elements that are measured in all samples (most of the ions are in this category), but less reliable for elements that are measured in approximately 100 samples (most of the elements are in this category).

#### **4.1.2. Comparison of the Precipitation Data with the Literature and the EMEP Network**

Comparison of atmospheric data with literature and other stations is essential to assess the pollution level in the area under study and rank it among the other stations. Areas under study are classified as; urban, rural and remote. In this study, the data set which represents a rural area, long term variation refers to the seasonal variations in the concentration of elements and corresponding factors affecting these variations. The main factors to determine the concentration of elements and ions in the Eastern Mediterranean region are the frequency of air mass movements from different sectors, particle scavenging and source strengths.

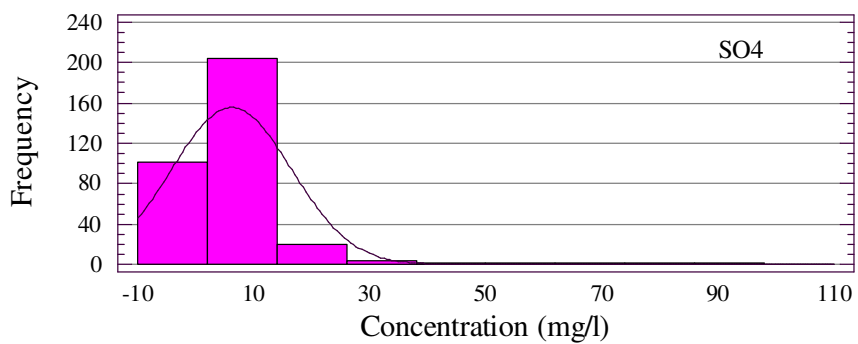
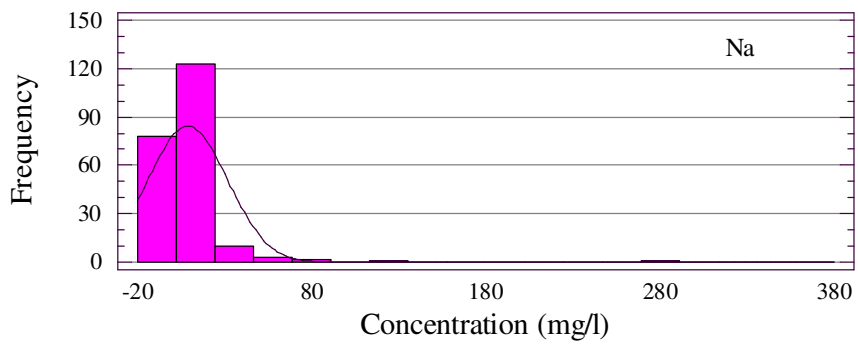
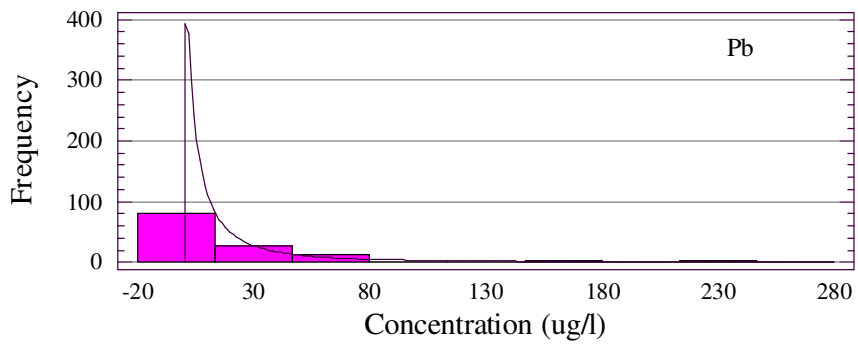
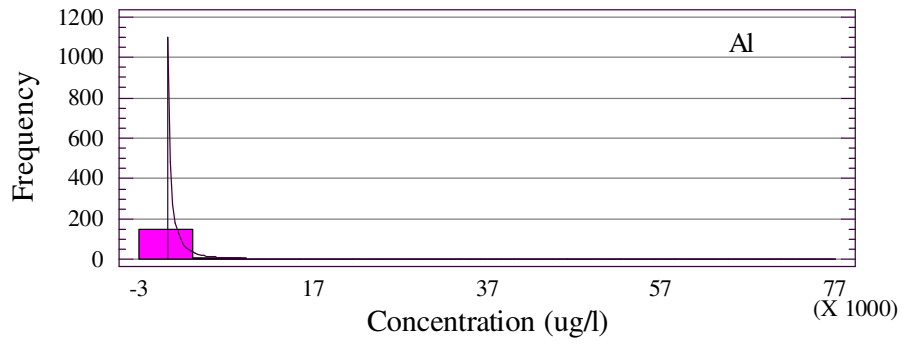


Figure 4.1 Frequency distributions and best fit curves for Al, Pb, Na<sup>+</sup> and SO<sub>4</sub><sup>2-</sup>.

The most frequent air mass movements occur from the North, Northwest and West sectors indicating the contributions of high emission areas such as western Europe, former USSR countries Ukraine and Russia and western parts of Turkey, which provide the potential pollution source regions to intercept in the eastern Mediterranean atmosphere away from local and anthropogenic sources, are investigated and compared with literature and EMEP stations data.

Major ions and trace elements are separately compared with rural data from other parts of the world, because of the difficulty in finding data sets that includes both elements and ions. Major ion data generated in this study are compared with the corresponding concentrations measured in EMEP (European Monitoring and Evaluation Programme) network. Major ion data generated in EMEP network is suitable for comparison because, (1) EMEP stations are fairly uniformly distributed on whole Europe covering both polluted and unpolluted regions and (2) sampling and analysis methods used in the network are similar to those used in this study.

The stations used in EMEP monitoring network have the following characteristics:

- Located in rural areas,
- Established at least 50 km away from large pollution sources (such as towns, power plants, major motorways), 100 m away from small scale domestic heating with coal, fuel oil or wood, 100 m away from minor roads, 500 m away from main roads, 2 km away from application manure and 500 m away from grazing by domestic animals on fertilized pasture (EMEP Manual for Sampling and Chemical Analysis, 1996),
- Not located in valleys or on peaks of mountain tops,
- Not exposed to strong winds.

Volume weighted arithmetic mean of annual concentrations of major ions between the years 1991 and 1999 in 72 stations were used in comparison. The EMEP stations included in comparison and their locations were presented in Table 4.3.

Table 4.3 The location of the EMEP stations used for the comparison

<b>Station Codes</b>	<b>Country</b>	<b>Location</b>	<b>Latitude</b>	<b>Longitude</b>	<b>Altitude</b>
<b>AT2</b>	Austria	Illmitz	47° 46' N	16° 46' E	117
<b>AT3</b>	Austria	Achenkirch	47° 33' N	11° 43' E	960
<b>AT4</b>	Austria	St.Koloman	47° 39' N	13° 12' E	851
<b>CH2</b>	Switzerland	Payerne	46° 49' N	6° 57' E	510
<b>CS5</b>	Serbia&Montenegro				
<b>CS8</b>	Serbia&Montenegro				
<b>CZ1</b>	Czech Republic	Svratouch	49° 44' N	16° 2' E	737
<b>CZ3</b>	Czech Republic	Kosetice	49° 35' N	15° 5' E	534
<b>DE1</b>	Germany	Westerland	54° 55' N	8° 18' E	12
<b>DE2</b>	Germany	Langenbrügge	52° 48' N	10° 45' E	74
<b>DE3</b>	Germany	Schauinsland	47° 54' N	7° 54' E	1205
<b>DE4</b>	Germany	Deuselbach	49° 45' N	7° 3' E	480
<b>DE5</b>	Germany	Brotjacklriegel	48° 49' N	13° 13' E	1016
<b>DE7</b>	Germany	Neuglobsow	53° 10' N	13° 2' E	62
<b>DE8</b>	Germany	Schmücke	50° 39' N	10° 46' E	937
<b>DE9</b>	Germany	Zingst	54° 26' N	12° 44' E	1
<b>DK3</b>	Denmark	Tange	56° 21' N	9° 36' E	13
<b>DK5</b>	Denmark	Keldsnor	54° 44' N	10° 44' E	10
<b>DK8</b>	Denmark	Anholt	56° 43' N	11° 31' E	40
<b>EE9</b>	Estonia	Lahemaa	59° 30' N	25° 54' E	32
<b>EE11</b>	Estonia	Vilsandy	58° 23' N	21° 49' E	6
<b>ES1</b>	Spain	San Pablo de los Montes	39° 32' N	4° 20' W	917
<b>ES3</b>	Spain	Roquetas	40° 49' N	0° 29' E	44
<b>ES4</b>	Spain	Logroño	42° 27' N	2° 30' W	445
<b>FI4</b>	Finland	Ähtari	62° 32' N	24° 13' E	162
<b>FI9</b>	Finland	Utö	59° 46' N	21° 22' E	7
<b>FI17</b>	Finland	Virolahti II	60° 31' N	27° 41' E	4
<b>FI22</b>	Finland	Oulanka	66° 19' N	29° 24' E	310
<b>FR3</b>	France	La Crouzille	45° 50' N	1° 16' E	497
<b>FR5</b>	France	La Hague	49° 37' N	1° 49' W	133
<b>FR8</b>	France	Donon	48° 30' N	7° 8' E	775
<b>FR9</b>	France	Revin	49° 54' N	4° 38' E	390
<b>FR10</b>	France	Morvan	47° 16' N	4° 5' E	620
<b>FR12</b>	France	Iraty	43° 2' N	1° 5' W	1300
<b>GB2</b>	United Kingdom	Eskdalemuir	55° 18' N	3° 12' W	243
<b>GB6</b>	United Kingdom	Lough Navar	54° 26' N	7° 52' W	126
<b>GB13</b>	United Kingdom	Yarner Wood	50° 35' N	3° 42' W	119
<b>GB14</b>	United Kingdom	High Muffles	54° 20' N	0° 48' W	267
<b>GB15</b>	United Kingdom	Strath Vaich Dam	57° 44' N	4° 46' W	270
<b>HR2</b>	Croatia	Puntijarka	45° 54' N	15° 58' E	988
<b>HR4</b>	Croatia	Zavizan	44° 49' N	14° 59' E	1594
<b>HU2</b>	Hungary	K-puszta	46° 58' N	19° 35' E	125
<b>IE1</b>	Ireland	Valentina Observatory	51° 56' N	10° 14' W	11

<b>IE2</b>	Ireland	Turlough Hill	53° 2 N	6° 24' W	420
<b>IT1</b>	Italy	Montelibretti	42° 6 N	12° 38' E	48
<b>IT4</b>	Italy	Ispra	45° 48 N	8° 38' E	209
<b>LT15</b>	Lithuania	Preila	55° 21 N	21° 4' E	5
<b>LV10</b>	Lativa	Rucava	56° 13 N	21° 13' E	5
<b>NL9</b>	Netherlands	Kollumerwaard	53° 20 N	6° 16' E	1
<b>NO1</b>	Norway	Birkenes	58° 23 N	8° 15' E	190
<b>NO8</b>	Norway	Skreådalen	58° 49 N	6° 43' E	475
<b>NO15</b>	Norway	Tustervatn	65° 50 N	13° 55' E	439
<b>NO39</b>	Norway	Kårvatn	62° 47 N	8° 53' E	210
<b>NO41</b>	Norway	Osen	61° 15 N	11° 47' E	440
<b>PL2</b>	Poland	Jarczew	51° 49 N	21° 59' E	180
<b>PL3</b>	Poland	Sniezka	50° 44 N	15° 44' E	1603
<b>PL4</b>	Poland	Leba	54° 45 N	17° 32' E	2
<b>PT1</b>	Portugal	Braganca	41° 49 N	6° 46' W	690
<b>PT3</b>	Portugal	Viana do Castelo	41° 42 N	8° 48' W	16
<b>PT4</b>	Portugal	Monte Velho	38° 5 N	8° 48' W	43
<b>RU1</b>	Russia	Janiskoski	68° 56 N	28° 51' E	118
<b>RU13</b>	Russia	Pinega	64° 42 N	43° 24' E	28
<b>RU16</b>	Russia	Shepeljovo	59° 58 N	29° 7' E	4
<b>SE2</b>	Sweden	Rörvik	57° 25 N	11° 56' E	10
<b>SE5</b>	Sweden	Bredkälén	63° 51 N	15° 20' E	404
<b>SE11</b>	Sweden	Vavihill	56° 1 N	13° 9' E	175
<b>SE12</b>	Sweden	Aspvreten	58° 48 N	17° 23' E	20
<b>SK2</b>	Slovakia	Chopok	48° 56 N	19° 35' E	2008
<b>SK4</b>	Slovakia	Stará Lesná	49° 9 N	20° 17' E	808
<b>SK5</b>	Slovakia	Liesek	49° 22 N	19° 41' E	892
<b>SK6</b>	Slovakia	Starina	49° 3 N	22° 16' E	345
<b>TR1</b>	Turkey	Cubuk II	40° 30 N	33° 0' E	1169

The data generated in EMEP locations and in this study are presented in Figure 4.2. It is clear from the figure that all ions measured in this study, except for H<sup>+</sup> ion, are higher than those reported from 72 stations in the EMEP network. Some of these differences are due to natural sources, but some are due to anthropogenic emissions.

Higher SO<sub>4</sub><sup>2-</sup>, NO<sub>3</sub><sup>-</sup> and NH<sub>4</sub><sup>+</sup> concentrations measured in this study should be explained by contributions of anthropogenic sources. Since data generated in this study and in all EMEP stations are regionally representative, the observed difference can not be due to local influences and should be regional. This observation suggests that concentrations of SO<sub>4</sub><sup>2-</sup>, NO<sub>3</sub><sup>-</sup> and NH<sub>4</sub><sup>+</sup> in Eastern Mediterranean rain water are higher than those measured anywhere in Europe. High concentrations of these ions in Eastern Mediterranean aerosols were reported by a number of authors (Güllü et al.,

1998; Mihalopoulos et al., 1997; Luria et al., 1996) and explained by long range transport of these pollutants to the Eastern Mediterranean region.

One interesting feature shown in the Figure 4.2 is unexpectedly low  $H^+$  concentration in Antalya station. Hydrogen ion is the only ion which has lower concentrations than  $H^+$  concentrations reported in EMEP station. This looks like a dilemma, because  $SO_4^{2-}$  and  $NO_3^-$  are the two ions, which are responsible for acidity in rain water. Since concentrations of both  $SO_4^{2-}$  and  $NO_3^-$  are high in Antalya station, one would also expect high  $H^+$  ion concentration (low pH). The low H ion and high  $SO_4^{2-}$  and  $NO_3^-$  concentrations are due to extensive neutralization of rain water acidity as will be discussed in detail, later in the manuscript.

High concentrations of crustal and marine elements measured in this study are due to natural sources. Crustal elements such as  $Ca^{2+}$  and  $K^+$  were highly enriched in Antalya station, due to the  $CaCO_3$  rich soil and the Saharan dust transported from the North Africa (Güllü et al., 2003; Al-Momani et al., 1999; Güllü et al., 1998; Al-Momani et al., 1997; Guerzoni et al., 1995). Furthermore, dry and long summer season in the region increases the atmospheric loading of soil particles which are washed by precipitation. Sporadic, intense incursions of Saharan dust also results in high concentrations of  $Ca^{2+}$  and  $K^+$ , because Saharan dust transported to the region is generally associated with frontal passages and rain events (Al-Momani et al., 2003; Al-Momani et al., 1998).

Marine elements such as  $Na^+$ ,  $Cl^-$ ,  $Mg^{2+}$  and  $K^+$  ions have the highest concentration in Antalya due to close proximity of the station to the Mediterranean Sea.

The comparison of trace elements between EMEP stations and Antalya station is presented in Figure 4.3. For each element, the numbers below the red circle indicates the number of EMEP stations in which concentration is lower than that measured in this study. The number above the red circle represents the number of EMEP stations in which concentration is higher than that measured in this study. Except for the Cd and Cu elements, Antalya station has the highest concentration level among the EMEP stations. The higher concentrations could be accomplished by the long range

transport of these trace elements from particularly European Countries and Russia. The details will be introduced later in the manuscript.

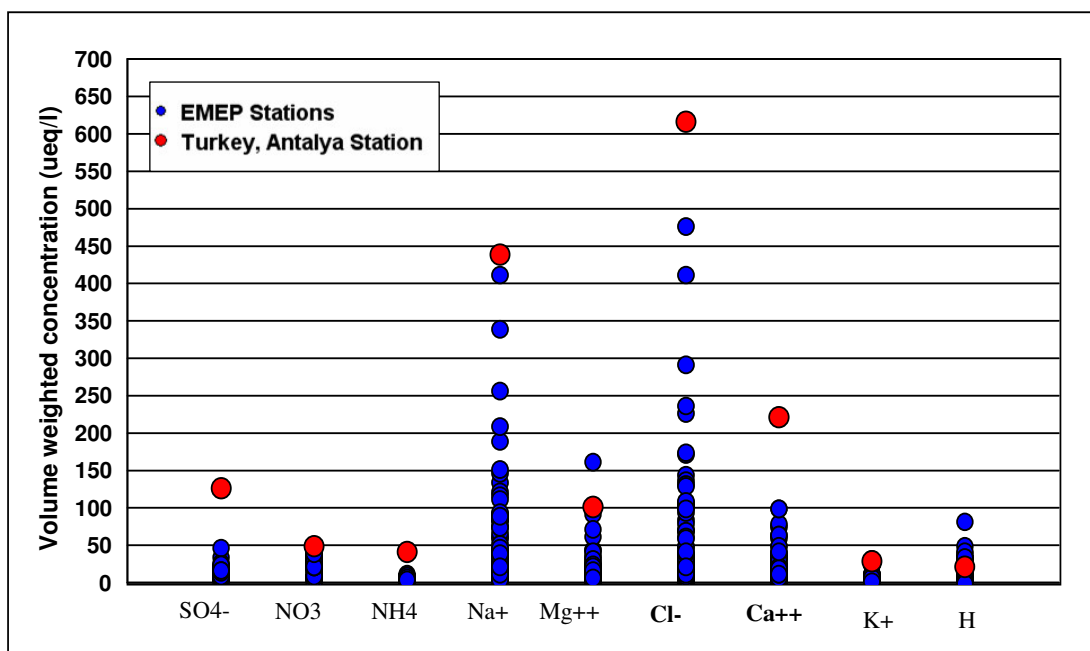


Figure 4.2 Comparison of volume weighted average concentrations of major ions of Antalya station with the results of other EMEP stations.

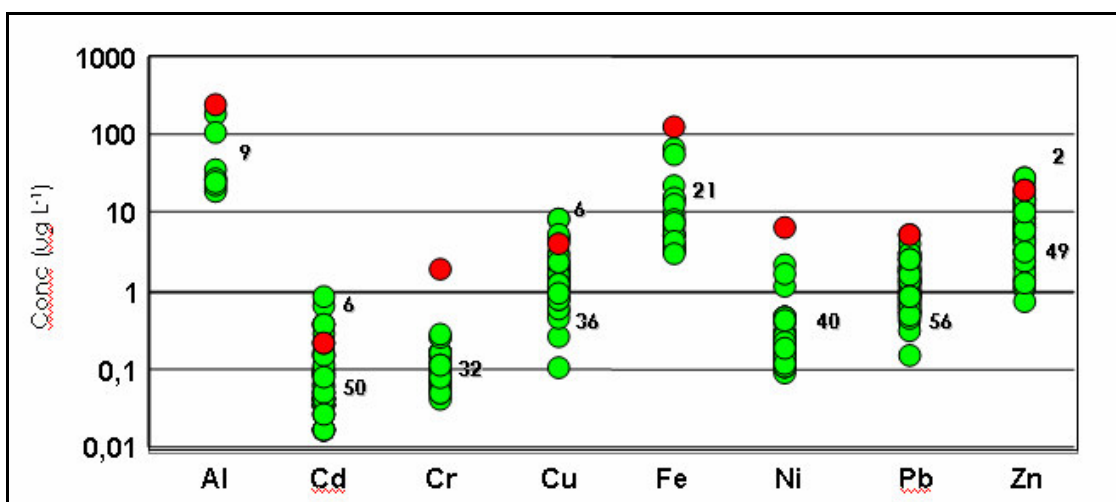


Figure 4.3. Comparison of concentrations of elements measured in this study with those reported for the EMEP stations.

Concentrations of trace elements measured in this study are compared with corresponding concentrations reported in literature for other parts of the world in Table 4.4. Crustal elements such as Al and Fe have second highest values reported

in other stations. The two important potential sources of Fe and Al are local soil and transported Saharan dust to the eastern Mediterranean. Higher concentrations of Cr and Ni can be explained by these elements rich in soil which is probably due to the presence of ophiolitic rocks in Mediterranean coast of Turkey ( Kubilay and Saydam, 1995; Tolun and Pamir, 1975).

Since there is no anthropogenic emission sources around the station, pollution derived elements are transported from the other parts of Turkey and from Europe (Al-Momani et al., 1997). Except for the element of Ni, all the pollution derived elements have the second highest values in Antalya Station, whereas the highest values belong to Amasra Station. Anthropogenic compounds of Cd, Cu, Pb, Zn, Al, Cr, Fe and Ni have significantly higher values compared to France, Rhode Island, Massachusetts, and Jordan Stations.

Table 4.4 Comparison of observed volume weighted average concentrations of trace elements with literature values ( $\mu\text{g/l}$ )

	<b>This Study</b>	<b>France<sup>1</sup></b>	<b>Northern Jordan<sup>2</sup></b>	<b>Black Sea Turkey<sup>3</sup></b>	<b>Rhode Island<sup>4</sup></b>	<b>Western Massachusetts<sup>5</sup></b>
<b>Cd</b>	0.75	0.024	0.42	5.17		0.31
<b>Cu</b>	4.97	0.534	3.08	100		0.95
<b>Pb</b>	8.17	1.31	2.57	12.32		4.5
<b>Zn</b>	46.62	3.08	6.52	100	4.5	3.7
<b>Al</b>	762.04		382	10110	71	53
<b>Cr</b>	8.28		0.77	11.73		0.14
<b>Ni</b>	21.12	0.46	2.62	18.17		0.75
<b>Fe</b>	645.17	18.91	92	7540	38	65

1. Cabon et al., 1999.

2. Al-Momani, I.F., 2003.

3. Alagha, O., 2000.

4. Heaton et al., 1990.

5. Dasch and Wolff , 1989.

## 4.2. Ionic Composition of Wet Deposition

### 4.2.1. Ion Balance

The ratio of total anions to that of total cations ( $\sum \text{anion} / \sum \text{cation}$ ) is an indicator of the completeness of measured parameters. If all the major anions and cations are included in the measurement, the ratio is expected to be unity. Deviation from unity indicates the exclusion of some ions.

The plot of the equivalent sum of anions ( $\text{SO}_4^{2-}$ ,  $\text{NO}_3^-$  and  $\text{Cl}^-$ ) against sum of cations ( $\text{Ca}^{2+}$ ,  $\text{Mg}^{2+}$ ,  $\text{Na}^+$ ,  $\text{K}^+$ ,  $\text{H}^+$  and  $\text{NH}_4^+$ ) is given in Figure 4.4. The average ( $\sum \text{anion} / \sum \text{cation}$ ) ratio was 0.77. Two potential anions can alter these ratio were organic species and bicarbonate ion (Anna and Avila, 2003; Al-Momani et al., 2000; Al-Momani et al., 1995a). Organic anions are generally important in regions with extensive forestry, such as tropics, but are not expected to be significant in temperate latitudes (Lacaux et al., 1992; Keene et al., 1983). Consequently anion deficiency observed in this study is expected to be presence of  $\text{HCO}_3^-$  anion, which is not measured in this study. The  $\text{HCO}_3^-$  forms by dissolution of atmospheric  $\text{CO}_2$  in rain and its concentration depends on the pH of the rain water. Generally bicarbonate ion concentration is not large enough to affect ion balance when rain water is acidic and its concentration increases as rain water becomes more and more basic.

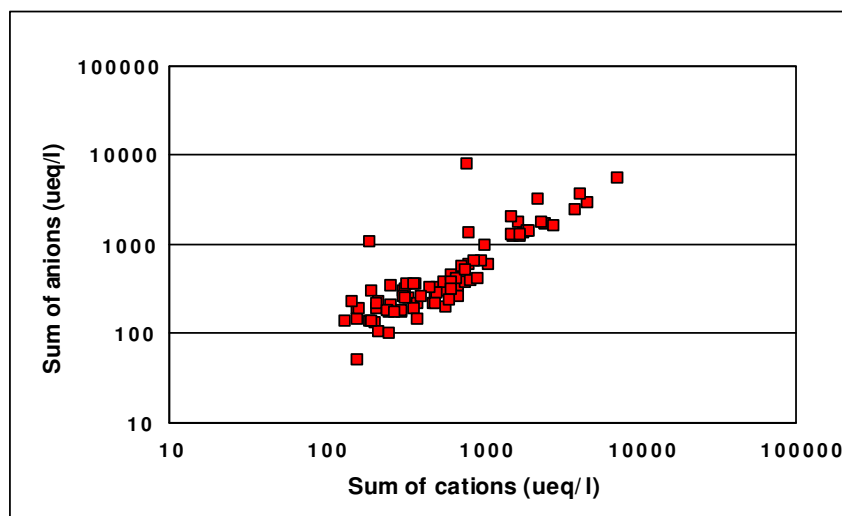


Figure 4.4 The plot of the equivalent sum of anions to equivalent sum of cations.

Since Antalya Region has calcareous soil and fairly high pH, the observed deficiency can be referred to the exclusion of bicarbonate ions from the measurements (Al-Momani et al., 1995c). Although the bicarbonate ion is not measured in this study, its concentration is calculated in each sample using the equation (2.2) in page 8. Calculations showed that average bicarbonate ion concentration in the study period is  $1855 \mu\text{eqL}^{-1}$ . When this is included in ion balance,  $(\sum\text{anion}) / (\sum\text{cation})$  ratio becomes 0.99.

The good agreement in  $(\sum\text{anions})$  and  $(\sum\text{cations})$  demonstrate that measurements are reliable and all of the major ions are measured in this study.

#### **4.2.2. Contributions of Ions to Total Ion Mass**

Contributions of ions to total ion, total cation and total anion mass in each year, in wet and dry seasons and during the period November 1991 and August 1999 are given in Table 4.5.

In Figure 4.5, contribution of ions to total ion mass for the period 1991 to 1999 is represented. The highest portion is belonging to  $\text{Cl}^-$  ion, which has 32.75% contribution to total ion mass. Sodium has the second highest contribution with 19.49%. Sodium and chloride together account for 52.24 % of total ion mass. Sodium and chloride originate from sea salt and their high contribution to total ion mass is due to location of the station, which is on the coast.

$\text{Ca}^{2+}$ ,  $\text{Mg}^{2+}$  and  $\text{K}^+$  are mainly from crustal source. Their contributions to total ion mass are 16.88 %, 7.14% and 1.39%, respectively.  $\text{NH}_4^+$  has a 6.9% contribution to total ion mass. A total contribution of  $\text{Ca}^{2+}$  and  $\text{NH}_4^+$  is 23.78%. This is important, because it indicates neutralization potential in rainwater. Contributions of acid forming ions, namely  $\text{SO}_4^{2-}$  and  $\text{NO}_3^-$  are 10.68%, 3.96% respectively. And that of  $\text{H}^+$  ion is 0.82%.

Table 4.5 Contributions of ions to total ion, total cation and total anion mass in each year, in wet and dry season and during the period November 1991 and August 1999.

	Cations						Anions		
	H <sup>+</sup>	NH <sub>4</sub> <sup>+</sup>	Na <sup>+</sup>	Mg <sup>2+</sup>	Ca <sup>2+</sup>	K <sup>+</sup>	SO <sub>4</sub> <sup>2-</sup>	NO <sub>3</sub> <sup>-</sup>	Cl <sup>-</sup>
<b>1991 (13)*</b>									
% Total	1.84	1.44	0.00	0.00	0.00	0.00	10.53	1.71	84.48
% Cations	56.02	43.98	0.00	0.00	0.00	0.00			
% Anions							10.88	1.77	87.35
<b>1992 (44)</b>									
% Total	2.03	5.93	21.34	9.11	9.99	1.22	15.77	8.34	26.27
% Cations	4.10	11.95	43.00	18.37	20.14	2.45			
% Anions							31.30	16.55	52.15
<b>1993 (50)</b>									
% Total	1.54	6.86	21.79	11.46	11.86	0.97	7.69	6.26	31.56
% Cations	2.83	12.60	39.99	21.04	21.76	1.78			
% Anions							16.89	13.76	69.35
<b>1994 (66)</b>									
% Total	0.27	3.56	71.21	5.04	6.32	0.73	3.05	1.38	8.44
% Cations	0.31	4.08	81.73	5.79	7.25	0.83			
% Anions							23.69	10.73	65.58
<b>1995 (49)</b>									
% Total	3.96	22.93	0.00	0.00	0.00	0.00	17.85	7.16	48.10
% Cations	14.73	85.27	0.00	0.00	0.00	0.00			
% Anions							24.42	9.80	65.78
<b>1996 (59)</b>									
% Total	0.90	10.95	15.84	3.28	14.34	1.43	10.36	2.18	40.72
% Cations	1.92	23.43	33.90	7.02	30.67	3.06			
% Anions							19.45	4.09	76.45
<b>1997 (41)</b>									
% Total	0.10	0.00	17.74	3.22	17.99	1.88	13.34	3.88	41.87
% Cations	0.24	0.00	43.35	7.86	43.95	4.59			
% Anions							22.58	6.56	70.86
<b>1998 (41)</b>									
% Total	0.17	2.75	17.95	10.07	23.81	1.51	12.72	3.96	27.07
% Cations	0.30	4.88	31.91	17.90	42.32	2.68			
% Anions							29.08	9.06	61.87
<b>1999 (24)</b>									
% Total	0.80	3.72	16.17	5.98	36.16	0.97	9.67	3.27	23.27
% Cations	1.26	5.83	25.35	9.37	56.67	1.52			
% Anions							26.70	9.02	64.27
<b>Wet season during the period 1991-1999 (269)</b>									
% Total	0.89	5.71	23.43	7.19	14.59	1.28	8.92	3.08	34.90
% Cations	1.68	10.75	44.14	13.54	27.49	2.41			
% Anions							19.02	6.57	74.41
<b>Dry season during the period 1991-1999(118)</b>									
% Total	0.38	11.75	15.91	7.35	21.08	1.51	14.28	7.84	19.91
% Cations	0.65	20.26	27.44	12.68	36.37	2.61			
% Anions							33.97	18.65	47.38
<b>During the period 1991-1999 ( 387)</b>									
% Total	0.82	6.90	19.49	7.14	16.88	1.39	10.68	3.96	32.75
% Cations	1.55	13.12	37.04	13.57	32.08	2.64			
% Anions							22.54	8.35	69.11

\*Number of data points analyzed is given in parenthesis.

Contribution of anions to total anion mass and contribution of cations to total cation mass were presented in the Figure 4.6. Chloride has the highest contribution with 69.11%, among the total anion mass. Sulfate has the second highest contribution with 22.54% and  $\text{NO}_3^-$  has 8.35% contribution.

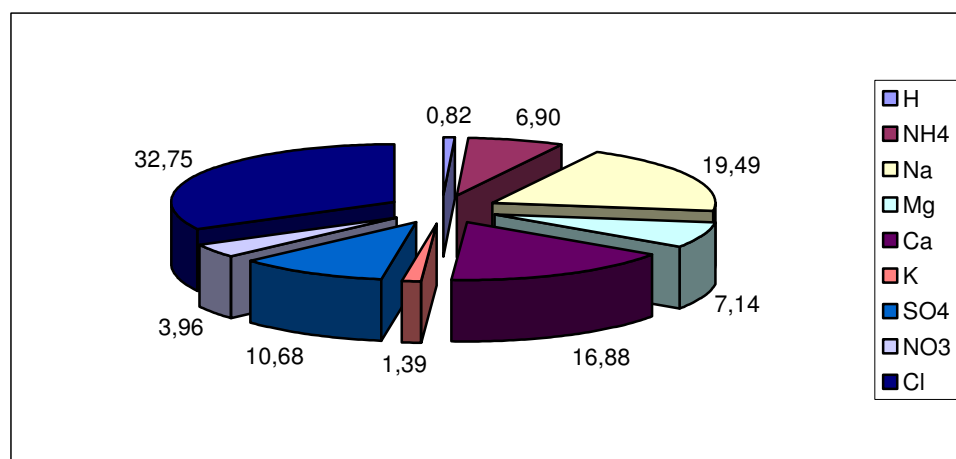


Figure 4.5 Contribution of ions to total ion mass

The highest cation contribution to total cation mass was observed for  $\text{Na}^+$  ion with 34.04%. The second highest contribution was belong to  $\text{Ca}^{2+}$  ion with 32.08%.  $\text{Mg}^{2+}$ ,  $\text{NH}_4^+$ ,  $\text{K}^+$  and  $\text{H}^+$  have the contributions with 13.57%, 13.12%, 2.64% and 1.55%, respectively. These percentages indicate strong dominance of sea salt on ionic composition of rain water in the Eastern Mediterranean. The observed pattern does not change significantly from one year to another.

Seasonal variations in the contributions of ions to total ion mass were presented in Figure 4.7. Wet season was accepted as the period from the beginning of October to the end of March and dry season was taken as the period from the beginning of April to the end of September.

Contribution of marine elements  $\text{Na}^+$  and  $\text{Cl}^-$  to total ion mass are 23.43% and 34.90% respectively in wet, and 15.79% and 19.91%, respectively in and dry season. In wet season, marine elements  $\text{Cl}^-$  and  $\text{Na}^+$  have higher contributions compared to dry season due to the more extensive sea salt generation during stormy winter season.

Contributions of crustal elements  $\text{Ca}^{2+}$ ,  $\text{Mg}^{2+}$  and  $\text{K}^+$  to total mass are 14.79%, 7.19%, 1.28%, respectively in the winter and 21.08%, 7.35%, 1.51%, respectively in the summer. Crustal elements of  $\text{Ca}^{2+}$ ,  $\text{Mg}^{2+}$  and  $\text{K}^+$  ion mass have higher contributions in dry season, which can be explained by easier resuspension of soil aerosol during summer (Al-Momani et al., 1997; Kubilay and Saydam, 1995).

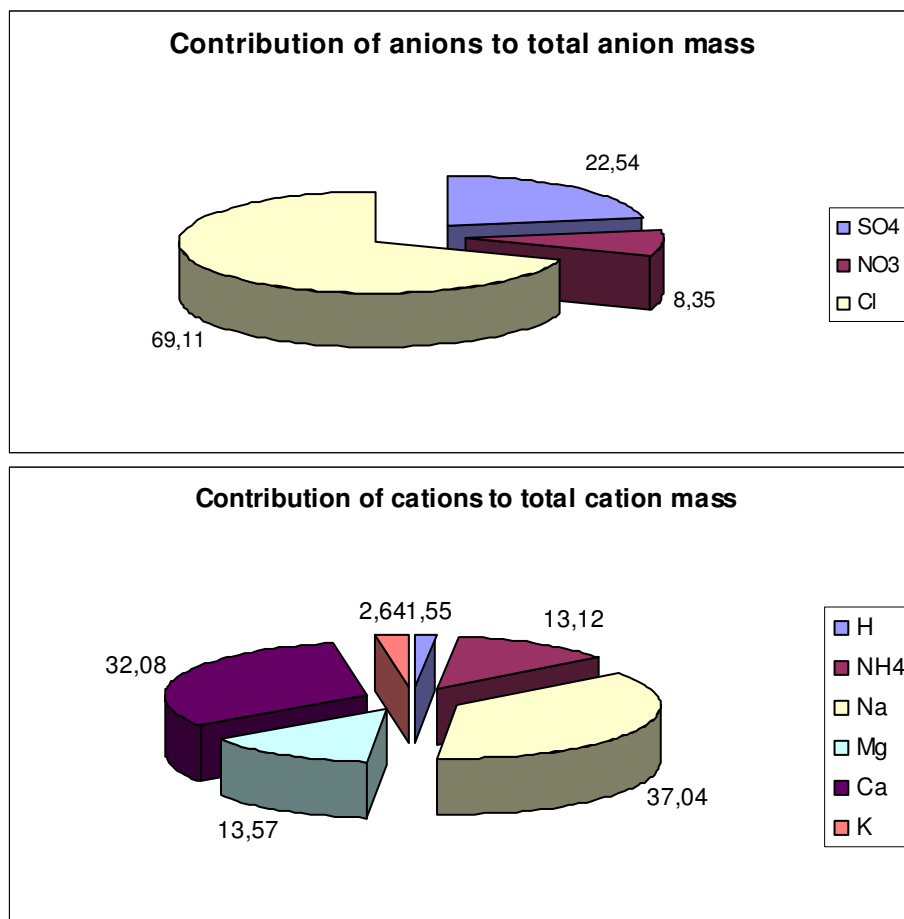


Figure 4.6 Contribution of anions to total anion mass and contribution of cations to total cation mass.

$\text{NH}_4^+$  contribution to total ion mass in wet season and dry season were, 5.71% and 11.75%, respectively. Higher contribution of  $\text{NH}_4^+$  to total ion mass in summer is probably due to widespread application of  $\text{NH}_4^+$  containing fertilizer in the region. These fertilizers are applied in spring and evaporation of  $\text{NH}_3$  from these is enhanced in summer

$\text{SO}_4^{2-}$  and  $\text{NO}_3^-$  ion contributions in wet and dry season were, 8.92%, 3.08% and 14.28%, 7.84%, respectively.  $\text{SO}_4^{2-}$  and  $\text{NO}_3^-$  contributions are higher in dry season

compared to wet season, due to enhanced photochemistry during summer months (Al-Momani, 1995c).  $H^+$  ion contribution to total ion mass in wet season was 0.89% and in dry season 0.38%. Lower contribution of  $H^+$  ion in dry season is due to the neutralization process, which occurs during dry season.

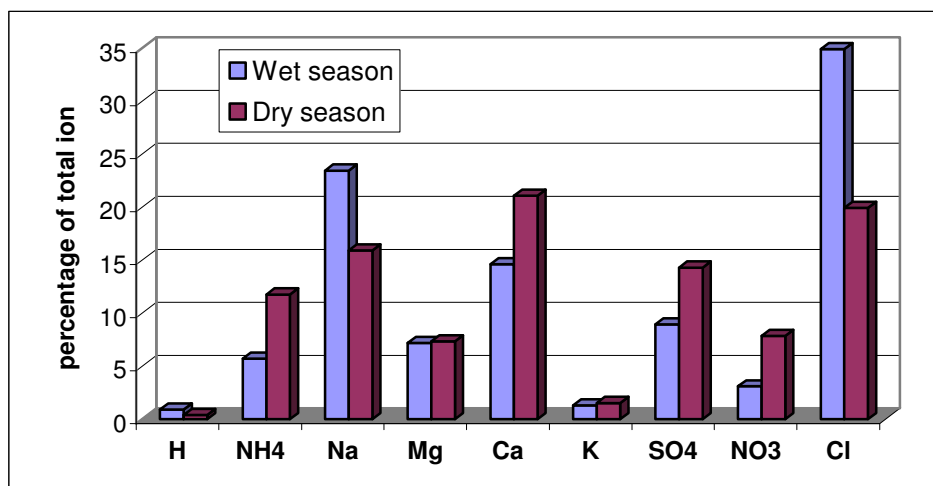


Figure 4.7 Seasonal variations in the contributions of ions to total ion mass

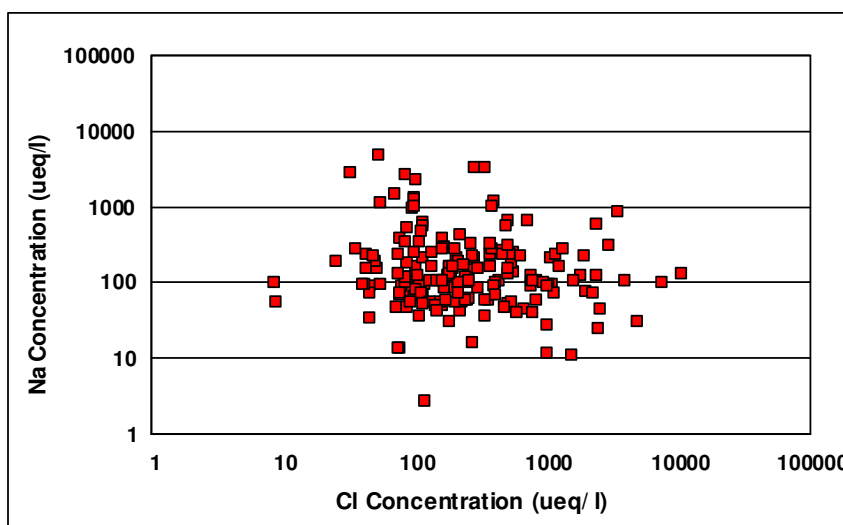


Figure 4.8 Plot of equivalent Na concentration to equivalent Cl concentration

Equivalent ratio of  $Na^+$  to  $Cl^-$  was plotted and presented in Figure 4.8. The median Cl-to-Na mass ratio was calculated as 2.0. This value is close to the Cl-to-Na ratio in fresh sea salt, which is 1.8 and suggests that there is no significant  $Cl^-$  loss in particles captured by rain droplets in our station. This is probably due to close proximity of the station to the sea, because in aged air masses  $Cl^-$  is evaporated from

particles and the Cl-to-Na ratio is generally < 1.8 (Tunçer, 2000). It should be noted that since the rain water composition is determined by capturing of particles by rain droplets, the Cl-to-Na ratio in particles reflects to the corresponding ratio in rain water

Since crustal material and sea salt are the most abundant components of elements and ions in rain water, it may be worthwhile to calculate fractions of elements and ions measured in this study that originate from soil and the sea. In such calculation, of Na is used as tracer element for sea salt and Al is used as tracer element for crustal material. Crustal contribution was calculated using the following relation:

$$Cr - C_x = \left( C_{Al(sample)} * \frac{C_{x(soil)}}{C_{Al(soil)}} \right) \quad (4.3)$$

Where, (Cr-C<sub>x</sub>) was the crustal contribution on parameter x, (C<sub>Al</sub>)<sub>sample</sub> is Al concentration of a single sample (C<sub>Al</sub>)<sub>soil</sub> is the concentration of Al in Mason's (1966) global soil compilation and (C<sub>x</sub>)<sub>soil</sub> is the concentration of ion X in the Mason's average soil composition.

Marine contribution was calculated by using Na that has more conservative nature, in Goldberg's sea water composition (Goldberg, 1963). The formula 4.3 is revised by replacing Al with Na for calculating the marine contribution. After calculating the crustal and marine contribution, both values are added. Then this total value is subtracted from the total concentration to find the other contributions. Sources contributing to observed concentrations of ions and elements in Eastern Mediterranean region were presented in Table 4.6.

It was observed that crustal material in precipitation accounts for Al and Fe elements. The contribution of Mg<sup>2+</sup>, K<sup>+</sup> and Ca<sup>2+</sup> to crustal material had lesser extend. This is probably due to differences in the composition of soil in the Eastern Mediterranean region and in Mason's (1966) average soil. The region is highly enriched in alkaline soil, which is rich in alkaline earth elements, particularly in Ca<sup>2+</sup>. The contribution of other elements to crustal content was insignificant. Na<sup>+</sup> and Cl<sup>-</sup> have the highest

contribution to marine content. Furthermore,  $Mg^{2+}$ ,  $K^+$  and  $SO_4^{2-}$  have considerable contributions to sea salt content. Other ions do not have significant effects on concentrations of sea salt.

Sea salt and crustal components can account for less than 10% of the observed concentrations of Cd, Cu, Pb, Ni, Zn and Cr. More than 90% of their concentrations are unaccounted for by natural sources. This is not surprising, because it is well documented that anthropogenic emissions are main sources of these chalcophilic elements in the atmosphere. The  $SO_4^{2-}$  which is well-known anthropogenic ion has approximately 20% contribution from the sea salt.

Table 4.6 Sources contributing to observed concentrations of ions and elements in the Eastern Mediterranean

	<b>Crustal (%)</b>	<b>Marine (%)</b>	<b>Other (%)</b>
<b><math>SO_4^{2-}</math></b>	0.1	22.1	77.8
<b>Cl<sup>-</sup></b>	0	89.9	10.1
<b><math>Mg^{2+}</math></b>	11.5	66.4	22.1
<b><math>Ca^{2+}</math></b>	5.1	5.1	89.8
<b><math>K^+</math></b>	22.7	30.0	47.3
<b><math>Na^+</math></b>	3	100	0
<b>Cd</b>	0.2	0	99.8
<b>Cu</b>	5.2	0	94.8
<b>Pb</b>	0.7	0	99.3
<b>Al</b>	100	0	0
<b>Ni</b>	1.7	0	98.3
<b>Cr</b>	5.6	0	94.4
<b>Zn</b>	1.1	0	98.9
<b>Fe</b>	60.7	0	39.3

The approach used to estimate the marine and crustal contribution fractions of elements involves some assumptions that sea water and soil have similar characteristics to general sea water and soil composition. The major ion composition of sea water does not change significantly from one location to another. However, the case was not the same for soil composition. Mason's average soil composition

does not reflect the real characteristics of Antalya soil. Therefore, observed differences in concentrations of  $\text{Ca}^{2+}$ ,  $\text{Mg}^{2+}$  and  $\text{K}^+$  were due to the used soil composition. Unexplained portion of Fe was expected to be the contribution of anthropogenic sources.

### **4.3. Acidity of Wet Deposition**

#### **4.3.1. Rainwater pH**

Acid precipitation is an efficient removal mechanism of acidic substances such as sulfuric acid and nitric acids from atmosphere by wet deposition (Losno et al., 1991; Pio et al., 1991). pH of precipitation is defined as a consequence of acid-base of chemical species from incorporation of atmospheric gases and aerosols by in-cloud and sub-cloud scavenging (Khwaja and Husain, 1990). While nitric and sulfuric acids or their precursors so as  $\text{NO}_x$  and  $\text{SO}_2$  dissolves in water to give hydrogen ions, they ultimately turn to nitrate ions ( $\text{NO}_3^-$ ) and sulfate ions ( $\text{SO}_4^{2-}$ ).  $\text{CO}_2$  dissolves in water and forms a weak acid of  $\text{HCO}_3^-$  (Losno et al., 1991). Furthermore, organic acids may contribute to the acidity of rain water (Sanusi et al., 1996; Tuncel and Ungör, 1996).

Among the 302 samples that collected between November 1991 and August 1999, the median, minimum and maximum pH values are calculated as 5.29, 2.96 and 6.93, respectively. In Antalya Station, air masses from Europe is associated with high anthropogenic content and low pH value and air masses transported from South and East have less anthropogenic content and high pH values (Al-Momani et al., 1995a; Al-Momani et al., 1999).

The frequency distribution of pH is illustrated in Figure 4.9. The histogram clearly demonstrates that the rain water is not acidic. The pH of rain is controlled by two factors: (1) Abundance of acid forming ions, namely  $\text{SO}_4^{2-}$  and  $\text{NO}_3^-$  and (2) abundance of neutralizing ions, namely  $\text{NH}_4^+$  and Ca (representing  $\text{CaCO}_3$ ). High free acidity in rain suggests the abundance of acid forming ions and low free acidity indicates the abundance of neutralizing agent. Furthermore, the rain water pH between 4.5 and 5.6 represent the dissolution of naturally produced  $\text{CO}_2$ ,  $\text{NO}_x$  and

SO<sub>2</sub> gases in clouds and rain water droplets. The samples having pH values less than 4.5 represent anthropogenic sources and pH values greater than 5.6 represent crustal contribution, which is rich in CaCO<sub>3</sub> in the Eastern Mediterranean region (Al-Momani et al., 1998). In the data set 18.5% of the data is have pH less than 4.5 and 42.7% of the data have pH greater than 5.5.

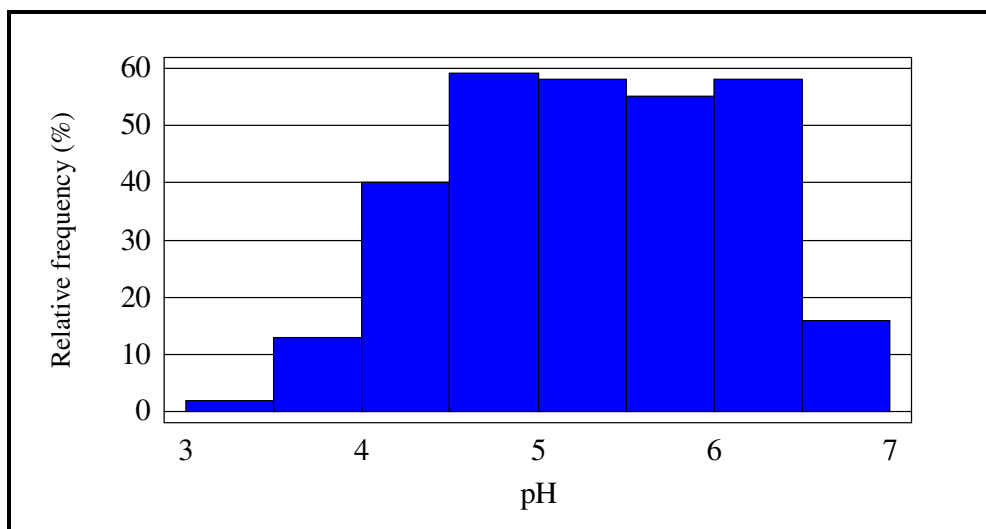


Figure 4.9 Frequency distribution of pH

Median concentrations of ions for pH<5, pH≥5 and whole data set are introduced in Table 4.7. Except for the elements of Fe, Zn and Cu, all major ions and trace elements concentrations have been increased with the elevated pH values.

In the data set pH higher than 5, although acidifying compounds have higher concentrations (SO<sub>4</sub><sup>2-</sup> and NO<sub>3</sub><sup>-</sup> were 3.99 and 1.61 mg/l, respectively), the higher concentrations of neutralizing agents (Ca<sup>2+</sup> and NH<sub>4</sub><sup>+</sup> were 3 and 0.614 mg/l, respectively) does not allow pH to decrease to the values expected from SO<sub>4</sub><sup>2-</sup> and NO<sub>3</sub><sup>-</sup> levels. The evidences indicate that the pH in the rain water is not only under the control of acidifying compounds but also existing of neutralizing species. High pH values does not indicate the lacking of acid forming ions in the precipitation, but rather associate with neutralization of acidity during the rain event by washout mechanism.

Table 4.7 Concentrations of ions for pH&lt;5, pH≥5 and whole data set.

	Concentration	pH<5	pH>=5	Whole data
<b>pH</b>	pH unit	4.52 (113)*	5.82 (189)	5.29 (302)
<b>H<sup>+</sup></b>	mgL <sup>-1</sup>	0.03 (113)	0.0015 (189)	0.0051 (302)
<b>SO<sub>4</sub><sup>2-</sup></b>	mgL <sup>-1</sup>	2.34 (105)	4.00 (166)	3.22 (336)
<b>nSO<sub>4</sub><sup>2-</sup></b>	mgL <sup>-1</sup>	1.64 (54)	2.78 (99)	2.42 (164)
<b>NO<sub>3</sub><sup>-</sup></b>	mgL <sup>-1</sup>	1.55 (95)	1.61 (151)	1.54 (297)
<b>NH<sub>4</sub><sup>+</sup></b>	mgL <sup>-1</sup>	0.53 (80)	0.61 (78)	0.78 (223)
<b>Cl<sup>-</sup></b>	mgL <sup>-1</sup>	7.16 (105)	9.59 (166)	7.29 (341)
<b>Mg<sup>2+</sup></b>	mgL <sup>-1</sup>	0.46 (70)	0.60 (122)	0.55 (218)
<b>Ca<sup>2+</sup></b>	mgL <sup>-1</sup>	1.37 (70)	3.00 (122)	2.12 (218)
<b>K<sup>+</sup></b>	mgL <sup>-1</sup>	0.22 (70)	0.43 (122)	0.34 (219)
<b>Na<sup>+</sup></b>	mgL <sup>-1</sup>	2.98 (70)	3.09 (122)	2.82 (218)
<b>Cd</b>	μgL <sup>-1</sup>	0.20 (30)	0.24 (41)	0.57 (114)
<b>Cu</b>	μgL <sup>-1</sup>	2.66 (42)	2.49 (71)	4.90 (139)
<b>Pb</b>	μgL <sup>-1</sup>	4.25 (43)	4.71 (62)	7.32 (130)
<b>Al</b>	μgL <sup>-1</sup>	191.0 (54)	224.51 (82)	427.2 (164)
<b>Ni</b>	μgL <sup>-1</sup>	11.33 (39)	12.18 (59)	12.84 (120)
<b>Cr</b>	μgL <sup>-1</sup>	3.06 (37)	5.85 (56)	7.92 (114)
<b>Zn</b>	μgL <sup>-1</sup>	19.42 (39)	15.03 (60)	29.28 (125)
<b>Fe</b>	μg/l	231.2 (34)	221.0 (69)	414.4 (121)

\* is the number of samples is given in parenthesis.

In Figure 4.10, the trajectory plots representing pH greater than 5 and pH lower than 5 are introduced. The red colored lines show parts of the trajectories, which are below 1000 m altitude. The yellow color shows trajectory segments that are between 1000 and 1500 m, green color indicates segments with altitudes 1500 – 2000 m and violet color indicate trajectory segments that are higher than 2000 m. Trajectories belong to pH greater than 5 are incorporated with the transportation alkaline nature of air masses from the North Africa to the region. On the contrary, the trajectories less than 5 indicate the transportation from Western European Countries, such as Spain, Italy, France and Balkan countries of Ukraine to the region where emissions are high due to industrialization and lack of emission control in Eastern European countries.

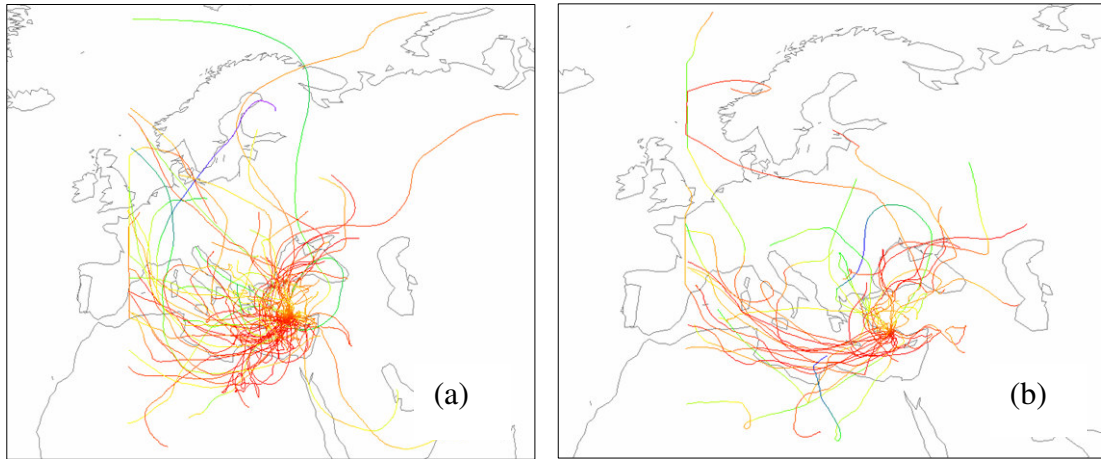


Figure 4.10 Trajectory plots of pH a) greater than 5 b) lower than 5.

Neutralization is the key feature of the rain and will be discussed briefly in the following sections.

#### 4.3.2. Neutralization of Acidity

Deposition of alkaline particles plays an integral role in relation to the issue of acidification through the ability of alkaline particles to neutralize acidity (Rodhe et al., 2002; Draaijers et al., 1997; Avila, 1996; Hedin et al., 1994).

Conducted studies have explained the fact that in higher annual pH values is not a direct indication of lack of pollution, but indicates a balance between  $\text{SO}_4^{2-}$  and  $\text{NO}_3^-$  ions and neutralizing species  $\text{Ca}^{2+}$  and  $\text{NH}_4^+$  (Rodhe et al., 2002; Tunçer et al., 2001; Kaya and Tuncel, 1997; Avila, 1996; Sanusi et al., 1996; Tuncel and Ungör, 1996; Al-Momani et al., 1995a; Guerzoni et al., 1995; Khwaja and Husain, 1990).

$\text{SO}_4^{2-}$  and  $\text{NO}_3^-$  ion concentrations imply the relative contribution of  $\text{H}_2\text{SO}_4$  and  $\text{HNO}_3$  to the rain water acidity, respectively. These relative contributions can change from one place to another. Until a decade ago, it was accepted that  $\text{H}_2\text{SO}_4$  and  $\text{HNO}_3$  was responsible from the 70% and 30% of the rain water acidity, respectively (NRC, 1983). However, today with more effective S removal in sources compared to  $\text{NO}_x$  control, relative contributions of  $\text{SO}_4^{2-}$  and  $\text{NO}_3^-$  to acidity in rain are approximately 50% each. The ratio of  $\text{SO}_4^{2-}$  to  $\text{NO}_3^-$  in rainwater is a measure of relative contributions of  $\text{H}_2\text{SO}_4$  and  $\text{HNO}_3$  to acidity. There is no acidity in rain water in the

Eastern Mediterranean region; consequently the term “relative contribution to acidity” is irrelevant. However, the  $\text{SO}_4^{2-}$  to  $\text{NO}_3^-$  ratio can be used as a crude indicator of source regions, because  $\text{SO}_4^{2-}/\text{NO}_3^-$  ratio is expected to be different at different parts of Europe. In the Western Europe effective S control in effect since mid-80s. However,  $\text{NO}_x$  control is not as effective (Lehmann, et al., 2005; Hayward, 2004; EPA, 2004; Avila and Alarcon, 2003; EEA, 2003; Puxbaum et al., 1998; Lynch et al., 1995; Hedin et al., 1994; Khwaja and Husain, 19991; Erisman et al., 1989). Therefore, low  $\text{SO}_4^{2-}/\text{NO}_3^-$  ratio is expected in air masses transported from western parts of Europe. In Eastern Europe and in Balkan countries, including Turkey, neither S nor  $\text{NO}_x$  control are effective, which means the ratio should be approximately 2.5 in air masses transported from Eastern Europe.

In Table 4.8, monthly average ( $\text{SO}_4^{2-}/\text{NO}_3^-$ ) ratios are presented together with (H/nss- $\text{SO}_4^{2-}+\text{NO}_3^-$ ), which will be discussed later in the manuscript. In Antalya station the ratio of  $\text{SO}_4^{2-}/\text{NO}_3^-$  is 2.65, that indicates the contribution of  $\text{H}_2\text{SO}_4$  and  $\text{HNO}_3$  are 73% and 27%, respectively. This high ratio is partly due to the lack of national S emission reductions and also indicates that Eastern Mediterranean region is influenced from pollution transport from Eastern European and Balkan countries.

Table 4.8 Median (H/nss- $\text{SO}_4^{2-}+\text{NO}_3^-$ ) and ( $\text{SO}_4^{2-}/\text{NO}_3^-$ ) ratios calculated for the whole dataset and for all months.

	H/nss- $\text{SO}_4^{2-}+\text{NO}_3^-$	$\text{SO}_4^{2-}/\text{NO}_3^-$
<b>Whole data set</b>	$3.44*10^{-5}$	2.653
<b>January</b>	$1.67*10^{-4}$	2.671
<b>February</b>	$4.45*10^{-5}$	4.803
<b>March</b>	$8.17*10^{-6}$	3.321
<b>April</b>	$1.36*10^{-5}$	3.053
<b>May</b>	$1.28*10^{-5}$	1.946
<b>June</b>	$1.18*10^{-5}$	1.151
<b>July</b>	$5.40*10^{-6}$	2.445
<b>August</b>	$3.13*10^{-6}$	1.639
<b>September</b>	$5.28*10^{-6}$	2.185
<b>October</b>	$1.86*10^{-5}$	1.292
<b>November</b>	$2.07*10^{-4}$	2.295
<b>December</b>	$2.71*10^{-4}$	4.217

In Figure 4.11 the monthly variations of median equivalent ratio of ( $\text{SO}_4^{2-}/\text{NO}_3^-$ ) was illustrated the case clearly. ( $\text{SO}_4^{2-}/\text{NO}_3^-$ ) ratio is higher during wet season compared to dry season. There are two reasons for this seasonal pattern. First it indicates that the region is influenced from western parts of the Europe in summer and Eastern part of Europe in winter. However, it is also known that coarse particles are scavenged out from atmosphere more efficiently than fine particles (Tuncel and Ungör, 1996), and a significant fraction of  $\text{NO}_3^-$  (approximately 70%) is associated with coarse particles, whereas almost all  $\text{SO}_4^{2-}$  is associated with fine particles in the atmosphere. Consequently, during the wet season,  $\text{NO}_3^-$  is removed faster from the atmosphere by wet deposition than  $\text{SO}_4^{2-}$ , resulting in higher  $\text{SO}_4^{2-}/\text{NO}_3^-$  ratio in particles. Since particle composition reflects in rain water composition, similar ratio is also observed in rain water. Probably both of these mechanisms do contribute to very significant difference in  $\text{SO}_4^{2-}/\text{NO}_3^-$  ratio between summer and winter seasons.

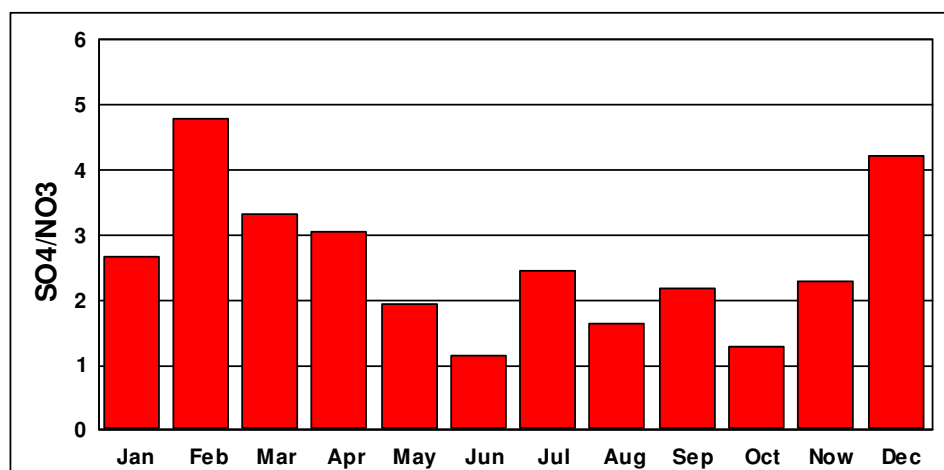


Figure 4.11 Monthly variations for the equivalent ratio of  $\text{SO}_4^{2-}/\text{NO}_3^-$  in rainwater.

Although  $\text{SO}_4^{2-}/\text{NO}_3^-$  ratio do provide insights on possible source regions affecting chemical composition of precipitation in the Eastern Mediterranean region, it does not tell anything about the extend of neutralization in rain water. Another ratio, namely ( $\text{H}^+/(n\text{ssSO}_4^{2-} + \text{NO}_3^-)$ ) is more informative for this purpose.

If the acidity is primarily originated from the  $\text{H}_2\text{SO}_4$  and  $\text{HNO}_3$  and if there is no neutralization, since these are strong acids and dissociate 100%,  $\text{H}^+/(n\text{ss-SO}_4^{2-} + \text{NO}_3^-)$  ratio approaches to unity. However, if all of the acid in rain water is neutralized than the ratio approaches to 0. Therefore,  $\text{H}^+/(n\text{ssSO}_4^{2-} + \text{NO}_3^-)$  ratio takes values between

0 and 1 and values close to zero indicate extensive neutralization in rain water, whereas values close to one indicates lack of neutralization.

Monthly variation of median for the equivalent ratio of  $(H^+/(nss-SO_4^{2-} + NO_3^-))$  in rainwater is presented in Figure 4.12. The median value of this ratio for the whole year is 0.000035, indicating that 99.99% of the acidity is neutralized in the Eastern Mediterranean rain water. However, the ratio shows a very strong seasonality with much more extensive neutralization during summer months. Please note in the figure that even in November, December and January, which are the months with the least neutralization, 75% - 85% of the acidity in rain is neutralized. Higher neutralization capacity was consistent with the atmospheric abundance of  $NH_3$  and  $CaCO_3$  which are the main neutralizing agents in rainwater and both of which have higher concentrations during summer months.

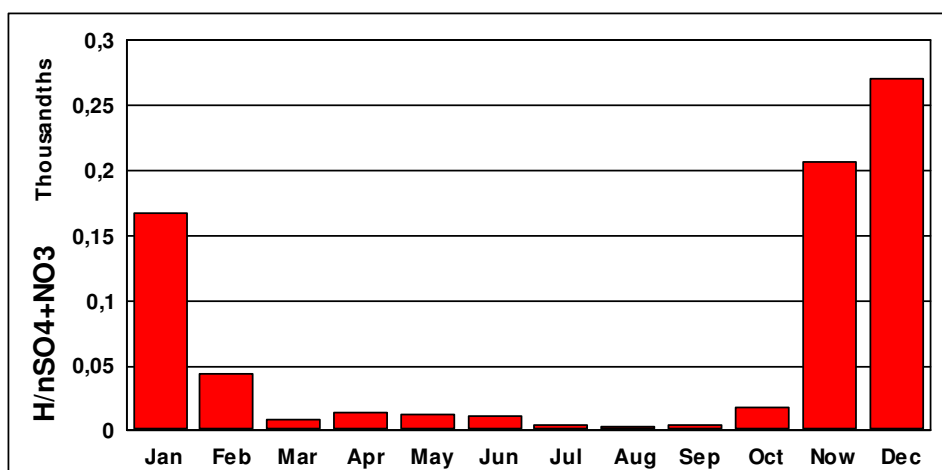


Figure 4.12 Monthly variations for the equivalent ratio of  $H^+/(nss-SO_4^{2-}+NO_3^-)$  in rain water.

The relationship between rainwater composition and rainfall amount is also reported in the literature. This may be significant in this study, because summers are extremely dry (with only 20% of the precipitation occurring between April and October) and winter months are very wet. This precipitation pattern seems to agree with monthly variation of  $H^+/(nssSO_4^{2-} + NO_3^-)$  ratio. We have investigated the relation between rainfall and  $H^+/(nssSO_4^{2-} + NO_3^-)$  ratio. The results are presented in Figure 4.13, where  $H^+/(nss-SO_4^{2-}+NO_3^-)$  ratio is plotted against precipitation amount. The ratio indicated that there was no clear correlation between  $H^+/(nss-SO_4^{2-}+NO_3^-)$

ratio and precipitation amount. Therefore, one could not expect higher neutralization of acidity with lower precipitation amounts in summer or vice versa.

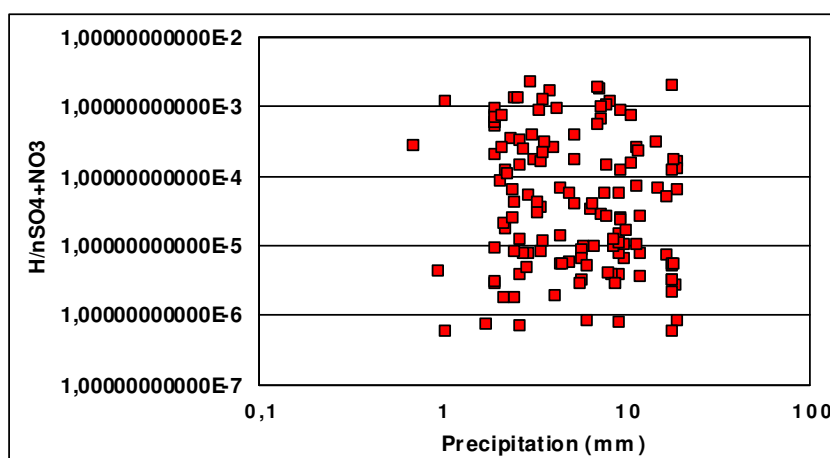


Figure 4.13 The relation between  $H^+/(nss-SO_4^{2-}+NO_3^-)$  ratio and the precipitation amount

Neutralization reactions take place in cloud and rain droplets, via in cloud and below cloud processes. Incorporation of bases in cloud droplets initiates the neutralization. By the way the transport of clouds from source region to receptor makes the in-cloud process regional. Below cloud neutralization is a local process that needs the bases of receptor site. (Tunçer, 2000)

Deposition of alkaline particles plays an important role in that they have ability to neutralize the acidified compounds (Draaijers et al., 1997; Hedin et al., 1994). The main neutralizing agents in the precipitation were  $CaCO_3$  and  $NH_3$  (Sanusi et al., 1996). The main sources of  $NH_3$  in precipitation are fertilizer applications.  $CaCO_3$  is produced from the  $CaCO_3$  rich in local soil and incursion of Saharan dust to the region.  $CaCO_3$  have coarse particles and have very short residence times in atmosphere. Therefore, neutralization by  $CaCO_3$  is a local process and occurs via below-cloud process (Tunçer, 2000; Al-Momani et al., 1997; Tuncel and Ungör, 1996).  $NH_3$  can be incorporated in rainwater through both in-cloud and below-cloud process (Al-Momani et al., 1997).

If precipitation acidity was originated from  $H_2SO_4$  and  $HNO_3$  and the neutralizing species are  $CaCO_3$  and  $NH_3$ , the sum of  $H^+$ ,  $Ca^{2+}$  and  $NH_4^+$  is expected to linearly

related with the sum of  $\text{SO}_4^{2-}$  and  $\text{NO}_3^-$ . In Figure 4.14, the plot of  $(\text{SO}_4^{2-} + \text{NO}_3^-)$  versus  $(\text{H}^+ + \text{Ca}^{2+} + \text{NH}_4^+)$  was given. The ratio of 0.79 indicates complete neutralization of acids by  $\text{CaCO}_3$  and  $\text{NH}_3$  species.

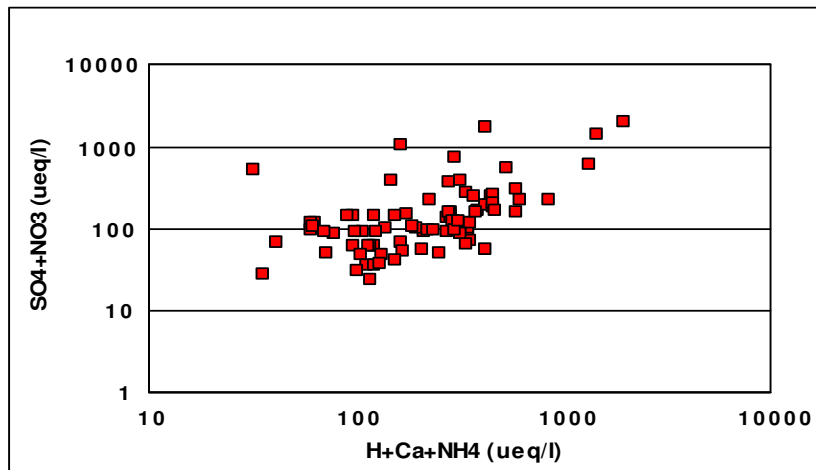


Figure 4.14 The plot of  $(\text{H}^+ + \text{Ca}^{2+} + \text{NH}_4^+)$  versus  $(\text{SO}_4^{2-} + \text{NO}_3^-)$  ( $\mu\text{eq/l}$ )

#### 4.4 Temporal Variability of Wet Deposition

Temporal variation of wet deposition provides information about the mechanism of particle transport from source region to receptor sites and their generation mechanisms. Temporal variations, is classified as short term (daily) variation and long term (seasonal) variations. Short term variations, which refer to few days long sudden increases and decreases in concentrations of measured species or episodes that provide information about the point sources, source regions and transport patterns (Güllü et al., 1998). Long term variations provide information about factors affecting ion compositions seasonally at the receptor site. Long term or seasonal variations can provide useful information on dependence of atmospheric burdens of species on seasonal changes in meteorology, such as changes in precipitation rate, or change in transport patterns, change in photochemistry etc.

Local and distant rain events have a profound influence on the chemical composition of aerosols and precipitation in the Mediterranean basin, in this respect rainfall amounts of 80% and 20%, in wet and dry season, respectively, have significance in explaining temporal variations (Al-Momani et al., 1998; Güllü et al., 1998; Kubilay and Saydam, 1995). Furthermore, seasonal differences in the frequencies of air mass

transport from different wind sectors are important, since these changes influence temporal behaviors of measured elements and ions (Güllü et al., 1998).

Detected episodic deviations in short term variations and seasonal variations in long term variations of ions will be discussed in the subsequent sections.

#### **4.4.1. Short Term (Daily) Variation**

Short term variations of  $\text{SO}_4^{2-}$ ,  $\text{NO}_3^-$  and  $\text{H}^+$  and backtrajectories corresponding to the episodes were presented in Figure 4.15.  $\text{H}^+$  ion has clearly higher concentrations in winter season.  $\text{SO}_4^{2-}$  and  $\text{NO}_3^-$  do not show a well defined seasonal pattern. Europe is a potential source of these ions particularly in winter season. However, more of the pollution derived elements that incorporate to clouds can reach to the Eastern Mediterranean region during summer season, since in winter season most of the particles are scavenged by wet deposition before reaching to our site (Al-Momani et al., 1998). In this respect, pollution derived elements were expected to be scavenged by wet deposition in summer season.  $\text{H}^+$  ion shows more regular seasonal pattern that episodic peaks occur mostly in winter season, because there is not much free  $\text{H}^+$  ion in the atmosphere during summer, as discussed in the previous section. Trajectories corresponding to  $\text{H}^+$  ion episodes do not show a specific directional preference, probably because  $\text{H}^+$  ion episodes are not only determined by transport of high concentrations of free acidity to the region, but also determined by the lack of neutralizing ions, namely  $\text{Ca}^{2+}$  and  $\text{NH}_4^+$ .

$\text{SO}_4^{2-}$  ion concentrations show strong episodic nature. This is not only specific to  $\text{SO}_4^{2-}$  ion but is observed for most of the elements and ions and not only in this study, but also in most of the studies performed in the Mediterranean region. The selected trajectories corresponding to  $\text{SO}_4^{2-}$  episodes have different directional preferences. Some of the trajectories follow a path along the western coast of the Mediterranean Sea, indicating that countries such as Italy, Greece, Spain and France can be the regions affecting  $\text{SO}_4^{2-}$  concentrations in the Eastern Mediterranean rain water. Some of the trajectories originate from North pointing Countries like Russia and Ukraine as potential source regions. There are also few trajectories that extend toward east and southeast.

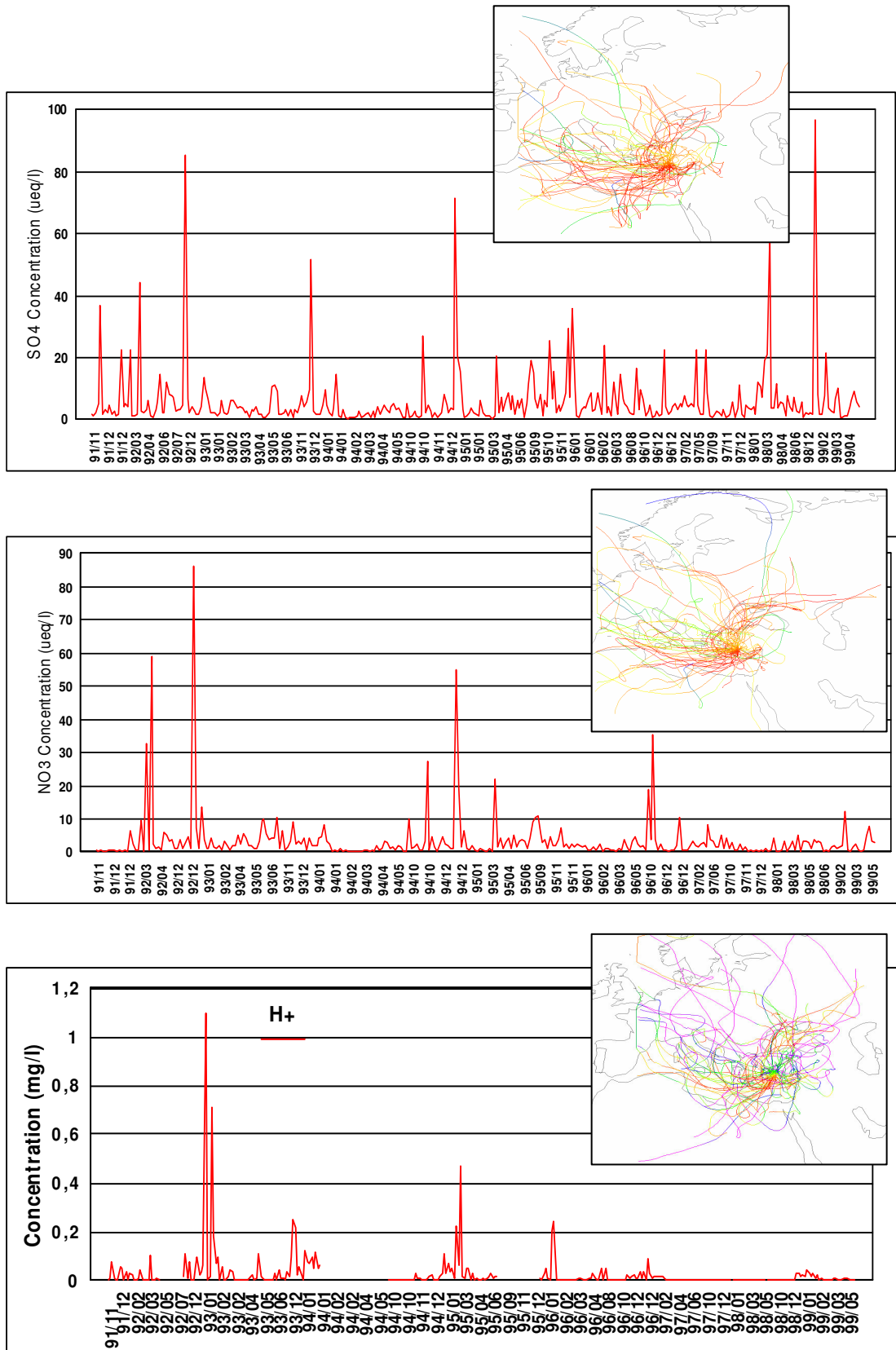


Figure 4.15 The time trend plot of SO<sub>4</sub><sup>2-</sup>, NO<sub>3</sub><sup>-</sup> and H<sup>+</sup> and corresponding backtrajectories.

The short term variability in  $\text{NO}_3^-$  concentrations and associated trajectories are very similar to those observed for the  $\text{SO}_4^{2-}$  ion. This is expected, because  $\text{SO}_4^{2-}$  and  $\text{NO}_3^-$  are always found to be strongly correlated with  $\text{NO}_3^-$  in most studies.

In Figure 4.16, time trend plot of  $\text{NH}_4^+$  was presented.  $\text{NH}_4^+$  concentrations does not indicate significant seasonal trend, although the contribution to the neutralization was significant and clearly observed.

The long term variations and episodic transport of  $\text{Ca}^{2+}$ ,  $\text{Mg}^{2+}$  and  $\text{K}^+$  were illustrated in Figure 4.17 and those of Al and Fe in figure 4.18. Concentrations of  $\text{Ca}^{2+}$ ,  $\text{Mg}^{2+}$  and  $\text{K}^+$ , Al and Fe also show strong variability. However, unlike anthropogenic elements, variability in concentrations of crustal elements is owing to natural sources. There are two sources of soil related elements; one of them is the resuspension of local soil by wind and the other one is incursion of Saharan dust. Generation of soil aerosol by wind and transport of dust from North Africa are both sporadic processes. The first one depends on the wind speed. Strong winds which blow for a day or two can generate a strong peak in concentrations of crustal elements. Similarly, Saharan dust incursion is also random in certain parts of the year. But when such transport from North Africa occurs, atmospheric loading of dust and concentrations of crustal elements increase to very high values. These concentrations go back to pre-plume values after the passage of Saharan dust plume, generating an episode in the concentrations of crustal elements. Most of the dust transport episodes are associated with rain, probably due to increased number of cloud condensation nuclei in the atmosphere during these events. When high loading of soil aerosol is washed with rain it generates an episode in rain as well.

The long term variations and episodic transport of sea salt elements were illustrated in Figure 4.19. Sea salt elements have higher concentrations and stronger variability particularly in winter season. The episodic behavior of sea salt elements is due to the variations in their source strengths that are closely related with meteorology. So that, sea salt elements were produced over the sea surface through bubble-bursting process that commonly associated with stormy weather (Güllü et al., 1998; Kubilay and Saydam, 1995). It was observed that sea salt elements  $\text{Na}^+$  and  $\text{Cl}^-$  have similar episodic patterns.

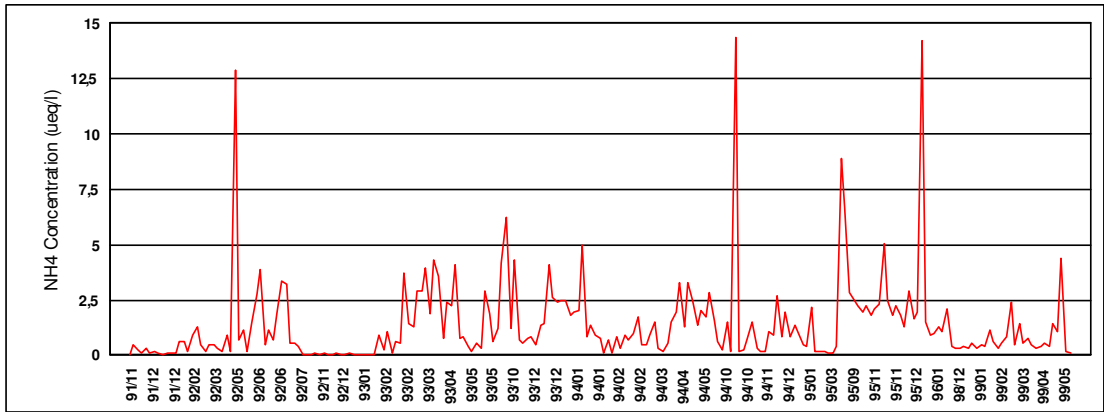


Figure 4.16 The time trend plot of NH<sub>4</sub><sup>+</sup>.

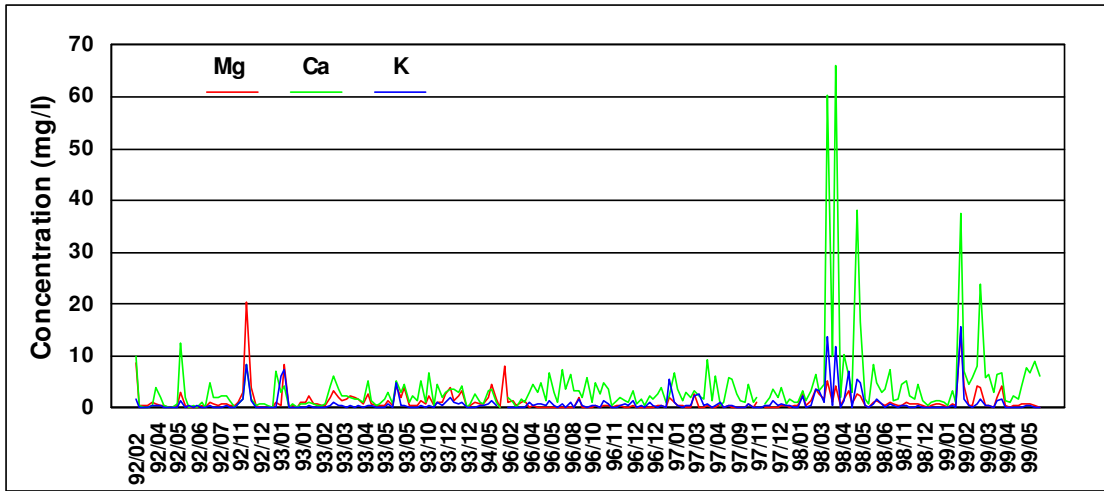


Figure 4.17 The time trend plot of Mg<sup>2+</sup>, Ca<sup>2+</sup> and K<sup>+</sup>.

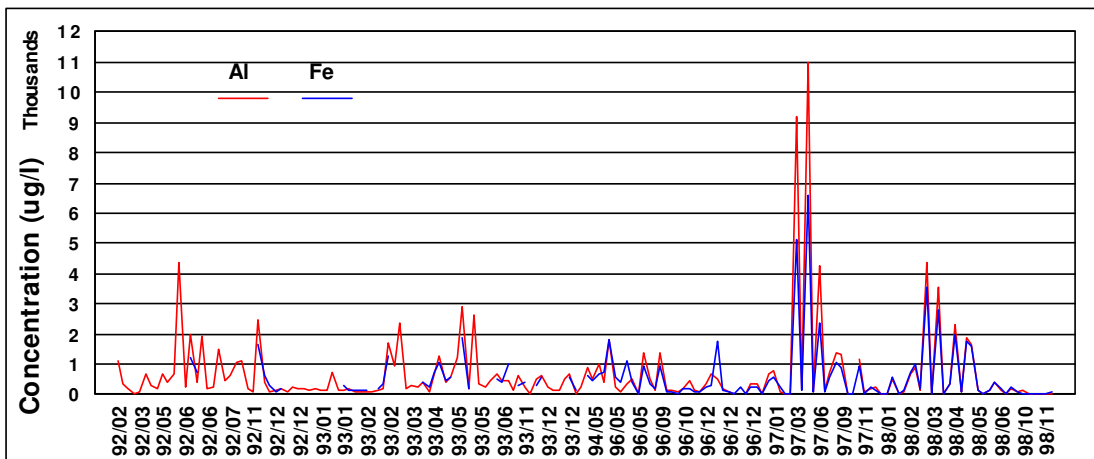


Figure 4.18 The time trend plot of Al and Fe.

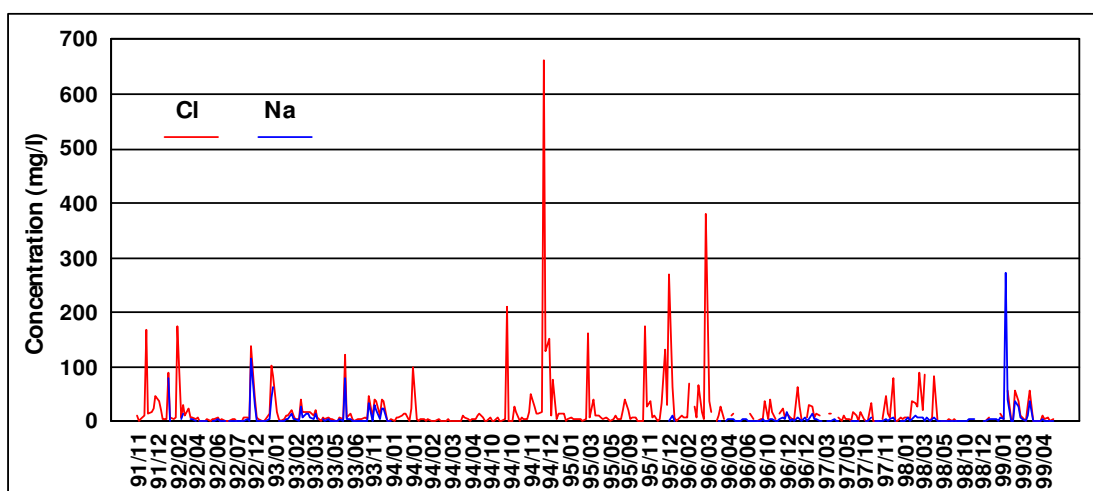


Figure 4.19 The time trend plot of  $\text{Na}^+$  and  $\text{Cl}^-$ .

In Figure 4.18, the time trend plot of Al and Fe was illustrated. Al and Fe show very close fluctuation pattern, which indicates that they have common sources of emissions and transport properties. Higher concentrations were observed during summer season compared to winter season due to the dried and suspended soil in summer season.

In Figure 4.20, time trend plot of Ni and Cr was illustrated. Ni and Cr show very close fluctuation pattern, which indicates that they have common sources of emissions and transport properties. The high Cr and Ni levels over the eastern Mediterranean basin is due to the presence of ophiolitic rocks that enriched with Cr and Ni bearing minerals, frequently outcrop on the coastal hinterland of the basin (Kubilay and Saydam, 1995; Tolun and Pamir, 1975).

Long term variation of Pb was illustrated in Figure 4.21, which does not show clear seasonal and episodic trends. Since being pollution derived elements, it was expected to have higher concentrations during summer season, which was similar to anthropogenic elements of  $\text{SO}_4^{2-}$  and  $\text{NO}_3^-$ .

Anthropogenic species is carried from Central and Western Europe to former USSR countries and Central Anatolia by the Atlantic polar frontal system. Further transport of pollutants from White Russia and Ukraine is occurred by Siberian frontal system.

Besides these, few episodes have been observed through Azor anticyclone which is effective from Eastern Mediterranean countries such as Italy and Greece and Basra frontal system through Middle East. (Tunçer, 2000; Al-Momani, 1995c)

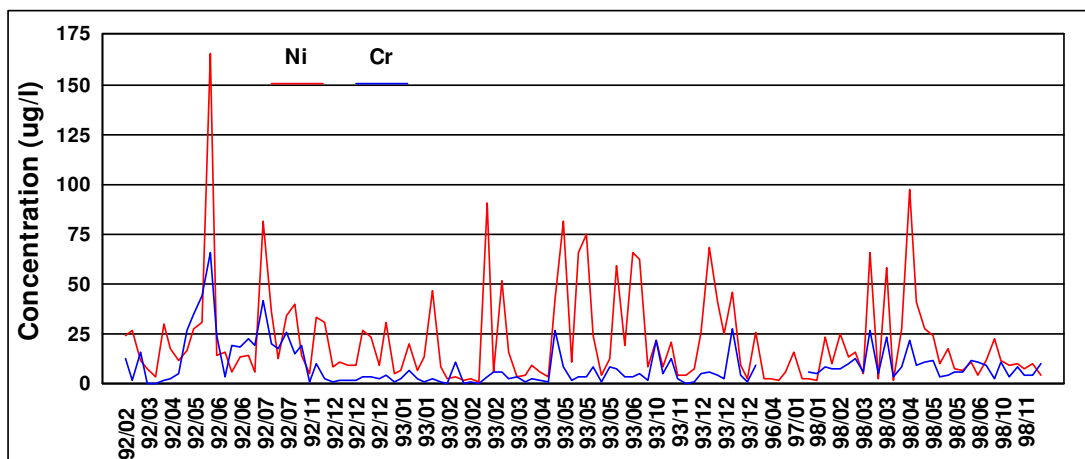


Figure 4.20 The time trend plot of Ni and Cr.

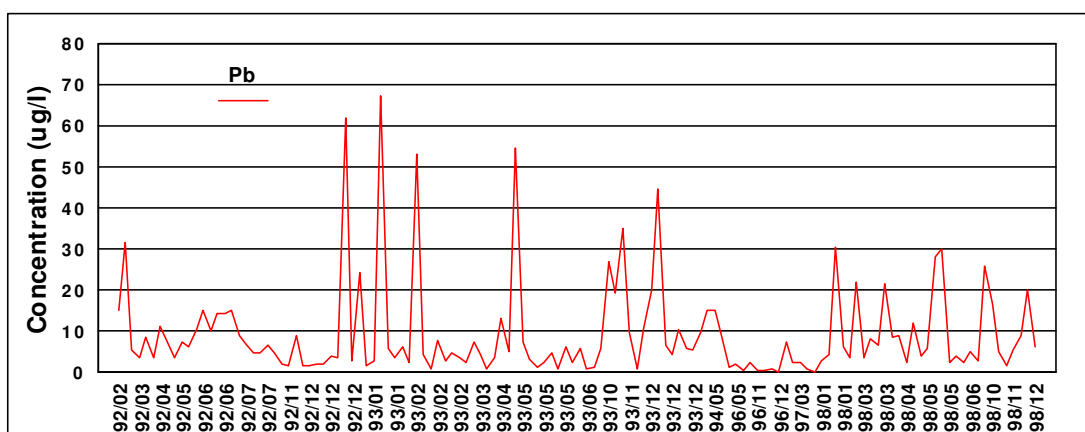


Figure 4.21 The time trend plot of Pb.

#### 4.4.1.1 Baseline concentrations of measured parameters

Background concentrations represent the regionally uniform concentrations of elements in a region without contribution of anthropogenic and natural transport of emissions. Regional background levels of elements and ions are important since the difference between the regional background and geometric mean is an indication of impact of episodic transport. There are different ways of calculating the regional background concentrations of elements which are as follows:

- (1) Manually deleting all the peak values of the data set,
  - (2) After fitting a curve to frequency distribution of the data, the maximum point for this curve is defined as the background level,
  - (3) Getting the most frequently occurring value as the background concentration.
- (Doğan, G., 2005)

In this study, baseline concentrations of elements and ions were calculated using the second approach, namely by drawing the best fit curve to the frequency distributions of the concentrations of elements and assigning the maximum point on the curve as the baseline concentration, and the results are represented in Table 4.9.

Table 4.9 Regional background concentrations.

	<b>Median</b>	<b>Whole dataset</b>	<b>Dry Season</b>	<b>Wet Season</b>	<b>Wet/dry</b>	<b>Percent concentrations Transported by episodes (%)</b>
<b>H<sup>+</sup></b>	0.0051	0.00015	0.00014	0.000155	1.11	97.06
<b>SO<sub>4</sub><sup>2-</sup></b>	3.22	1.2	1.765	1.06	0.60	62.73
<b>Nss-SO<sub>4</sub><sup>2-</sup></b>	2.42	0.8	1.03	0.68	0.66	66.94
<b>NO<sub>3</sub><sup>-</sup></b>	1.54	0.25	0.79	0.168	0.21	83.77
<b>NH<sub>4</sub><sup>+</sup></b>	0.78	0.082	0.264	0.062	0.23	89.49
<b>Cl<sup>-</sup></b>	7.29	1.265	1.49	1.46	0.98	82.65
<b>Na<sup>+</sup></b>	2.81	0.73	0.7	0.95	1.36	74.02
<b>Mg<sup>2+</sup></b>	2.16	0.14	0.136	0.134	0.99	93.52
<b>Ca<sup>2+</sup></b>	0.34		0.7			
<b>K<sup>+</sup></b>	2.81		0.112			
<b>Cd</b>	0.29	0.072	0.143	0.062	0.43	75.17
<b>Cu</b>	3.14	1.37	1.83	1.19	0.65	56.37
<b>Pb</b>	5.51	1.34	2.54	0.97	0.38	75.68
<b>Al</b>	242.57	37.2	93.5	28.4	0.30	84.66
<b>Ni</b>	12.84	4.3	4.65	4.14	0.89	66.51
<b>Cr</b>	5.34	1.49	2.84	1.255	0.44	72.10
<b>Zn</b>	18.75	2.85	6.9	1.4	0.20	84.80
<b>Fe</b>	245.63	27.6	107.6	20.7	0.19	88.76

As pointed before, the difference between the baseline concentration and average concentration for a measured parameter is an indication of the magnitude of episodic

variation in the concentrations. For anthropogenic elements and ions this shows the magnitude of episodic transport to the Eastern Mediterranean atmosphere.

The largest difference between baseline and average concentrations is observed for  $H^+$  ion (97%). This is because  $H^+$  ion concentration is determined by the concentrations of  $SO_4^{2-}$ ,  $NO_3^-$ ,  $Ca^{2+}$  and  $NH_4^+$ , all of which is highly episodic themselves.

For marine and crustal elements more episodic behavior was expected compared to pollution derived elements, because their short term variability is determined by variations in source strengths due to variability in wind speed, which is known to be highly variable. This is indeed what is observed, contributions of episodes on observed concentrations of elements and ions are between 80% and 90% for crustal and sea salt elements, but between 60% and 70% for anthropogenic elements and ions. The only exceptions of these ranges are observed for  $NH_4^+$  and  $NO_3^-$ , for which the episodic contributions were higher than 80%.

The baseline concentrations for sea salt elements were expected to be higher in winter than in summer. Winter to summer ratio is 0.98 for  $Cl^-$  and 1.36 for  $Na^+$ . The case can be explained by the increased wind speeds that generated more bubbles and so that the sea salt elements in winter season.

For combined crustal and marine elements of  $Ca^{2+}$ ,  $K^+$  and  $Mg^{2+}$  some missing values observed. For  $Mg^{2+}$ , summer and winter season background concentrations were very close to each other.

For anthropogenic trace metals such as Cd, Cu, Pb and Zn have lower wet to dry ratio, indicating that summer background concentration were significantly higher than winter background concentrations. Similarly, crustal originated elements of Al, Fe, Ni and Cr have the same trend compared to above anthropogenic trace metals. The case can not be explained by local sources since the station is away from pollution sources. Pollution derived elements reach to eastern Mediterranean region by long range transportation from Western Europe and rain out by these rains.

For the anions  $\text{SO}_4^{2-}$ ,  $\text{nss-SO}_4^{2-}$ ,  $\text{NO}_3^-$  background concentrations were higher in summer and lower in winter can be explained by the above reasons that long range transport of these elements and wash out by summer rains. The  $\text{NH}_4^+$  background concentrations were similarly higher in summer, which reflects the case of extensive usage of fertilizers and volatilization with higher temperatures in dry season.

The baseline concentrations of elements studied are not temporally uniform (probably also not spatially uniform as well), which we expected to see in the beginning of the exercise. Obviously, non episodic fractions in the concentrations of elements and ions are also influenced by local generation and transport processes. It is also interesting to note that for all elements and ions measured in this study, more than half of their average concentrations are due to episodic processes.

#### **4.4.2 Long Term (Seasonal) Variations**

Long term variation refers to the seasonal variations in the concentration of elements and corresponding factors affecting these variations. The main factors to determine the concentration of elements and ions in the Eastern Mediterranean region are the frequency of air mass movements from different sectors, particle scavenging and source strengths.

The most frequent air mass movements occur from the North, Northwest and West sectors indicating the contributions of high emission areas such as Western Europe, former USSR countries Ukraine and Russia and western parts of Turkey, which provide the potential pollution source regions to intercept in the eastern Mediterranean atmosphere (Güllü et al., 1998).

Monthly variation of  $\text{H}^+$  was illustrated in Figure 4.22.  $\text{H}^+$  ion concentration was clearly lower in summer season and higher in winter season. This was discussed previously and attributed to extensive neutralization occurs during summer season.

In the region, most of the rain fall shows dramatic differences between summer and winter seasons (with 80% in winter and 20% in summer) (Güllü et al., 1998; Kubilay and Saydam, 1995), which exhibits an important parameter to explain the seasonal

variations. Acidity was primarily occurred by  $\text{SO}_4^{2-}$  and  $\text{NO}_3^-$  ions in precipitation in the region. Monthly median concentration of  $\text{SO}_4^{2-}$  and  $\text{NO}_3^-$  ions was depicted in Figure 4.23.

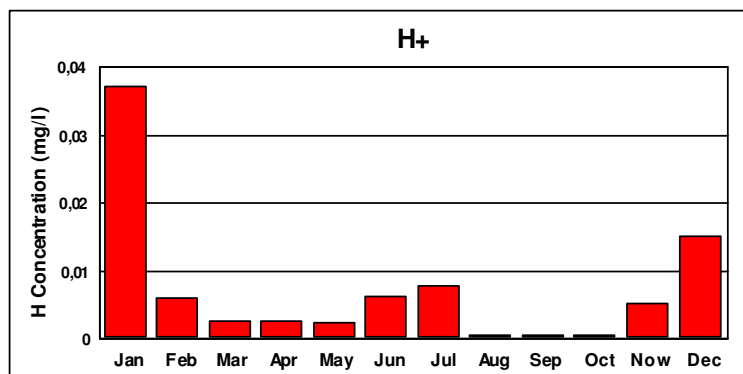


Figure 4.22 Monthly median concentrations of H<sup>+</sup>.

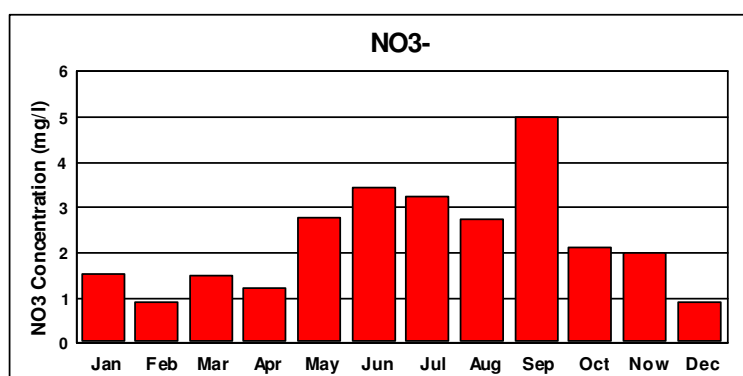
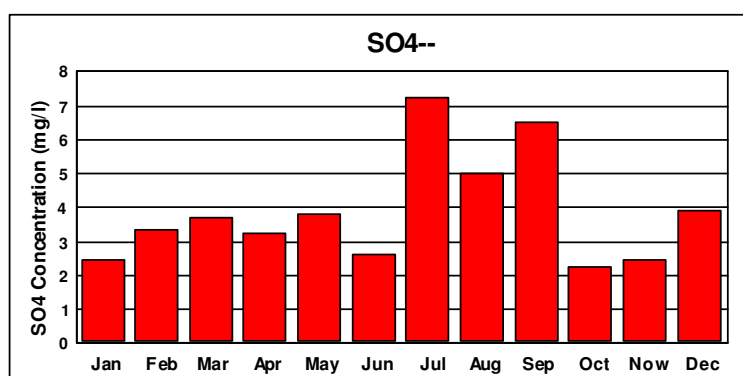


Figure 4.23 Monthly median concentrations of  $\text{SO}_4^{2-}$  and  $\text{NO}_3^-$ .

Increased concentrations of these ions during summer season and lower concentrations during winter season were observed. As previously mentioned, long range transport of these ions from Europe was dominant in eastern Mediterranean atmosphere, and higher concentrations during summer rains is due to more effective

scavenging during transport from distant source regions in summer months. Because of this, pollution derived ions and elements cannot survive to reach Eastern Mediterranean in winter either as particles or in cloud droplets. Furthermore, during summer season, higher solar flux enhances the photochemistry, which leads to formation of  $\text{SO}_4^{2-}$  and  $\text{NO}_3^-$ .

In Figure 4.24, monthly median concentrations of  $\text{NH}_4^+$  are presented. It was observed that  $\text{NH}_4^+$  ions dominate during summer season which can be explained by the extensive usage of  $\text{NH}_3$  containing fertilizers in agricultural activities and enhanced volatility of it during higher temperatures of summer season. An increase in  $\text{Ca}^{2+}$  and  $\text{NH}_4^+$  concentrations clearly explain the reduced  $\text{H}^+$  ions during summer season.

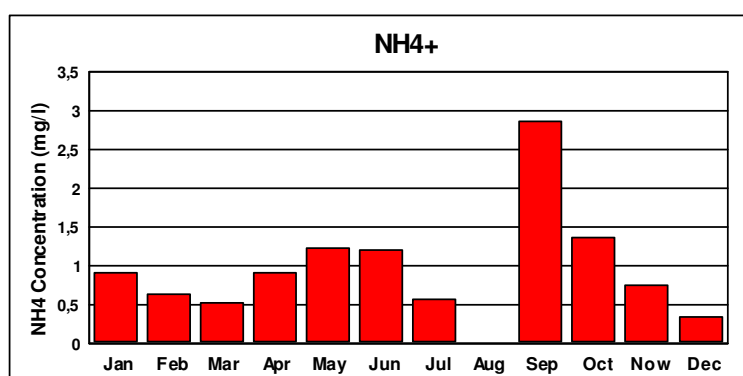


Figure 4.24 Monthly median concentrations  $\text{NH}_4^+$ .

Monthly median concentrations of marine elements of  $\text{Na}^+$  and  $\text{Cl}^-$  were depicted in Figure 4.25. These elements show consistent seasonal variations with higher concentrations in winter season and lower in summer season. As mentioned previously, in wet season, due to the increased wind speeds, bubble-bursting over sea surface generates sea salt elements and therefore increase their contribution to the atmosphere.

Median concentrations of crustal originated Al, Fe,  $\text{Ca}^{2+}$ , Ni and Cr are presented in Figure 4.26. They all show higher concentrations in the summer season. This is explained by local generation of soil aerosols in the atmosphere which are subsequently captured in rain water. Resuspension of surface soil is the main source for these elements. Resuspension is very limited in winter when surface soil is wet

(muddy), but during summer, when surface soil becomes dry, soil particles can easily resuspend into atmosphere by the wind action. This mechanism generates higher concentrations of crustal elements in summer period. Resuspension of surface soil is not the only source for Ni and Cr. Concentrations of these elements have anthropogenic components as well. However, soil on the Mediterranean coast of Turkey is highly enriched in Ni and Cr, as mentioned previously, which masks anthropogenic fractions of Ni and Cr.

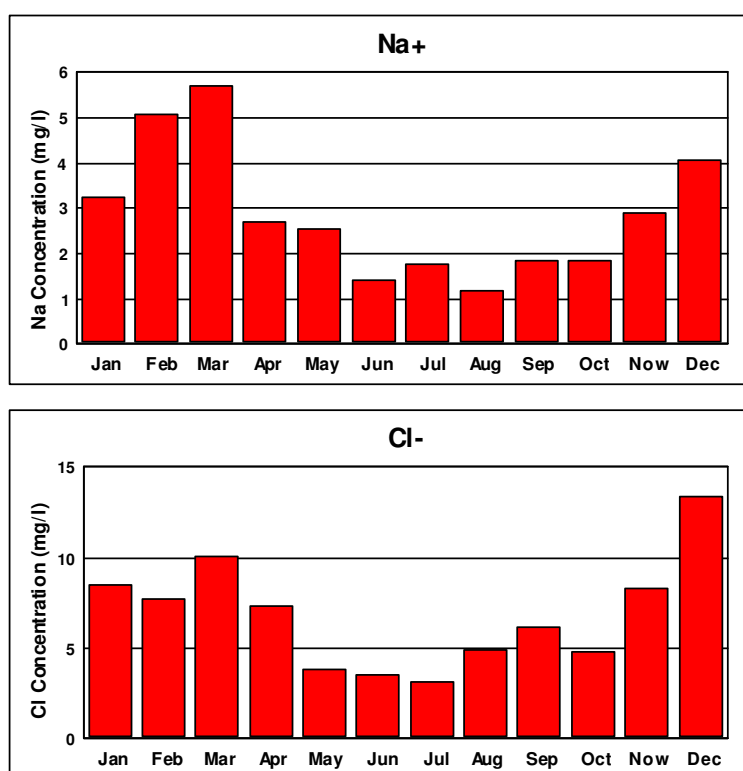


Figure 4.25 Monthly median concentrations of Na<sup>+</sup> and Cl<sup>-</sup>.

Figure 4.26 show similar trends, that concentrations of Fe, Ni, Cr and Ca<sup>2+</sup> were higher in summer season and lower in winter season, can be explained by the same reason with Al element. Monthly median concentrations of Mg<sup>2+</sup> and K<sup>+</sup> are depicted in Figure 4.27. These two elements have mixed crustal and marine sources. The seasonal pattern observed in Mg concentration closely resembles the patterns observed in purely marine elements, indicating that Sea salt is the main source of Mg. Seasonal pattern observed in K<sup>+</sup> is more in between in the patterns observed in crustal and marine elements, suggesting that sea salt and soil contributes approximately equally to observed K concentrations.

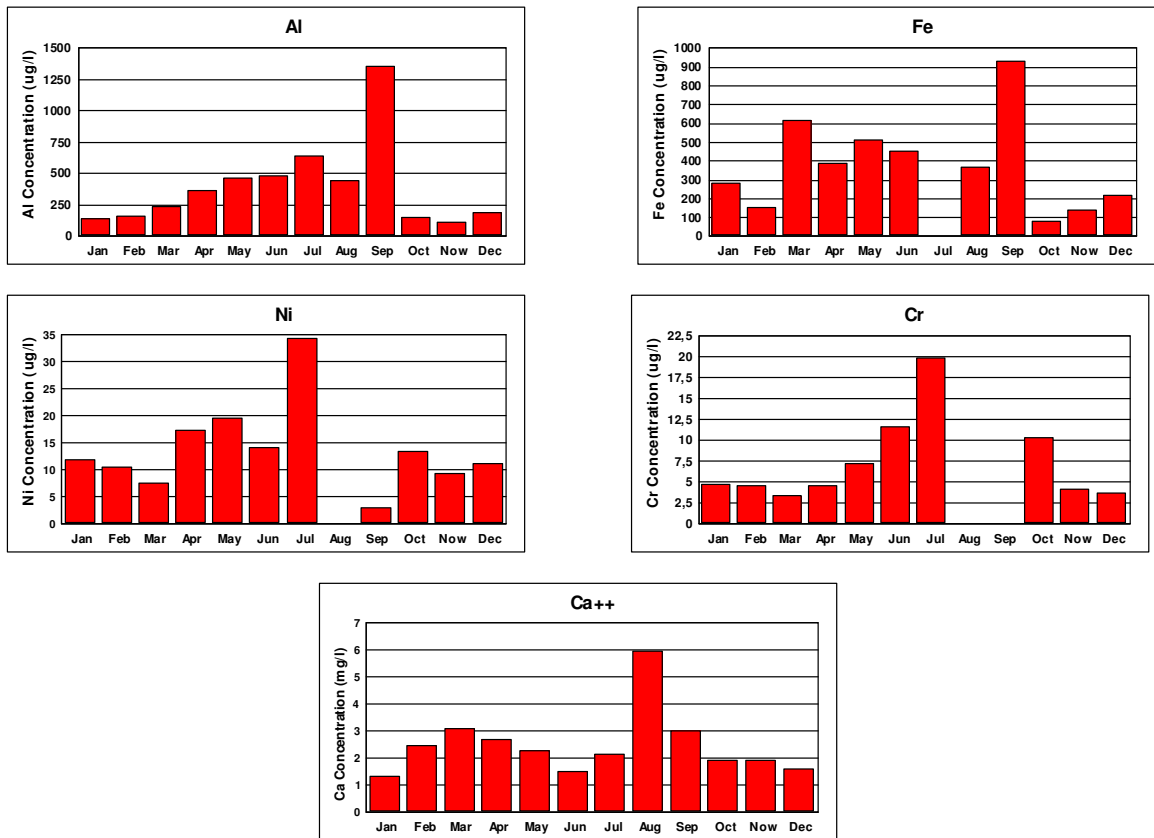


Figure 4.26 Monthly median concentrations of Al, Fe, Ni, Cr and Ca<sup>2+</sup>.

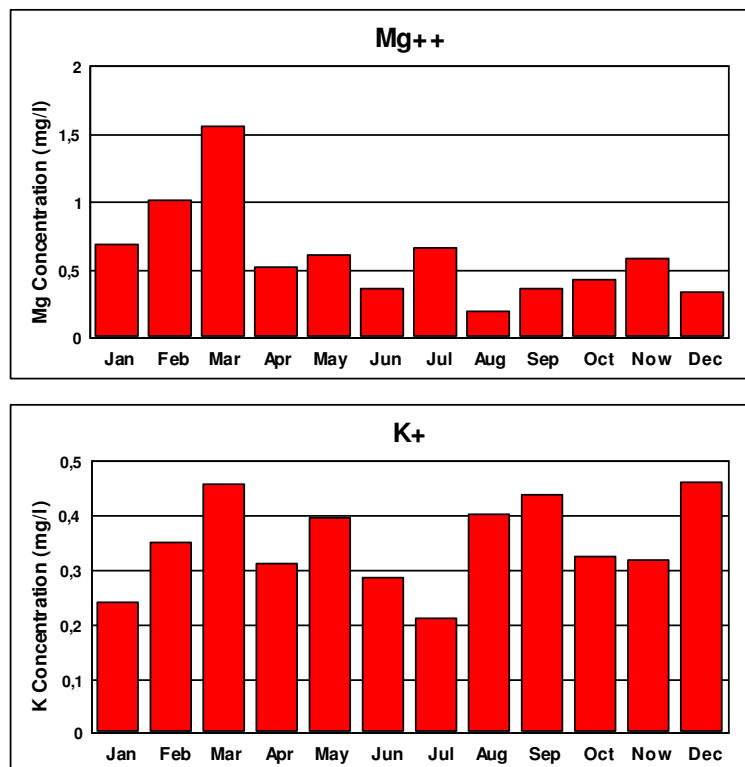
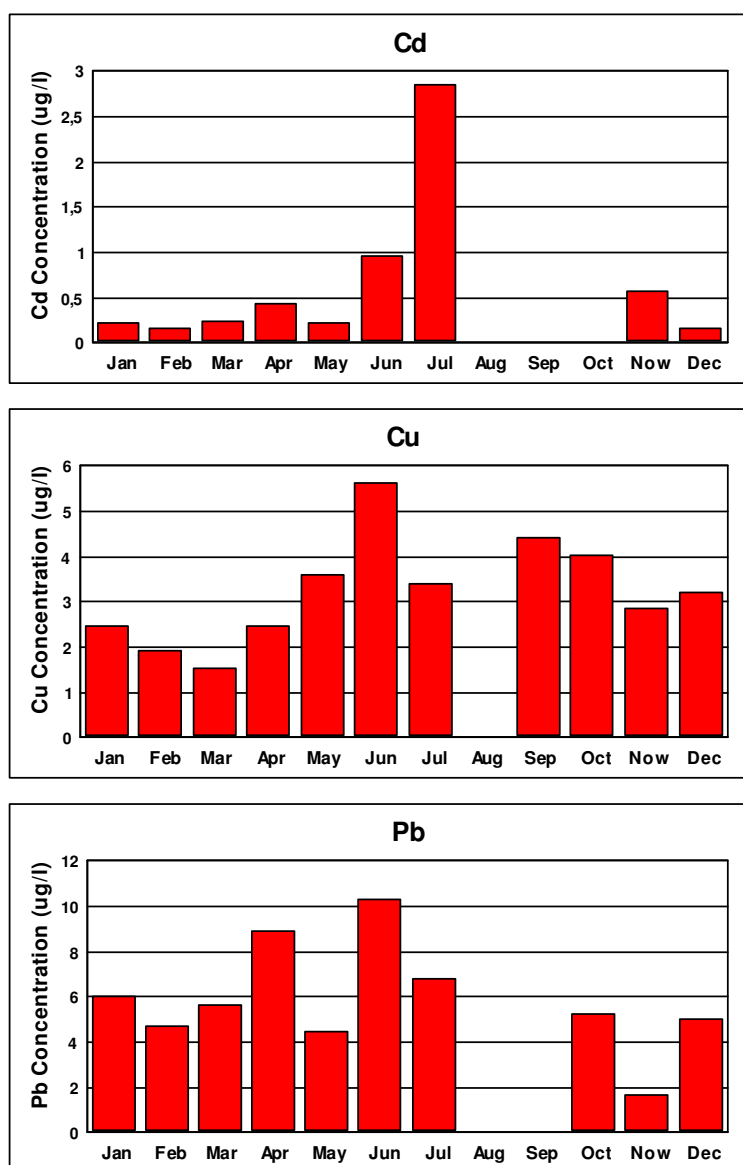


Figure 4.27 Monthly median concentrations of Mg<sup>2+</sup> and K<sup>+</sup>.

Seasonal variations on the concentrations of anthropogenic elements Cd, Cu, Pb and Zn were depicted in Figure 4.28. Some missing values of these elements prevent clear illustrations. Elements Pb, Cd and Cu have higher concentrations in summer. These are typical patterns expected from elements, which are transported to the Eastern Mediterranean by long range transport. As discussed with  $\text{SO}_4^{2-}$  and  $\text{NO}_3^-$ , this pattern is due to more extensive scavenging of these elements from atmosphere in winter season. Zinc on the other hand does not show a clear seasonal pattern. In the previous studies it was demonstrated that elements with local sources do not show a clear seasonal pattern as they are not scavenged as effectively as the elements transported from distant sources. This may also be the reason for lack of seasonal pattern observed in Zn concentrations.



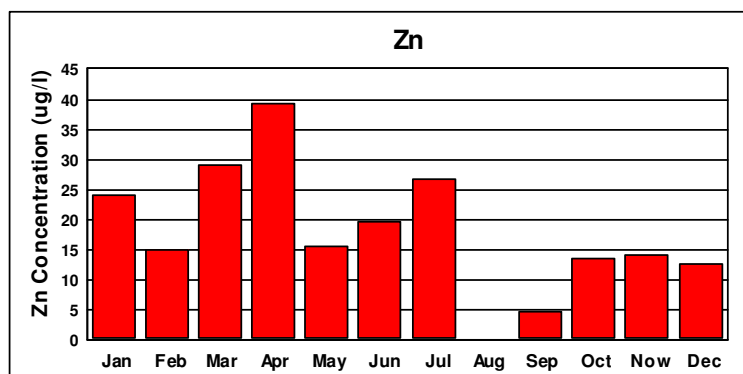


Figure 4.28 Monthly median concentrations of Cd, Cu, Pb and Zn.

#### 4.5. Time Trend Analysis

Time trend analysis was performed to observe the behavior of ions and elements in time and in this respect to set emission reduction policies on regional scale. In Europe, the general trend of acidifying compounds tends to decrease due to the strict emission reduction policies applied. In Europe, the EU countries and Accession Countries have achieved 39% and 53% reduction in acidifying compounds, which are mainly sulfur compounds between the years 1990 and 2000 (EEA, 2003b). On the other hand it was implied that in Turkey, the emissions of acidifying compounds have been increased as 66% between the years 1990 and 2002 (EEA, 2005).

Time trend analysis of ions and elements were performed by using least squares general linear model. Logarithmic concentrations of elements were used since they have nearly normal distributions (Lynch et al., 1995).

$$\text{Log}(C_y) = b_o + b_1 y \quad (4.4)$$

Where  $C_y$  is the measured concentration of a given ion at time  $y$ ,  $b_o$  is the intercept,  $b_1$  is the slope of the long term log-concentration trend and  $y$  is the corresponding day of sampling.

The results of the time trend analysis for major ions and elements were presented in Table 4.10. The ions and elements that denote significant trend was evaluated by the p-value and Durbin Watson Statistics. The ions and elements have p values lower

than 0.1 show significant trend at 90% or more confidence level.  $\text{H}^+$ ,  $\text{NO}_3^-$ ,  $\text{NH}_4^+$ ,  $\text{Mg}^{2+}$ ,  $\text{Ca}^{2+}$ ,  $\text{K}^+$ , Cd, Al, Cr, Zn and Fe show significant trend for 90% or more confidence level. Among these,  $\text{H}^+$ ,  $\text{NO}_3^-$ , Mg and Al show a decreasing trend in time, whereas  $\text{NH}_4^+$ , Ca, K, Cd, Cr, Zn and Fe show an increasing trend between 1991 and 2000. Some of these assessments are uncertain due to limited number of data included in statistics. Although time-span of measurements is approximately 10 years, data for some of the elements is scarce, as they are not measured in all of the collected samples. Data for  $\text{H}^+$ ,  $\text{SO}_4^{2-}$ ,  $\text{NO}_3^-$  and  $\text{NH}_4^+$  are adequate for trend assessments.

Studies performed in Europe demonstrated a significant decrease in concentrations of not only ions but also of anthropogenic elements. The variation  $\text{H}^+$ ,  $\text{SO}_4^{2-}$ ,  $\text{NO}_3^-$  and  $\text{NH}_4^+$  in EMEP network is depicted in Figure 4.29. An obvious decrease in the concentrations of  $\text{SO}_4^{2-}$ ,  $\text{H}^+$  and  $\text{NH}_4^+$  can be clearly seen in the Figure. In some parts of the Europe this decrease is as high as 70% in last 10 years. The decrease in the concentrations of  $\text{NO}_3^-$  is not as obvious as those observed in the concentrations of  $\text{H}^+$ ,  $\text{SO}_4^{2-}$  and  $\text{NH}_4^+$ . This is because the protocol that leads to reductions observed in concentrations of pollutants became effective much later for  $\text{NO}_x$ .

The time dependent decreases in the concentrations of measured parameters observed in this study are not as obvious as those observed in other parts of Europe. And in some cases we observed increase in concentrations, rather than expected decrease. This is not only true for rain water composition investigated in this study, but also observed in aerosol composition as well.

This observation is important, because it means that, over the time concentrations of ions measured in the Eastern Mediterranean precipitation is expected to become smaller than the corresponding concentrations measured in other parts of Europe. This is what is observed both in the compositions of rain water and particles. The same observation also suggests that the concentrations of ions in the Eastern Mediterranean precipitation is determined by the pollutants emitted in regions such as Balkan Countries, parts of Turkey and countries such as Ukraine and Russia, because these are the regions in Europe where  $\text{SO}_2$  emissions are not effectively reduced.

Table 4.10 Linear Regression analysis to determine time trends.

Variable	Unit	Number of samples (N)	Intercept (b <sub>0</sub> )	Slope (b <sub>1</sub> )	Coefficient of determination r <sup>2</sup> (%)	Durbin Watson Statistics	P value
H <sup>+</sup>	mg/l	302	-1.85	-0.00032	10.08	0.90	0.0000*
SO <sub>4</sub> <sup>2-</sup>	mg/l	336	0.48	0.00004	0.60	1.43	0.1560
NO <sub>3</sub> <sup>-</sup>	mg/l	297	0.27	-0.00008	1.13	1.47	0.0672*
NH <sub>4</sub> <sup>+</sup>	mg/l	223	-0.30	0.00012	2.43	0.79	0.02*
Cl <sup>-</sup>	mg/l	341	0.90	3.76*10 <sup>-7</sup>	2.62*10 <sup>-5</sup>	1.33	0.9925
Mg <sup>2+</sup>	mg/l	218	-0.11	-0.00008	1.67	1.17	0.0566*
Ca <sup>2+</sup>	mg/l	218	0.005	0.00021	15.60	1.54	0.0000*
K <sup>+</sup>	mg/l	219	-0.54	0.00009	2.30	1.49	0.0254*
Na <sup>+</sup>	mg/l	218	0.61	-0.00006	0.96	1.41	0.1505
Cd	µg/l	87	-0.62	0.00025	11.54	0.91	0.0013*
Cu	µg/l	139	0.58	-0.00006	1.59	1.63	0.139
Pb	µg/l	130	0.76	-0.00005	0.68	1.44	0.35
Al	µg/l	164	2.60	-0.00014	4.17	1.95	0.0087*
Ni	µg/l	120	1.20	-0.00007	1.75	1.61	0.1500
Cr	µg/l	114	0.64	0.00009	3.01	1.24	0.0065*
Zn	µg/l	125	1.45	0.00015	5.45	0.81	0.0088*
Fe	µg/l	121	2.74	0.00023	8.63	1.98	0.0011*

\* show significant trend

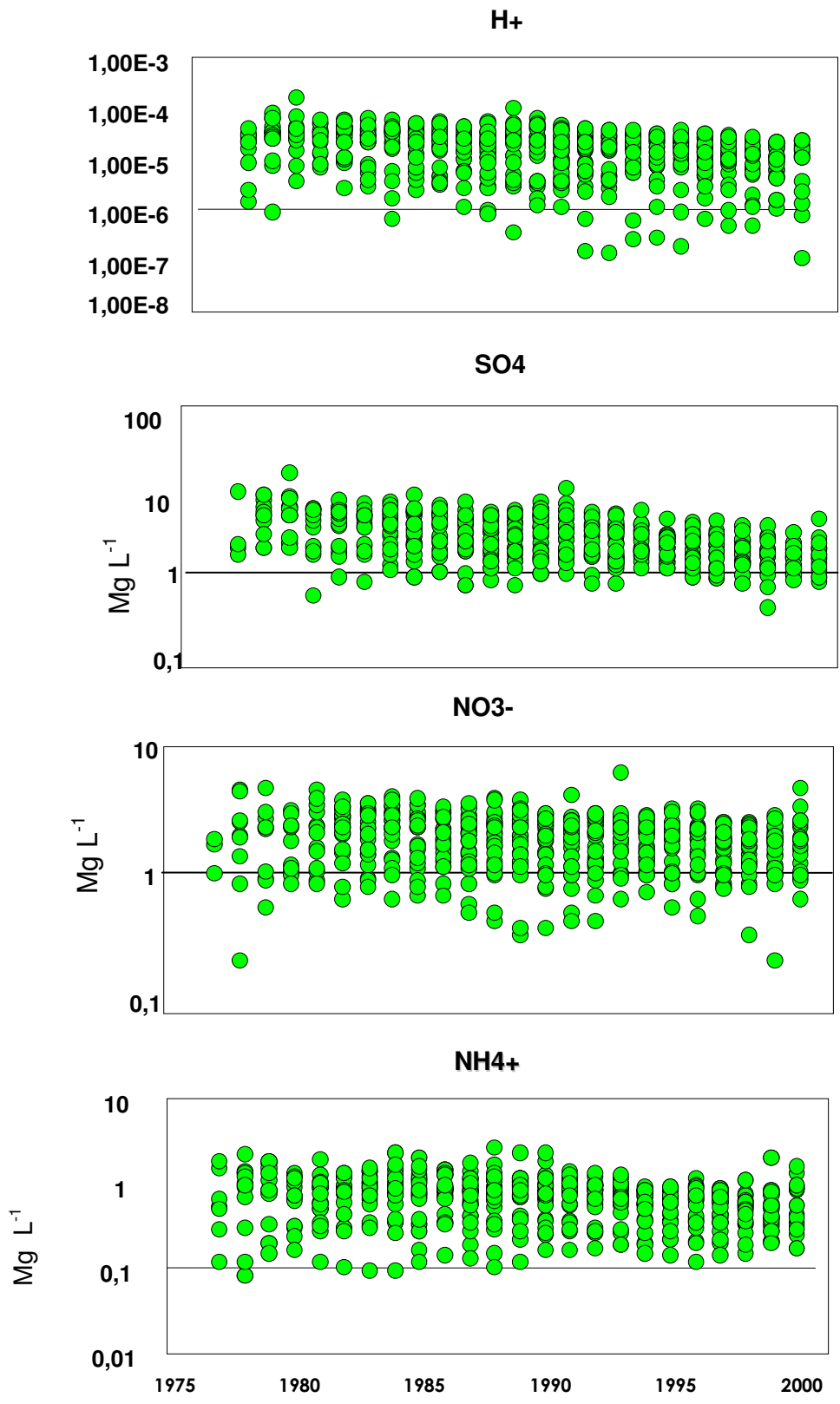


Figure 4.29 The time trend distribution of H<sup>+</sup>, SO<sub>4</sub><sup>2-</sup>, NO<sub>3</sub><sup>-</sup> and NH<sub>4</sub><sup>+</sup> among the EMEP Stations between the years 1991-1999.

For further indication of significant trend we have investigated Durbin Watson Statistics. The ions and elements having DW Statistics higher than 1.4, indicate lack of auto correlation between residuals, which verify the assumption of normally distributed residuals of the regression model. The ions and elements of  $H^+$ ,  $NH_4^+$ ,  $Cl^-$ ,  $Mg^{2+}$ , Cd, Cr and Zn show significant trend in terms of DW statistics as well.

One interesting feature observed in trends of elements is the increasing trend consistently observed for all crustal elements. The reason for this observation is not clear, but may indicate increased aridity in the region or increased frequency of transport of North African dust can cause observed increases in the concentrations of soil related elements. However, these are serious proposals and needs to be investigated further.

#### **4.6. Wet Deposition Fluxes**

Atmospheric input of pollutants such as trace elements is particularly important in semi-enclosed seas such as Mediterranean and Black sea, which are close to potential pollution sources in Northern Europe (Al-Momani, 1995c).

In this study, the wet deposition flux of any elements and ions was calculated by multiplying daily precipitation amount (in mm) and concentration of that specie in that sample (in  $mg L^{-1}$ ). Wet deposition fluxes calculated per event basis were then added appropriately to calculate monthly, seasonal and annual wet fluxes of elements and ions.

Many factors affect the major ions and trace elements to display different seasonal variations depending on their nature and strength of their contamination sources, monthly precipitation amounts, major wind directions, mixing heights and hours of dry weather (Hu and Balasubramanian, 2003; Kaya and Tuncel, 1997).

The dependence of wet deposition on precipitation amount is explained by the following power relation (Khwaja and Husain, 1991; Lindberg, 1982):

$$D = a * P^b \quad (4.5)$$

Where D is the deposition flux, P is the precipitation amount and a and b are constants. Regression analysis was performed by taking the logarithm of the deposition fluxes of the whole ions and elements as the dependent variable and the logarithm of the precipitation amounts as the independent variable. The results of regression analysis of wet deposition fluxes with precipitation were presented in Table 4.11. Correlation coefficients ranging between 0.85 and 0.99 clearly demonstrate that the wet deposition flux is logarithmically related with the precipitation amount, as suggested by Khwaja and Husain (1991) and Lindberg (1982). Furthermore, b values near unity indicate that the relation is approximately linear. However, note that the regression was performed on log-transformed deposition data and linear relation between precipitation amount and log-deposition flux indicates a logarithmic relation between deposition flux and rainfall. A similar logarithmic relation between wet deposition flux and rainfall was also proposed in previous studies (Khwaja and Husain, 1991). Log-log plots for wet deposition flux of  $H^+$ ,  $SO_4^{2-}$ ,  $NO_3^-$ ,  $NH_4^+$ ,  $Ca^{2+}$ ,  $Cl^-$ , Cu and Al vs. precipitation amount are given in Figure 4.30. The plots in the figure show a clear correlation between the wet deposition flux and precipitation amount for all the species included.

Table 4.11 Results of regression analysis of wet deposition fluxes with precipitation.

<b>Variable</b>	<b>Intercept (log a)</b>	<b>Slope (b)</b>	<b>r</b>
<b>H<sup>+</sup></b>	-2.70	1.19	0.93
<b>SO<sub>4</sub><sup>2-</sup></b>	0.64	0.93	0.99
<b>NO<sub>3</sub><sup>-</sup></b>	0.52	0.84	0.98
<b>NH<sub>4</sub><sup>+</sup></b>	-0.01	0.94	0.95
<b>Cl<sup>-</sup></b>	0.62	1.13	0.99
<b>Mg<sup>2+</sup></b>	-0.36	1.08	0.98
<b>Ca<sup>2+</sup></b>	0.41	0.96	0.98
<b>K<sup>+</sup></b>	-0.49	1.02	0.99
<b>Na<sup>+</sup></b>	0.23	1.13	0.99
<b>Cd</b>	-2.92	0.70	0.93
<b>Cu</b>	-2.37	0.91	0.99
<b>Pb</b>	-2.13	0.92	0.97
<b>Al</b>	-0.21	0.78	0.96
<b>Ni</b>	-2.04	0.98	0.97
<b>Cr</b>	-1.92	1.04	0.96
<b>Zn</b>	-1.92	1.08	0.97
<b>Fe</b>	-0.28	0.85	0.95

#### 4.6.1. Seasonality of Wet Deposition Fluxes

Annual and seasonal average wet deposition fluxes corresponding to the measured ions were introduced in Table 4.12. In the calculation of annual wet deposition fluxes, median monthly concentrations of each ion and elements were found and are multiplied by the rainfall for the corresponding month, which were obtained from the General Directorate of Meteorology. This approach provides a better wet deposition flux values over long periods, because some of the rain events may not be sampled over the years and if those are not included, wet deposition fluxes can be underestimated. Such a problem can be avoided if met rainfall and monthly averages are used in flux calculations. Total masses of elements and ions deposited to the Eastern Mediterranean basin, where have a catchment area of 650000 km<sup>2</sup>, were calculated and presented in Table 4.13.

Deposition fluxes of all of the ions and elements increased until 1997 remained the same in 1998 and decreased in 1999. However, the decrease in wet deposition of all species observed in 1999 is an artifact, because in that particular year data were available until August and wet deposition fluxes were low, because half of the wet season (October – December) were not included in calculations. The observed trend in wet deposition fluxes of elements and ions are consistent with the variation of annual rainfall in the same period. Wet fluxes are significantly high in wet season since the 80% of the rain in Eastern Mediterranean falls in this season. For all the ions and elements, wet to dry ratios range between 6 and 47. For all elements and ions winter deposition fluxes (wet season) are higher than summer wet fluxes. This is due to higher rainfall during winter period. However, the magnitude of the wet-to-dry season flux ratio depends not only on the differences in summer and winter rainfall, but also due to differences in seasonal average concentrations. For the elements and ions which have higher concentrations during winter, such as H<sup>+</sup>, Na and Cl the ratio is > 15. However for the elements that has higher concentrations during summer season, such as crustal and anthropogenic elements, the ratio varies between 5 and 10.

Table 4.12 Annual and seasonal average wet deposition fluxes corresponding to the measured ions (mg/m<sup>2</sup>).

	1991	1992	1993	1994	1995	1996	1997	1998	1999	Wet Season	Dry Season	Wet/Dry
<b>H<sup>+</sup></b>	10.3	4.6	13.3	14.6	11.1	20.8	13.5	17.5	11.4	114.8	2.4	47.6
<b>SO<sub>4</sub><sup>2-</sup></b>	2735.2	2178.3	2894.4	3581.1	3839.4	4717.8	5115.5	4345.4	1949.2	27989.4	3366.9	8.3
<b>NO<sub>3</sub><sup>-</sup></b>	738.0	976.6	1585.0	2019.1	2077.8	1764.4	2392.6	1827.1	874.1	12251.2	2003.4	6.1
<b>Cl<sup>-</sup></b>	9320.8	6413.5	7571.6	10300.4	11541.5	14291.7	13778.6	12933.8	5375.2	86320.4	5206.8	16.6
<b>NH<sub>4</sub><sup>+</sup></b>	289.3	395.2	796.5	1060.1	860.2	936.4	1165.1	932.6	481.2	5883.9	1032.7	5.7
<b>Mg<sup>2+</sup></b>	270.3	526.0	723.1	768.4	975.6	921.3	841.8	890.9	608.8	6059.5	466.7	13.0
<b>Ca<sup>2+</sup></b>	1174.4	1449.6	1913.7	2400.3	2648.2	2734.9	3112.0	2641.7	1378.2	17043.7	2409.2	7.1
<b>K<sup>+</sup></b>	323.5	259.4	324.4	426.4	460.5	536.3	576.3	499.7	208.4	3298.4	316.4	10.4
<b>Na<sup>+</sup></b>	2850.4	2631.8	3389.5	4071.2	4678.9	5391.4	5043.3	5066.2	2699.0	33834.4	2187.3	15.5
<b>Cd</b>	0.2	0.2	0.2	0.3	0.5	0.3	0.5	0.3	0.2	2.1	0.5	4.5
<b>Cu</b>	2.3	1.7	2.6	3.7	3.3	3.9	4.6	3.7	1.4	24.0	3.0	8.0
<b>Pb</b>	3.4	2.8	4.9	5.9	4.9	7.5	7.9	6.9	3.7	41.0	6.9	5.9
<b>Al</b>	134.0	131.7	202.2	203.0	222.4	260.0	388.8	255.2	120.0	1480.9	436.4	3.4
<b>Ni</b>	7.9	6.6	11.5	14.2	12.7	16.3	16.7	15.3	7.0	93.8	14.5	6.5
<b>Cr</b>	2.7	2.6	5.0	7.1	5.3	6.7	7.0	6.4	2.9	40.8	4.9	8.3
<b>Zn</b>	9.4	12.5	18.9	20.7	23.4	25.6	25.6	25.1	14.7	152.1	23.7	6.4
<b>Fe</b>	153.1	210.7	294.3	246.5	361.4	340.5	434.0	347.5	206.6	2168.4	426.3	5.1

Table 4.13 Total and seasonal average wet deposition fluxes corresponding to the measured ions.

	Total wet deposition flux (1991-1999)				Winter		Summer		Wet / Dry
	mg.m-2.y-1		tons.y-1		mg.m-2.y-1		tons.y-1		
	mg.m-2.y-1	tons.y-1	mg.m-2.y-1	tons.y-1	mg.m-2.y-1	tons.y-1	mg.m-2.y-1	tons.y-1	
H	117.21	76186.5	114.8	74620	2.41	1566.5	2.41	1566.5	47.63
SO4	31356.35	20381628	27989.4	18193110	3366.92	2188498	3366.92	2188498	8.31
NO3	14254.6	9265490	12251.2	7963280	2003.38	1302197	2003.38	1302197	6.12
Cl	91527.09	59492609	86320.4	56108260	5206.77	3384401	5206.77	3384401	16.58
NH4	6916.64	4495816	5883.92	3824548	1032.71	671261.5	1032.71	671261.5	5.7
Mg	6526.18	4242017	6059.5	3938675	466.68	303342	466.68	303342	12.98
Ca	19452.97	12644431	17043.7	11078405	2409.2	1565980	2409.2	1565980	7.07
K	3614.79	2349614	3298.42	2143973	316.36	205634	316.36	205634	10.43
Na	36021.72	23414118	33834.4	21992360	2187.26	1421719	2187.26	1421719	15.47
Cd	2.60	1690	2.13	1384.5	0.47	305.5	0.47	305.5	4.53
Cu	27.04	17576	24.03	15619.5	3.01	1956.5	3.01	1956.5	7.98
Pb	47.89	31128.5	41.00	26650	6.90	4485	6.90	4485	5.94
Al	1917.21	1246186.5	1480.86	962559	436.35	283627.5	436.35	283627.5	3.39
Ni	108.32	70408	93.79	60963.5	14.53	9444.5	14.53	9444.5	6.45
Cr	45.74	29731	40.83	26539.5	4.91	3191.5	4.91	3191.5	8.32
Zn	175.81	114276.5	152.09	98858.5	23.73	15424.5	23.73	15424.5	6.41
Fe	2594.65	1686522.5	2168.35	1409427.5	426.31	277101.5	426.31	277101.5	5.09

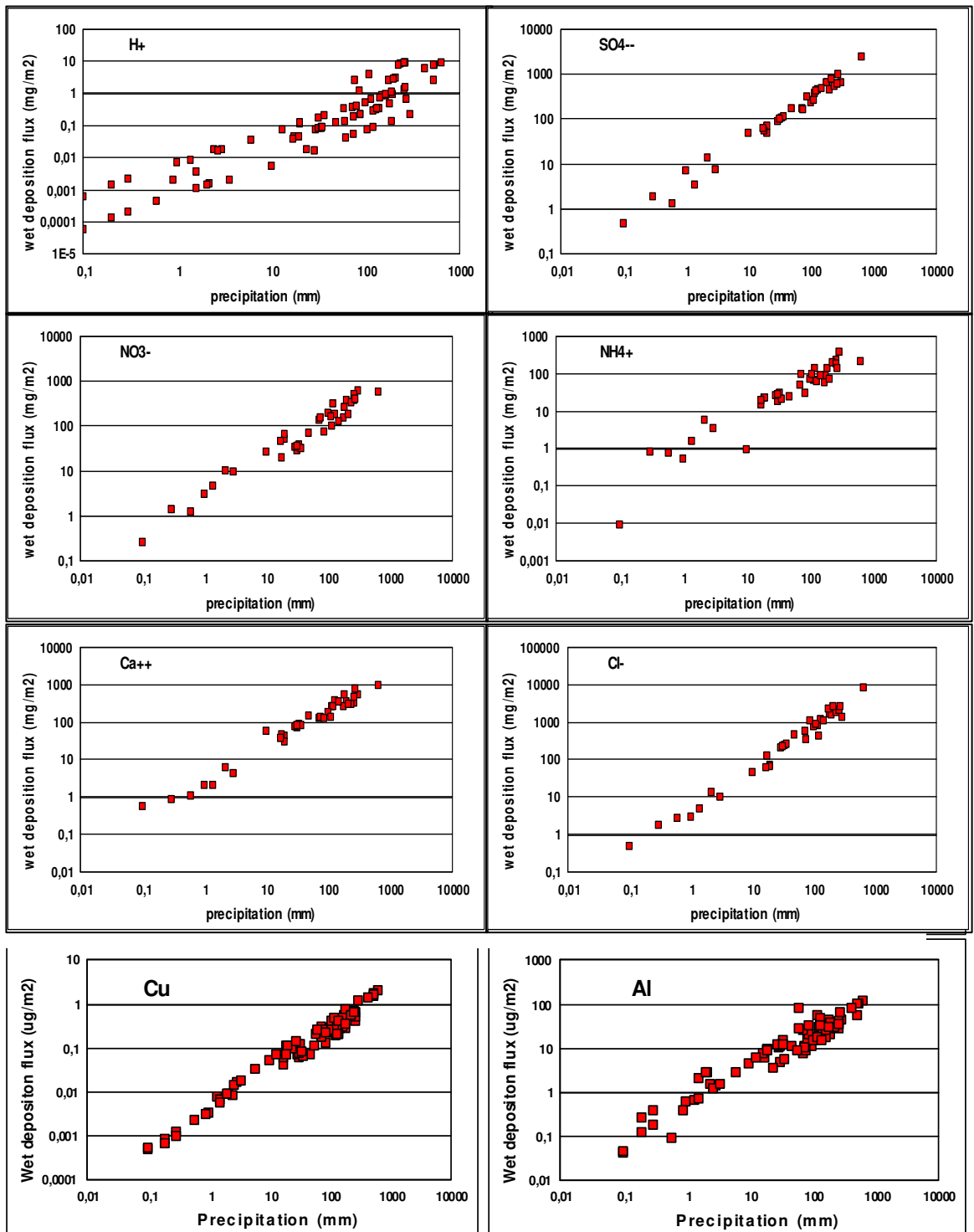


Figure 4.30 Plot of wet deposition flux of  $H^+$ ,  $SO_4^{2-}$ ,  $NO_3^-$ ,  $NH_4^+$ ,  $Ca^{2+}$ ,  $Cl^-$ , Cu and Al with precipitation amount.

#### 4.6.2. Comparison of the Wet Deposition Fluxes with the EMEP Network

Wet deposition fluxes of EMEP Stations and Turkey Antalya Station were compared for the major ions between the years 1991 and 1999 and presented in Figure 4.31. For the calculation of wet deposition fluxes, annual ion concentrations were multiplied by corresponding precipitation amounts.

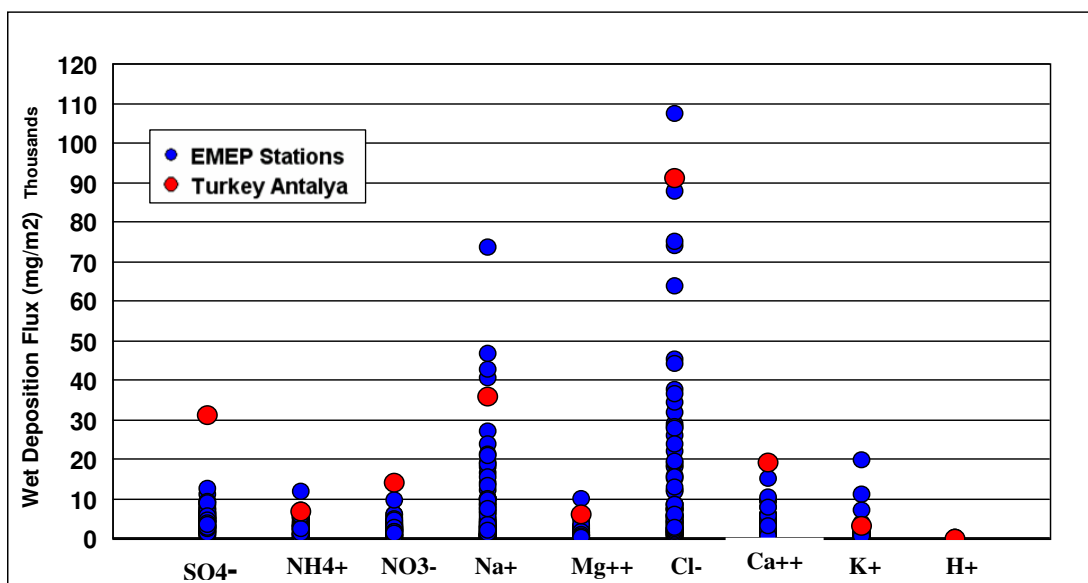


Figure 4.31 Comparison of wet deposition fluxes of EMEP Stations and Turkey Antalya Station between the years 1991 and 1999.

For the acidifying compounds, wet deposition fluxes in Antalya Station were the highest one among the all EMEP stations included. In Antalya Station, the annual median precipitation amount was  $1246 \text{ mm yr}^{-1}$  whereas; it was  $710 \text{ mm yr}^{-1}$  in the EMEP Stations that we have included for evaluation. Therefore, observed high wet fluxes of elements and ions in this study are partly due to high rainfall in Antalya and partly due high concentrations of these species, as discussed previously. Not only  $\text{SO}_4^{2-}$  and  $\text{NO}_3^-$  but wet deposition fluxes of all measured ions were found to be higher than those reported in EMEP network, but for different reasons. Calcium has the highest wet deposition flux among the EMEP Stations, because soil at Antalya and dust transported from North Africa, which are the two sources of crustal material at our sampling point, are highly enriched in  $\text{CaCO}_3$ . Wet deposition fluxes of  $\text{Cl}^-$  and  $\text{Na}^+$  are also higher than those reported for other EMEP sites, due to close

proximity of our sampling site to the sea.  $\text{NH}_4^+$ ,  $\text{Mg}^{2+}$  and  $\text{K}^+$  have moderate wet deposition fluxes compared to EMEP stations.

## 4.7. Sources of Measured Species

### 4.7.1. Correlation Matrix

The correlation coefficients can be used as a preliminary step to obtain information on potential sources of elements. The approach is only a preliminary step, because over reading binary correlation coefficients can give misleading conclusions, because in the correlation matrix only strong correlations can be seen, weaker correlations can not be easily seen. Also, some of the correlations can be due to transport or atmospheric chemistry. These minor sources and artifacts complicate the information obtained from binary correlation matrix. However, the information can be useful if only strong correlations are related to sources. (Khwaja and Husain, 1991). Binary correlation coefficients between ions were presented in Table 4.13, 4.14 and 4.15 for the whole data set, and the wet and dry seasons, respectively. The terms “correlation” or “correlated” in this section means that there is statistically significant correlation between the two parameters (in other words; probability of chance correlation is less than 5%; or  $[P(r,n)<0.05]$ ). Nitrate ion is correlated with  $\text{H}^+$ ,  $\text{SO}_4^{2-}$  and  $\text{Cl}$ . These correlations are not surprising, because  $\text{NO}_3^-$  is shown to be correlated with these ions in many data sets. Correlation of  $\text{NO}_3^-$  with  $\text{H}^+$  is due to formation of  $\text{HNO}_3$  in the atmosphere, as pointed previously. Its correlation with  $\text{SO}_4^{2-}$  is due to their similar sources. Both  $\text{SO}_4^{2-}$  and  $\text{NO}_3^-$  are secondary particles formed from gaseous precursors with similar gas-to-particle conversion mechanism. The correlation between  $\text{NO}_3^-$  and  $\text{Cl}$  is probably due to association of  $\text{NO}_3^-$  with sea salt particles. It is frequently shown in literature that approximately 70% of the  $\text{NO}_3^-$  in atmosphere are in the coarse fraction associated with sea salt particles (Kuloğlu and Tuncel, 2005). This association arises by the reaction of gaseous  $\text{HNO}_3$  in the atmosphere with  $\text{NaCl}$  in the sea salt.

Table 4.14 Correlation coefficients between ions and elements in whole data set.

	H	SO4	NO3	Cl	NH4	Mg	Ca	K	Na	Cd	Cu	Pb	Al	Ni	Cr	Zn	Fe
H	1.00																
SO4	-0.05	1.00															
NO3	<b>0.49</b>	0.31	1.00														
Cl	-0.06	<b>0.68</b>	<b>0.40</b>	1.00													
NH4	-0.08	0.09	0.03	0.05	1.00												
Mg	-0.02	<b>0.72</b>	0.00	<b>0.57</b>	0.00	1.00											
Ca	-0.02	<b>0.47</b>	0.07	0.16	0.06	<b>0.41</b>	1.00										
K	-0.04	<b>0.60</b>	-0.02	<b>0.42</b>	-0.10	<b>0.69</b>	<b>0.77</b>	1.00									
Na	-0.02	<b>0.71</b>	0.00	<b>0.60</b>	-0.04	<b>0.79</b>	0.32	<b>0.64</b>	1.00								
Cd	-0.09	0.23	-0.05	0.03	0.06	-0.01	<b>0.46</b>	0.22	-0.14	1.00							
Cu	-0.01	-0.04	0.01	-0.02	0.12	0.00	-0.05	-0.05	-0.03	0.07	1.00						
Pb	0.21	0.00	0.15	-0.02	0.06	0.04	0.02	0.00	-0.03	0.04	0.32	1.00					
Al	-0.08	0.05	-0.06	0.06	0.06	0.12	0.36	0.31	0.02	0.32	0.02	0.00	1.00				
Ni	0.06	-0.03	0.05	-0.05	0.12	0.11	0.28	0.20	-0.08	0.27	0.16	0.04	<b>0.51</b>	1.00			
Cr	-0.10	0.00	-0.02	-0.11	0.23	0.02	0.27	0.16	-0.12	<b>0.55</b>	0.26	0.08	<b>0.50</b>	<b>0.53</b>	1.00		
Zn	-0.03	-0.06	0.02	-0.06	0.36	0.03	0.01	-0.05	-0.05	0.05	0.07	0.25	-0.03	-0.01	0.04	1.00	
Fe	-0.09	0.04	-0.04	0.04	0.04	0.16	<b>0.45</b>	<b>0.45</b>	0.01	0.36	0.01	0.12	<b>0.97</b>	<b>0.48</b>	<b>0.54</b>	-0.02	1.00

Table 4.15 Correlation coefficients between ions and elements in wet season data set.

	H	SO4	NO3	Cl	NH4	Mg	Ca	K	Na	Cl	Cu	Pb	Al	Ni	Cr	Zn	Fe
H	1.00																
SO4	-0.05	1.00															
NO3	0.49	0.30	1.00														
Cl	-0.07	0.69	0.41	1.00													
NH4	-0.09	0.06	-0.01	0.07	1.00												
Mg	-0.03	0.74	-0.02	0.55	-0.01	1.00											
Ca	0.00	0.49	0.07	0.16	0.04	0.41	1.00										
K	-0.05	0.62	-0.04	0.35	-0.11	0.69	0.80	1.00									
Na	-0.03	0.72	-0.02	0.53	-0.04	0.80	0.36	0.67	1.00								
Cl	-0.08	0.37	-0.03	0.29	-0.13	0.05	0.67	0.43	-0.03	1.00							
Cu	0.02	-0.06	0.04	-0.06	0.05	-0.04	-0.10	-0.13	-0.05	-0.14	1.00						
Pb	0.23	-0.02	0.17	-0.05	0.02	0.00	0.00	-0.05	-0.06	0.03	0.24	1.00					
Al	-0.07	0.08	-0.07	0.01	0.17	0.17	0.46	0.42	0.00	0.36	-0.05	-0.01	1.00				
Ni	0.14	-0.04	0.10	-0.06	0.10	0.15	0.45	0.32	-0.01	0.11	0.08	0.17	0.44	1.00			
Cr	-0.08	0.03	-0.02	-0.04	0.40	0.12	0.58	0.43	-0.06	0.45	0.06	0.09	0.53	0.41	1.00		
Zn	-0.05	-0.08	0.01	-0.12	0.49	0.00	0.01	-0.08	-0.09	0.05	0.14	0.25	-0.01	0.01	0.18	1.00	
Fe	-0.03	0.07	-0.03	0.00	0.16	0.24	0.58	0.59	0.04	0.49	-0.09	0.08	0.96	0.59	0.75	0.00	1.00

Table 4.16 Correlation coefficients between ions and elements in dry season data set.

	H	SO4	NO3	Cl	NH4	Mg	Ca	K	Na	Cd	Cu	Pb	Al	Ni	Cr	Zn	Fe
H	1.00																
SO4	-0.17	1.00															
NO3	-0.08	<b>0.63</b>	1.00														
Cl	-0.10	0.39	0.33	1.00													
NH4	0.13	<b>0.55</b>	<b>0.62</b>	0.12	1.00												
Mg	-0.18	0.30	<b>0.43</b>	<b>0.61</b>	0.16	1.00											
Ca	-0.30	0.39	0.28	0.16	0.13	<b>0.42</b>	1.00										
K	-0.17	0.33	0.11	<b>0.75</b>	-0.07	<b>0.66</b>	<b>0.61</b>	1.00									
Na	-0.05	0.25	<b>0.45</b>	<b>0.84</b>	-0.10	<b>0.51</b>	0.06	<b>0.44</b>	1.00								
Cd	-0.12	<b>0.42</b>	-0.16	-0.09	0.07	0.07	0.38	0.11	-0.15	1.00							
Cu	-0.12	0.03	0.04	0.11	0.18	0.18	0.00	0.07	0.08	0.07	1.00						
Pb	-0.12	0.06	0.05	0.02	0.22	0.23	0.09	0.15	-0.01	0.16	<b>0.57</b>	1.00					
Al	-0.14	0.15	0.07	0.33	-0.09	0.20	0.28	0.26	0.17	0.21	0.02	0.09	1.00				
Ni	-0.06	0.20	0.03	0.11	0.15	0.31	0.18	0.21	-0.06	0.25	0.17	-0.03	<b>0.53</b>	1.00			
Cr	-0.32	0.25	0.10	-0.02	0.16	0.12	0.10	0.07	-0.07	<b>0.54</b>	0.32	0.22	<b>0.46</b>	<b>0.51</b>	1.00		
Zn	0.04	-0.04	0.25	0.03	0.20	<b>0.45</b>	0.05	0.06	-0.04	-0.09	<b>0.44</b>	<b>0.52</b>	0.00	0.34	0.19	1.00	
Fe	-0.15	0.13	-0.07	<b>0.43</b>	-0.19	0.17	0.31	0.32	0.41	0.08	0.03	0.18	<b>0.98</b>	0.34	0.32	0.04	1.00

The  $\text{SO}_4^{2-}$  is correlated with, in addition to  $\text{NO}_3^-$  ion, sea salt elements, namely Na, Cl and  $\text{Mg}^{2+}$ . This correlation of  $\text{SO}_4^{2-}$  with sea salt elements is not surprising because sea salt accounts for about 20% of  $\text{SO}_4^{2-}$  ion in the marine atmosphere. Neither  $\text{SO}_4^{2-}$  nor  $\text{NO}_3^-$  are strongly correlated with other anthropogenic elements, such as Cd, Pb etc., because anthropogenic elements like Pb, Zn etc are primary in nature, where as  $\text{SO}_4^{2-}$  and  $\text{NO}_3^-$  are secondary. In previous studies  $\text{SO}_4^{2-}$  and  $\text{NO}_3^-$  are shown to be related with other anthropogenic elements and this relation is attributed to similar transport mechanisms in the atmosphere (Güllü et al., 1998). Similarity in transport does not generate strong binary correlation coefficients. However, these minor relations due to similar transport patterns or similar chemistry in the atmosphere will be discussed later in the manuscript using more sophisticated multivariate statistical tools.

Crustal elements,  $\text{Ca}^{2+}$ ,  $\text{K}^+$ , Al and Fe are all correlated with each other forming a group. These strong correlations are due similar crustal sources of these elements. Similarly, sea salt elements Na, Cl and Mg also form a group of strong correlations between each other. Anthropogenic elements are generally correlated with each other. However they also show correlations with other groups. The three elements Pb, Cu, Zn are correlated among each other. Chromium, Cd and Ni are correlated with crustal elements as well. The correlation of Cr and Ni with elements like Al, Fe is due to enrichments of Cr and Ni bearing minerals on the Mediterranean coast of Turkey. However, such enrichments can not explain correlation between Cd and crustal elements. Association of Cd with coarse crustal particles were reported by Kuloğlu and Tuncel (2005) and attributed to attachment of fine anthropogenic particles onto coarse crustal particles. Such sticking of fine anthropogenic particles onto crustal ones can explain observed correlations

For the wet season, the same correlations were observed between the crustal and marine elements, respectively.  $\text{SO}_4^{2-}$  correlates strongly with marine elements during wet season and for the whole data. However, such relation between  $\text{SO}_4^{2-}$  and marine elements are not observed during dry season (summer). During summer  $\text{SO}_4^{2-}$  seem to be more related with other anthropogenic species, such as  $\text{NO}_3^-$ ,  $\text{NH}_4^+$ , and Cd and also to a host of crustal elements. Association of  $\text{SO}_4^{2-}$  with crustal species through reaction of atmospheric  $\text{H}_2\text{SO}_4$  with  $\text{CaCO}_3$  on crustal particles is

also reported in literature (Kuloğlu and Tuncel, 2005; Al-Momani et al., 2000; Jaradat et al., 1999). The lack of correlation between  $\text{SO}_4^{2-}$  and  $\text{Na}^+$  and  $\text{Cl}^-$  during summer season is due to reduced bubble bursting at the sea surface during summer months.

Binary correlations between other anthropogenic species do not show a significant difference between the summer and winter seasons.

#### 4.7.2. Enrichment Factors

In the absence of anthropogenic sources, concentrations of ions and elements should be explained by natural sources. Increased man-made sources and their emissions is made us to explain the enrichment of sources with known composition of crustal material, mainly called enrichment factor (EF). Enrichment factor is a double normalization technique to understand the existence of non crustal contribution to the observed level of elements in rain water at a given location. The crustal enrichment factor is calculated by the following relationship:

$$EF_x = \frac{\left( \frac{C_x}{C_R} \right)_{\text{Rain}}}{\left( \frac{C_x}{C_R} \right)_{\text{Reference}}} \quad (4.6)$$

Where  $C_x$  is the concentration of the ion in the sample and in the source and  $C_R$  is the concentration of reference element in sample and in source material which is either soil or sea water. Commonly used crustal indicators are Si, Al, Fe and Sc. In this study, Al was used as reference material to calculate the crustal enrichment factor.

For the elements containing soil origin are expected to have crustal enrichment factor ( $EF_c$ ) values around unity. For the values higher than unity, contribution of sources other than soil is expected for the crustal enrichment factors. These sources may be anthropogenic or natural sources that indicate other than soil or sea salt composite.  $EF_c$  values between 1 and 10 are considered relatively crustal materials.  $EF_c$  values between 10 and 500 were considered moderately enriched, indicating other sources

in addition to crustal materials, and  $EF_c$  greater than 500 indicate clear evidence of extreme enrichment, indicating severe contamination due to human activities.

#### 4.7.2.1. Crustal Enrichment Factors ( $EF_c$ )

Crustal enrichment factors were calculated by the formula 4.7, using Mason's average soil composition and Al as reference material and presented in Figure 4.32.

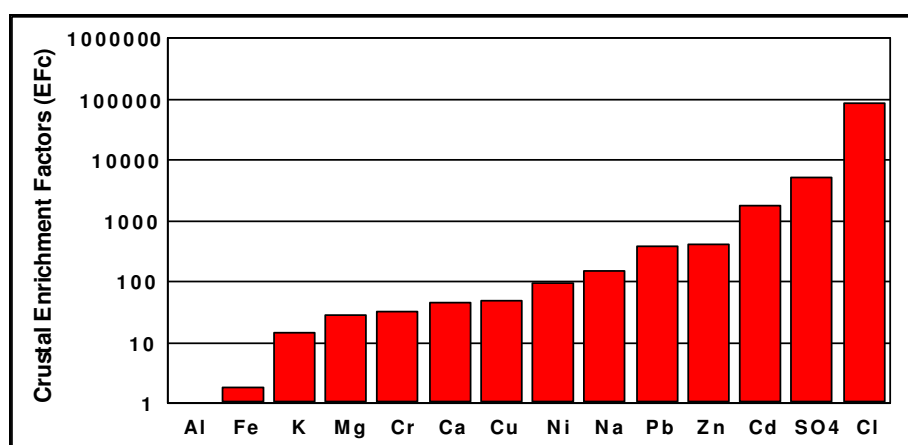


Figure 4.32 Crustal Enrichment Factor ( $EF_c$ ) of rainwater composition

The element of Fe was not enriched higher than 10, indicating that they have mainly originated from the airborne dust. The elements of  $K^+$ ,  $Mg^{2+}$ ,  $Ca^{2+}$ , Cr, Ni, Cu and  $Na^+$  were moderately enriched compared to the mean crustal composition indicating the presence of other sources contributing to the elements. The enrichment of  $Na^+$ ,  $Mg^{2+}$ ,  $Ca^{2+}$  and  $K^+$  was influenced from the sea salt, whereas Cr, Ni and Cu was from anthropogenic sources. The elements of Pb, Zn,  $SO_4^{2-}$ , Cd and Cl were highly enriched compared to mean crustal composition with anthropogenic origin.

Furthermore, the elements Fe, K, Mg, Ca, Na, Ni, Cu and Cr were associated with either soil or sea salt particles in the atmosphere. Since both sea salt and soil particles are in the coarse mode of the size spectrum, they scavenged out fairly efficiently by rain. Anthropogenic elements such as Pb, Zn, Cd and  $SO_4^{2-}$  were associated with sub-micron particles which are not scavenged out as efficiently as coarse particles by the rain. The difference in the scavenging efficiencies of coarse and fine particles can

be resulted in the observed difference in the enrichment factors of anthropogenic and lithophilic elements (Al-Momani et al., 1997).

The seasonal differences of crustal enrichment factors were presented in Figure 4.33. All ions and elements it was observed that dry season has lower enrichment factors compared to wet season, could be explained by the higher concentrations of airborne dust of Al during summer season, reduces the EF ratio slightly.

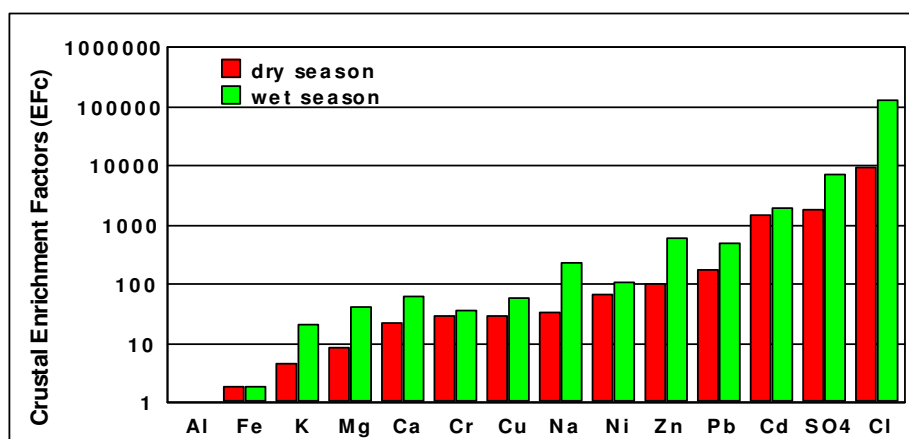


Figure 4.33 Seasonal differences of crustal enrichment factor of rain water composition

#### 4.7.3. Positive Matrix Factorization

The aim of the PMF is the identification of possible sources of components of measured parameters in rain water, because, every component could represent a different sources. The main principle in determining the factors in composition and separate the compounds into their factors, is the covariance. Therefore, the components do not indicate the separate factors invariably. In the formation of factors, sometimes, the cases of transportation, the chemical transformations such as neutralization and physical factors such as dissolution in the rain water could be effective.

PMF have considerable characteristics over the other receptor models, since for the missing values high uncertainties are assigned and their effect on least square fit is lowered. In PMF analysis, the accuracy of uncertainties have vitality since these

values are directly included in PMF analysis. Uncertainties in measured values should represent the real values since in PMF analysis; the uncertainties have the greatest influence on the species to determine the factors. Species with smaller uncertainty have more influence on the fit, whereas higher uncertainties that assigned for the missing values, which are non measured data due to some reason, and below detection limit value, have lower effect on the fit.

In PMF analysis, to assign the uncertainties of missing values and below detection limits, the approach that developed by Polissar et al., (2001) are used. For PMF analysis two data sheet are prepared, which are main data sheet and uncertainties data sheet. For the main data sheet, the concentrations higher than detection limit remain constant, while lower than detection limits are assigned as the half of the detection limit. Missing values are assigned as the geometric mean of each species for the whole data. In the uncertainties sheet, the concentration values higher than detection limit is assigned as the value of 0.05 times concentration plus detection limit, while lower than detection limit, standard deviations are assigned as 5/6 times detection limit. For the missing values, uncertainties are assigned as 4 times geometric mean. The effect of missing values and below detection limits on PMF are minimized by applying this method.

The PMF version 4.2 software developed by Paatero, 2002 is used for PMF analysis. To obtain the optimum results and to define the higher explained variations, some adjustments are applied during the PMF analysis. Initially, the robust mode is used to reduce the influence of possible outliers on the PMF solution. An outlier is explained as the residuals that exceeds  $\alpha$  times the standard deviation and expected to have lower in numbers since it associates with the unexplained portion. In this study, the value of  $\alpha$  is taken as 4 since it produces better fit. Higher outlier values are assigned to define the log-normal distribution and the overall composition of the whole data. Different seeds are applied to find the initial point by minimizing Q value and outlier values. Q value should be approximately equal to the number of points in the data matrix minus the total number of elements in the factor matrices (Paatero, 2000). Furthermore, the parameter FPEAK values are tried for several times to obtain the minimum Q values. In this respect, using the optimum seed and FPEAK values of each factor, explained variations and factor loadings are investigated. During the

investigations, three to eight factors are used and the suitable factor is selected considering the higher explained variations and defined source profiles. In this regard, the factor 5 is selected as the better factor to explain the Antalya rain water data. Scaled residual which is defined as the ratio of error to standard deviation, is the other parameter to determine the suitable factor. The values of scaled residuals should be in the pattern of positive and negative values between -2.0 and +2.0 (Paatero, 2000).

In this study, for the ions and elements,  $\text{NH}_4^+$ ,  $\text{Mg}^{2+}$ ,  $\text{Ca}^{2+}$ ,  $\text{K}^+$ ,  $\text{Na}^+$ , Pb, Ni, Cr, Zn and Fe, the scaled residuals are scatterly distributed between -10.0 and +10.0. Therefore, standard deviations are doubled for these ions and elements to obtain narrowly distributed scaled residuals. Finally, for this case and factor 5 the data is investigated deeply to solve the source profiles by factors. To figure out the most reasonable solution, crustal enrichment factors are calculated for each solution of the F-loading values by using Al as reference element. Explained variation of each element for each factor is used to identify the source profiles by factors. G factor which contains factor scores of each day and for each factor is produced by multiplying of factor scores, which are weight of each factor in sampling days, and daily concentrations of elements by each factor. G factors are analyzed for the each two factors that included in evaluations and it is expected to have nonlinear correlation between the applied two factors. G-loadings are used for the backtrajectory analysis that is plotted by PloTra2.1 software for the highest 20% contributions of the factors by totally 68 days of sampling. During the trajectory plots, a trajectory ending with the pressure of 900 mbar, which corresponds to 946 m., is used. For each of the anthropogenic factors, PSCF values are calculated using the highest 40% of the factor scores as polluted data set and plotted by using MapInfo 6.5. Bootstrap method is used for the calculation of PSCF by applying 3000 iterations.

In the interpretation of the data, the second step in the PMF analysis is to demonstrate that the partitioning of rain water composition into its components is correct. For this, the calculated total ionic mass is compared with the measured total ionic mass. The product of factor loading for a particular element in a particular factor and the G score for the same factor in a particular sample gives the

concentration of that element in that factor and at that particular day. Concentrations of elements and ions in each factor are calculated with this approach. The calculations are repeated for all of the 400 samples. The “calculated total ionic mass” is then determined by adding daily calculated concentrations of,  $\text{NO}_3^-$ ,  $\text{NH}_4^+$ ,  $\text{Cl}^-$ ,  $\text{Na}^+$ ,  $\text{Mg}^{2+}$ ,  $\text{K}^+$  and  $\text{Ca}^{2+}$  in each factor. These daily calculated concentrations of elements and ions are then compared with daily measured total ionic mass. The results are given in Figure 4.34, where calculated total ionic mass concentrations are plotted against measured total ionic mass concentrations. Number of data points in the graph is less than 395 samples we have, because observed total ionic mass concentrations are calculated only for samples in which data are available for all the ions included in total ionic mass calculations.

There is excellent agreement between calculated and measured total ionic mass concentrations with  $R^2 = 0.99$ . This demonstrates that calculations by the model are reliable for at least ions included in total ionic mass calculations.

In a second test, instead of calculating total ionic mass, observed-to-predicted ratios are calculated for each element separately. Median values of the observed-to-predicted ratios of elements are given in Figure 4.35.

Predicted concentrations of elements and observed to predicted ratios are calculated for each sample and median values of O/P ratio is used in the figure. The median O/P ratios of elements vary between 0.98 and 1.40. For most of the elements, the difference between observed and predicted concentrations is  $< 10\%$ . Indicating that the five factors account for a very large fraction of concentrations measured in this study. The only exception is Zn, for which O/P ratio is 1.4.

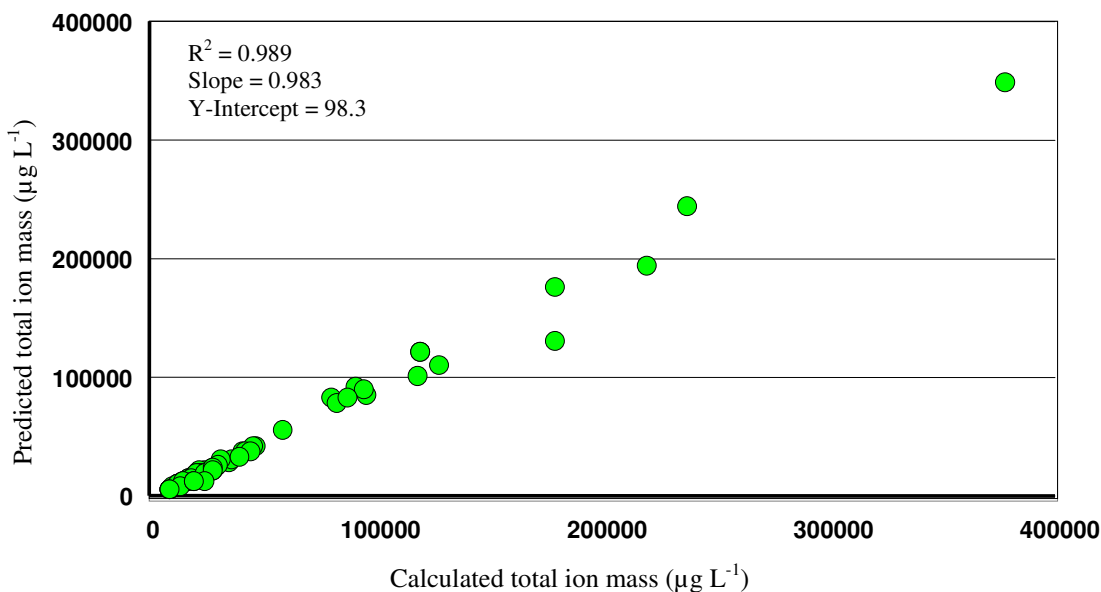


Figure 4.34 Calculated total ionic mass concentrations vs. measured total ionic mass concentrations.

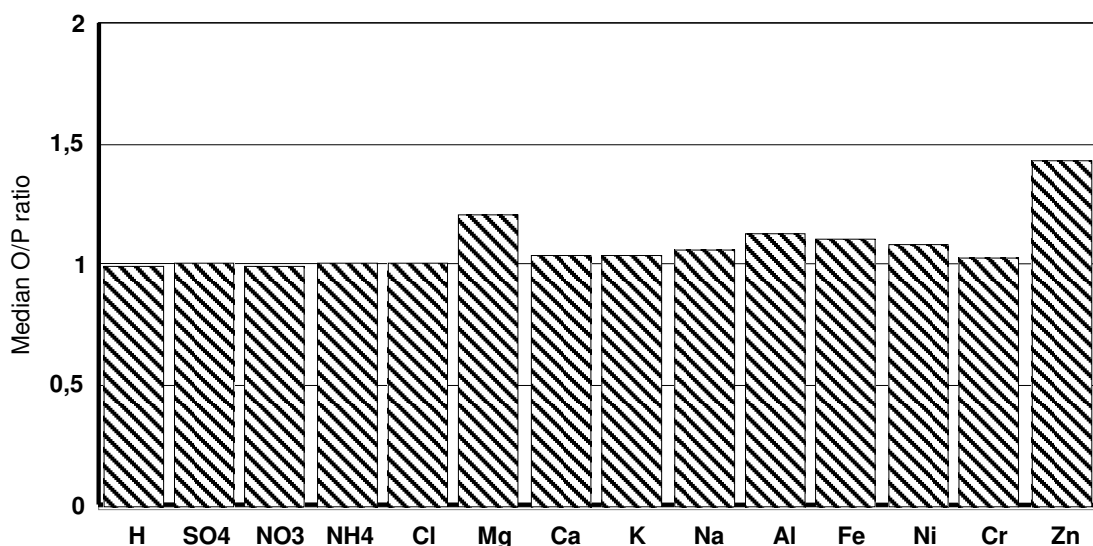


Figure 4.35 Median values of the observed-to-predicted ratios of elements.

After demonstrating that the results obtained from PMF using 5 factors is reliable, the physical meanings of the factors must be identified. This can be done by investigating which marker species are available in the factors with high loadings. However, although it sounds straightforward, the availability of marker elements in a factor is generally not enough to for a positive identification, because they generally occur in more than one factor and some of the factors are due to transport and chemistry. These factors contain all of the marker elements or none of them. For this reason we do not consider only the composition of factor loadings, but also

enrichment factors of elements in each factor, explained variances of elements in factors and seasonal variations observed in G factor scores, to relate factors to physical processes.

In Table 4.17, percent contribution of each factor on calculated concentrations of elements and ions are presented. Factor loadings (F-loading), Enrichment factors (EF<sub>c</sub>) of elements, Explained variances (EV) and monthly average values of G factor scores are given in Figure 4.36. Top and side views of the backtrajectories that correspond to highest 20% of the G scores can also be useful to identify factors. These are given in Figure 4.37.

Table 4.17 Percent contribution of each factor on calculated concentrations of elements and ions.

	<b>Factor 1</b>	<b>Factor 2</b>	<b>Factor 3</b>	<b>Factor 4</b>	<b>Factor 5</b>
<b>Na<sup>+</sup></b>	0,30	2,24	96,47	0,03	0,01
<b>Cl</b>	0,55	0,01	96,44	0,01	1,98
<b>Al</b>	0,00	92,74	2,07	3,94	0,01
<b>Fe</b>	0,01	92,15	0,00	0,00	7,84
<b>Ca<sup>2+</sup></b>	0,32	70,18	9,60	0,64	13,09
<b>K<sup>+</sup></b>	0,06	45,53	36,21	1,01	8,40
<b>Mg<sup>2+</sup></b>	0,61	51,96	39,60	1,61	0,00
<b>H<sup>+</sup></b>	98,52	0,24	0,17	0,15	0,41
<b>SO<sub>4</sub><sup>2-</sup></b>	0,42	1,74	1,26	2,38	91,79
<b>NO<sub>3</sub><sup>-</sup></b>	0,25	0,04	0,62	98,75	0,03
<b>NH<sub>4</sub><sup>+</sup></b>	0,00	98,03	0,01	1,94	0,02
<b>Cd</b>	0,30	54,71	0,03	27,31	10,88
<b>Cu</b>	0,53	36,41	3,28	34,15	14,69
<b>Pb</b>	4,47	39,60	0,35	28,69	9,87
<b>Ni</b>	1,51	61,30	1,67	27,16	0,62
<b>Cr</b>	0,00	53,35	0,01	44,14	1,18
<b>Zn</b>	2,98	60,16	0,19	15,25	9,13

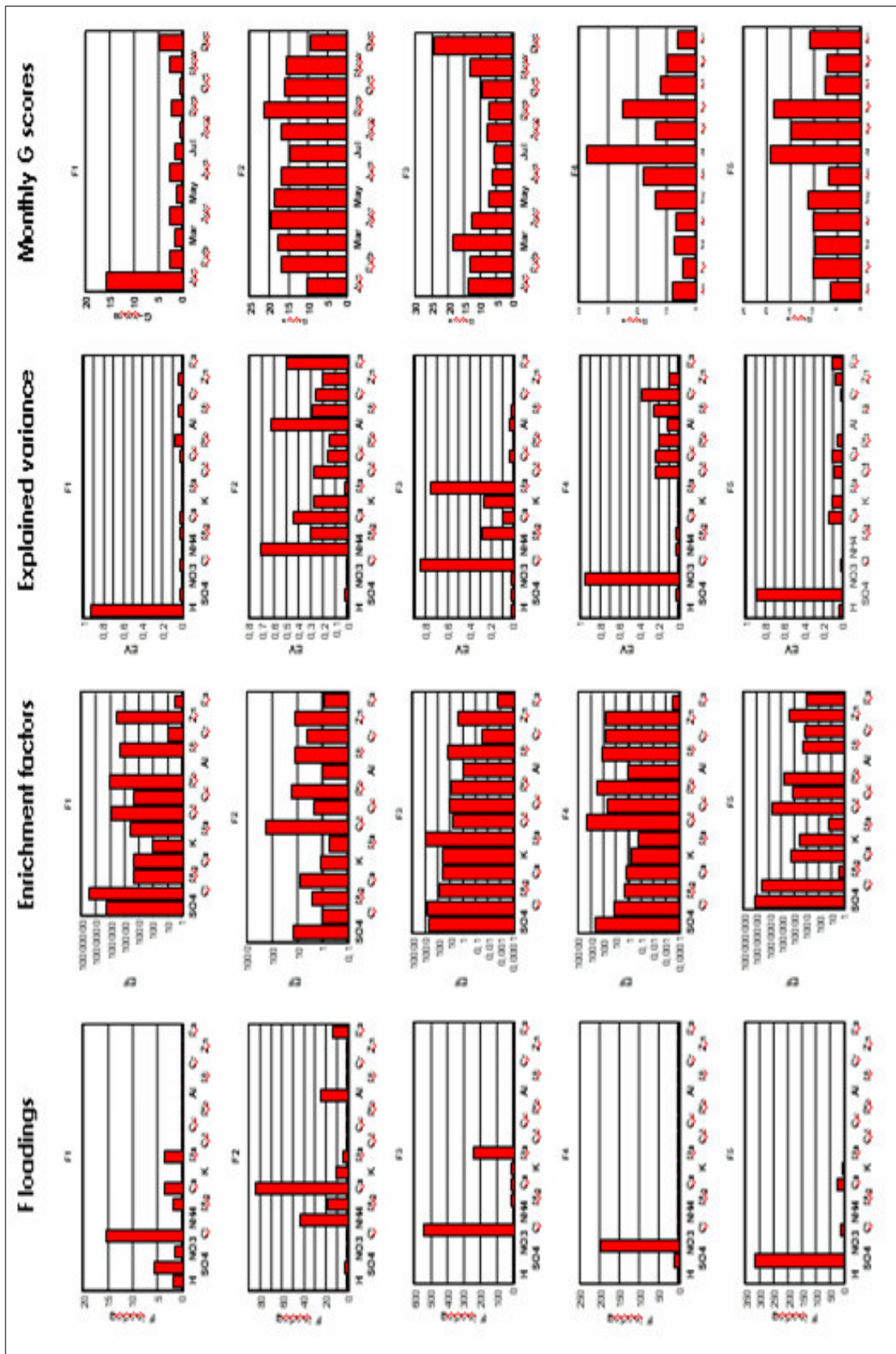


Figure 4.36 Factor loadings (F-loading), Enrichment factors (EFc) of elements, Explained variances (EV) and monthly average values of G factor scores.

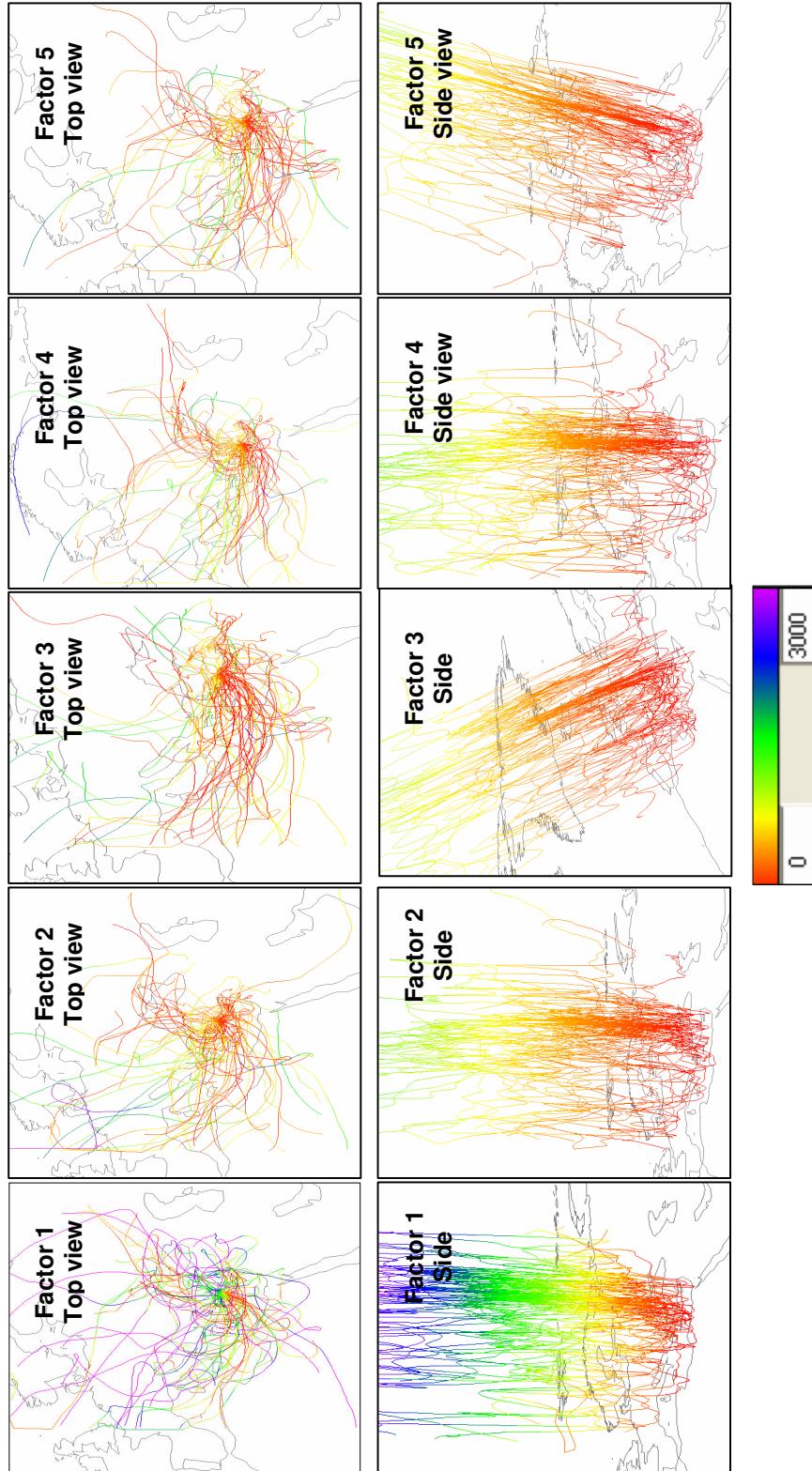


Figure 4.37 Top and side views of the backtrajectories that correspond to highest 20% of the G scores.

Factor 1 includes loadings from  $H^+$  ion,  $SO_4^{2-}$ ,  $NO_3^-$ , Cl, Mg, Ca and Na. All of the elements measured in this study, except for Cr and Fe are highly enriched relative to soil. Most importantly, Factor one explains most of the variance in  $H^+$  ion concentration and do not account for a large fraction of variance in any other specie. The percent contribution of  $H^+$  ion is 98.52% and the above mentioned ions account for less than 1%. Monthly variations of G score values closely resemble the seasonal variation of  $H^+$  concentration. This factor is identified as free acidity factor. It should be an artifact due to extensive neutralization in rain water. Normally, free acidity is generally observed in the same factor with  $SO_4^{2-}$  and  $NO_3^-$ . However, most of the acidity in Eastern Mediterranean rain water is neutralized and temporal variations in  $H^+$  ion concentration no longer depends on seasonal variations in  $SO_4^{2-}$  and  $NO_3^-$  concentrations. That is probably why H appears as a separate factor in the PMF.

The top view and vertical profiles of trajectories shown in Figure 4.37 provides interesting features that can explain the nature of the free acidity factor. The color coding in the trajectories is important. The red colored lines show parts of the trajectories, which are below 1000 m altitude. The yellow color shows trajectory segments that are between 1000 and 1500 m, green color indicates segments with altitudes 1500 – 2000 m and violet color indicate trajectory segments that are higher than 2000 m. The red color parts (segments below 1000 m) are the ones that are influenced most from the emissions. The top view for the trajectories for factor 1 shows that these are high lying trajectories. Which can be seen better in the vertical profiles. Most of the trajectories that have high factor one scores are transported to the sampling point at altitudes higher than 1000 m. And quickly advects at the sampling point to the below 1000 m altitude. Probably these trajectories bring in a lot of free acidity in them, and neutralized at the sampling point during advection by capturing  $CaCO_3$  in the immediate vicinity of the station. Only samples that contains too much  $H^+$  to be neutralized by available  $CaCO_3$  at the receptor appears in this factor.

Factor 2 has high concentrations of Ca,  $NH_4^+$  ion and Al and moderate concentrations of Mg, K, Na and Fe. None of the elements and ions is highly enriched, weak enrichments

of elements  $\text{SO}_4^{2-}$  ion, Cd, Pb, Ni and Zn. Enrichment factors of the other elements are between 1 and 10. The factor explains significant fraction of the variances of  $\text{NH}_4^+$  ion, Al and Fe, but also explains smaller fraction of variances of the other elements. The factor is identified as a crustal factor, representing crustal component in the water. The percent contribution of  $\text{NH}_4^+$ , Al, Fe and  $\text{Ca}^{2+}$  are 98.03%, 92.74%, 92.15% and 70.18%, respectively. The moderate contributions are accounted by Ni, Zn, Cd, Cr, Mg, K, Pb, and Cu with decreasing order of values from 61.3% to 36.41%, respectively. Higher G scores during summer season support this, because most of the crustal elements have higher concentrations during summer months.

The top view of the trajectories indicates that trajectories spend most of their time below 1000 m altitude, which means that they can pick up soil particles at any time of the transport. One interesting feature that can be seen in top and vertical view of the trajectories is that although some of the low lying trajectories penetrate deep into the Africa giving the impression that North African dust, but most of the trajectories do not spend any time over the Africa. Consequently Factor 2 does not represent transport of African dust. It probably represents the resuspension of local soil and soil particles incorporated in the rain during transport.

Factor 3 has high loadings of Na and Cl and much lower concentrations of Mg, Ca and K. The factor accounts for a significant fraction of variances in the same group of elements. Factor 3 is a clear marine factor and represent sea salt component in Eastern Mediterranean rain water. The percent contribution of  $\text{Na}^+$  is 96.47% and  $\text{Cl}^-$  is 96.44%. The moderate contributions of  $\text{Mg}^{2+}$ ,  $\text{K}^+$  and  $\text{Ca}^{2+}$  are 39.6%, 36.21%, 9.6%, respectively. It is interesting to note in the vertical profiles of trajectories that most of the low lying trajectories touch to the surface of the Mediterranean Sea, probably picking of sea salt in these instances.

Factors 4 and 5 are two anthropogenic factors. Factor 4 is a  $\text{NO}_3^-$  factor. It has very high loading of  $\text{NO}_3^-$  ion and explains a significant fraction of variances in  $\text{NO}_3^-$  and anthropogenic elements Cd, Cu, Pb, Ni, Cr and Zn. The percent contribution of  $\text{NO}_3^-$  is

98.75%. The moderate contributions belong to Cr, Cu, Pb, Cd, Ni and Zn with the values of decreasing order from 44.14% to 15.25%. G-score values of Factor 4 are significantly higher in summer. High summer values of any specie is an indication (not a conclusive evidence) of long range transport, because pollutants can not be transported over very low distances in winter due to extensive wet scavenging. Enrichment factors indicate that all of the anthropogenic species are enriched in this factor. There is also some mixing of crustal material to  $\text{NO}_3^-$  factor, because there are some small amounts of crustal elements in this factor and their enrichment factors are close to 1.0.

Top view of the trajectories associated with high factor 4 scores shows two flow patterns for low lying (red) trajectories. One of them is flow to the north where trajectories extend to the north of the Black Sea, towards the Caspian Sea and the other one is flow over the Mediterranean. The transport from north seems to indicate source regions of pollutants included in this factor is in the Russia. The flow over the sea makes western Mediterranean countries, and coastal and populated areas in North Africa potential source areas for  $\text{NO}_3^-$  factor.

Factor 5 is a  $\text{SO}_4^{2-}$  factor. It explains most of the variance in  $\text{SO}_4^{2-}$  concentration and a smaller fraction of variances in a number of other elements. Presence of Ca in this factor is probably, because some of the  $\text{SO}_4^{2-}$  is in the form of  $\text{CaSO}_4$  and presence elements like Cd, Cu, Pb and Zn indicates that these elements are probably transported along with  $\text{SO}_4^{2-}$  to the study area. The percent contributions factor 5 belong to  $\text{SO}_4^{2-}$  is 91.8%. The moderate contributions belong to Cu, Ca, Cd, Pb, Zn, K and Fe with the values has decreasing order from 14.7% to 7.8%. The G-scores for Factor 5 are higher in summer season, but the difference between summer and winter is not as pronounced as the difference observed in  $\text{NO}_3^-$  factor.

The top view and vertical profiles of trajectories corresponding to the highest 20% of the factor 5 scores are fairly similar with the corresponding figures for the nitrate factor. They both have a northerly component indicating transport from Russia and Ukraine; they both have a set of trajectories traveling over the Mediterranean Sea, suggesting

source regions in the Western Mediterranean, such as Italy, Spain and France. The only difference between the two factor trajectories is that Factor 5 trajectories have a third southeasterly component. Some of the low lying Factor 5 trajectories extends to the Eastern Turkey and the Middle East, namely Israel and Jordan. None of the Factor 4 trajectories originate from east and southeast. Please note that there are 6 large thermal power plants along the coast of Israel. These are strong  $\text{SO}_4^{2-}$  sources but not significant  $\text{NO}_3^-$  sources.

Factors 4 and 5 probably represent similar long-range transport component in rain water. They probably have similar source regions. They are separated, because  $\text{SO}_4^{2-}$  concentrations in the Eastern Mediterranean rain water are also influenced from emissions in the east of the station, namely Afşin Elbistan power plant in southeastern part of Turkey and emissions from power plants located on the coast of Israel, whereas  $\text{NO}_3^-$  factor is not affected from these sources.

#### **4.7.4. Potential Source Contribution Function**

In this study, PSCF values are calculated and their statistical significance is tested by using “bootstrap” technique and distribution maps are prepared using only statistically significant within 95% confidence interval PSCF values. Backtrajectories are calculated by using European Centre for Medium Range Weather Forecast (ECMWF) three-dimensional isentropic model. One backtrajectory is calculated for each sample in all stations. Trajectories used in this study are 5.5 days long, which gives the path of the air mass within 5.5 days before the sample collected. In previous studies backtrajectories are calculated by 3.5 days long, whereas 5.5 days long backtrajectories are available in newly published studies (Doğan, 2005; Yörük, 2004).

In the application of PSCF, the working area is divided into grids and polluted trajectory segments to total trajectory segments in each grid is included during the counts generated by Microsoft Visual C++. Trajectories ending with the pressure of 900 mbar and 3000 number of iterations are used for trajectory plots. Since PSCF is calculated by

the ratio of polluted trajectory segments to total trajectory segments are taken, uncertainty completely depends on the total trajectory segments in each grid. In case of there is only one segment in the grid which is completely polluted, that grid becomes a very strong source region. Therefore, the conclusions depending on the one segment in a grid accomplished with highly uncertain results. To prevent the contribution of fairly occurred episodic cases from highly uncertain results, the PSCF values of segments which have total number trajectory segments smaller than 5, are assigned as 0. This highly uncertainty case is mainly occur at the edge of the study area, since the trajectories ends at the station and number of segments increases when one approaches to the station.

The spatial distribution of PSCF values of Factor 1, 4 and 5 scores for the highest 40% of the concentrations are given in Figure 4.38 together with the spatial distribution of  $\text{SO}_4^{2-}$  ion concentrations. The source regions for the free acidity factor are located in the western Turkey, Greek Peninsula, north of Italy, south of Poland. However, as pointed out before free acidity factor can be an artifact originating from neutralization chemistry in rain water. The source regions are probably coincidental.

Real long range transport to the Eastern Mediterranean region through rain water is represented in factors 4 and 5. Source regions of factor 4 and 5 in Europe are fairly similar, indicating that  $\text{SO}_4^{2-}$ ,  $\text{NO}_3^-$  ions and anthropogenic elements are emitted from same source areas before being transported to the Eastern Mediterranean region. These source regions are located in Balkan Countries, Ukraine, central parts of Russia. There is also a common source area between the Black Sea and Caspian Sea. Central parts of Turkey are also moderate source regions for both factors 4 and 5. Although there are no known strong emission source regions at the Central parts of Turkey, this region appeared as moderate source regions, probably due to close proximity of these emissions to the sampling site.

The main difference between factor 4 and factor 5 source regions is that the Middle East region, starting from South East Turkey and extending to the south of Israel is a strong source region for factor 5. The same region is not a strong source region for  $\text{NO}_3^-$  factor.

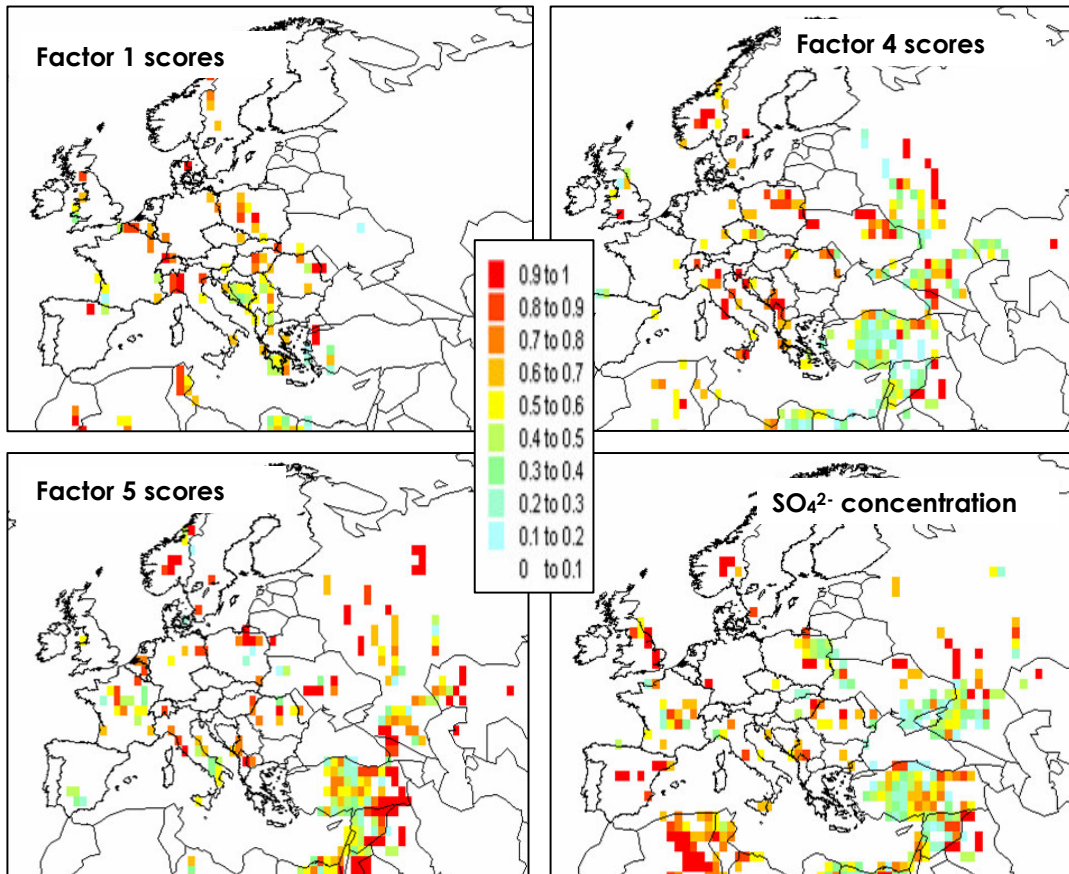


Figure 4.38 The spatial distribution of PSCF values of Factor 1, 4, 5 scores and  $\text{SO}_4^{2-}$  ion concentrations.

## CHAPTER 5

### CONCLUSION

In this study, the concentrations of major ions ( $\text{SO}_4^{2-}$ ,  $\text{NO}_3^-$ ,  $\text{NH}_4^+$ ,  $\text{H}^+$ ,  $\text{Na}^+$ ,  $\text{Cl}^-$ ,  $\text{Ca}^{2+}$ ,  $\text{Mg}^{2+}$ ,  $\text{K}^+$ ) and trace elements (Cd, Cu, Pb, Al, Ni, Cr, Zn, Fe) were investigated for 387 number of the wet deposition samples collected during November 1991 and August 1999 in Antalya Station, which is established in Mediterranean Coast of 20 km away from the city in rural area.

The frequency distributions show that most of the elements have right skewed distributions, whereas, only the  $\text{H}^+$  ion and elements Cu, Pb, Al, Ni, Zn and Fe have purely log-normal distributions. The distributions were determined by using skewness and Kolmogorov-Smirnov statistics.

The ionic composition was investigated by using ion balance, which is the ratio of sum of anions to sum of cations. The ratio was found as 0.77, which indicates anion deficiency. Since Antalya Region had calcareous soil, the observed deficiency could be referred to the exclusion of bicarbonate ions from the measurements. With the inclusion of  $\text{HCO}_3^-$  ion, the ion balance becomes as 0.99. The main species that contribute to total ion mass was found to be  $\text{Cl}^-$ ,  $\text{Na}^+$ ,  $\text{Ca}^{2+}$  and  $\text{SO}_4^{2-}$  that sorted with decreasing concentrations. Sea salt elements  $\text{Cl}^-$  and  $\text{Na}^+$  have the highest concentrations due to the close proximity of station to the sea. High concentrations of ions of  $\text{Ca}^{2+}$  and  $\text{SO}_4^{2-}$  were observed since they become airborne from the same source which is North African Saharan dust. Furthermore,  $\text{SO}_4^{2-}$  was an anthropogenic anion that contribution from the long range transport was dominantly observed.

In the region, the median pH of the rain water was found to be 5.29, which indicates the pH that occurred by the dissolution of naturally produced CO<sub>2</sub>, NO<sub>x</sub> and SO<sub>2</sub> gases in clouds and rain water droplets. Lower pH values do not indicate that lacking of acid forming ions in the precipitation, but rather associate with neutralization of acidity during the rain event by washout mechanism. In Antalya Station, air masses transported from Europe was commonly associated with high anthropogenic content and low pH values whereas, air masses from South and East have less anthropogenic content and high pH values.

To understand the contribution of ions to neutralization, multiple linear regression analysis was performed for acid forming compounds of SO<sub>4</sub><sup>2-</sup> and NO<sub>3</sub><sup>-</sup> ions. It was observed that most of the acidity was neutralized by Ca<sup>2+</sup> in Antalya region. However, in dry season, less amounts of contribution of NH<sub>4</sub><sup>+</sup> ion to the neutralization was observed due to the significant increase during hot and long summer months.

Short and long term variations and time trends were investigated briefly. Short term variations indicates the episodic changes in concentrations and transport pattern whereas, long term variations explain the seasonal composition change. H<sup>+</sup> ion has clear seasonal pattern that have higher concentrations during winter season and lower in summer season, which could be explained by the efficient neutralization mechanisms during summer season due to the increased Ca<sup>2+</sup> and NH<sub>4</sub><sup>+</sup> concentrations in rain water. In this respect, during summer season episodes were not allowed to happen. SO<sub>4</sub><sup>2-</sup> and NO<sub>3</sub><sup>-</sup> do not show a well defined seasonal pattern. Sea salt elements have higher concentrations during winter season. The episodic behavior of sea salt elements was due to the variations in their source strengths that are closely related with meteorology that generated by bubble-bursting process of stormy weather. Both crustal and marine elements of Ca<sup>2+</sup>, Mg<sup>2+</sup> and K<sup>+</sup> do not have a significant seasonal trend. The elements of Al, Fe, Ni and Cr have higher concentrations during summer season due to being crustal origin and their drying and resuspension with higher ambient temperatures. Cr and Ni concentrations higher in Eastern Mediterranean Region, due to the presence of ophiolitic rocks enriched with Cr and Ni bearing minerals.

$\text{SO}_4^{2-}$  and  $\text{NO}_3^-$  have higher concentrations during summer season, which has an indication (not a conclusive evidence) of long range transport, since pollutants can not be transported over very low distances in winter due to extensive wet scavenging. Furthermore, another indication was the increased photooxidation reactions in the atmosphere due to the higher temperatures. In seasonal variations,  $\text{Ca}^{2+}$  has significantly higher concentrations during summer season, due to the increased  $\text{CaCO}_3$  loading aroused from suspension of local soil and Saharan dust transported from North Africa.  $\text{NH}_4^+$  has a clear seasonal pattern with higher concentrations during summer season, which could be explained by extensive usage of fertilizers and their enhanced volatility during this season.  $\text{Mg}^{2+}$  ion has a seasonal pattern of higher concentrations during winter season due to being both crustal and sea salt elements. However,  $\text{K}^+$  does not have a clear seasonal pattern. Anthropogenic elements of Cu and Cd have a regular seasonal pattern with higher concentrations during summer season, where lower precipitation amounts results from higher concentrations. Anthropogenic elements of Pb and Zn do not show clear seasonal variations.

Time trend analysis was performed to observe the behavior of ions and elements during the time and to set emission reduction policies on a regional scale.  $\text{H}^+$  ion show a decreasing trend, although there was an increase in the  $\text{SO}_4^{2-}$  trend. The increase in neutralizing species of  $\text{Ca}^{2+}$  and  $\text{NH}_4^+$  and slight decrease in  $\text{NO}_3^-$  trend contribute to the overall picture of  $\text{H}^+$  ion. The  $\text{SO}_4^{2-}/\text{NO}_3^-$  ratio increase in time, which inversely reflect the situation in Europe and America. The ratio of  $(\text{H}^+ + \text{Ca}^{2+} + \text{NH}_4^+) / (\text{SO}_4^{2-} + \text{NO}_3^-)$  has an increasing trend, which indicate the increasing neutralization capacity increase with time by main neutralization species of  $\text{Ca}^{2+}$  and  $\text{NH}_4^+$ .

Deposition fluxes have clear and linear correlations with precipitation amount. Furthermore, the corresponding concentration of precipitation and scavenging mechanisms of the species were the other parameters that affecting the wet deposition amount. Annual and seasonal deposition fluxes show that there were significantly higher wet deposition fluxes during winter season, since 80% of the precipitation falls in during winter season in the eastern Mediterranean region.  $\text{Na}^+$ ,  $\text{Cl}^-$ ,  $\text{Mg}^{2+}$  and  $\text{K}^+$  have

higher concentrations during wet season and increased rainfall amounts; explain the higher wet to dry ratios. Crustal elements of Ca, Al, Fe, Ni and Cr have comparably smaller wet to dry ratios due to the increased concentrations during summer season.  $\text{SO}_4^{2-}$ ,  $\text{NO}_3^-$  and  $\text{NH}_4^+$  have close particle size in the accumulation mode and most efficiently removed by wet deposition by in-cloud process could be an additional explanation of high ratios of wet to dry season. The wet deposition fluxes were compared with EMEP Stations and the values in Antalya Station was comparably higher values. One of the main reason of this was in Antalya Station, the annual median precipitation amount was  $1246 \text{ mm yr}^{-1}$  whereas; it was  $710 \text{ mm yr}^{-1}$  in the EMEP Stations. Furthermore, for acidifying compounds of ( $\text{SO}_4^{2-}$  and  $\text{NO}_3^-$ ), the sea salt elements of ( $\text{Na}^+$  and  $\text{Cl}^-$ ) and crustal elements of  $\text{Ca}^{2+}$  have comparably higher concentrations in Antalya Station.

To identify the possible sources of components of measured parameters in rain water, the PMF were applied. Potential Source Contribution Function (PSCF) was applied to define the possible source regions by using “bootstrap” technique with 95% statistically significant confidence level. The source regions for the free acidity factor are located in the western Turkey, Five factors account for a very large fraction of concentrations measured in the rain water composition of Antalya Station. Factor 1 was the  $\text{H}^+$  factor, which was defined as free acidity. Due to the higher neutralization capacity,  $\text{H}^+$  ion no longer depends on seasonal variations in  $\text{SO}_4^{2-}$  and  $\text{NO}_3^-$ . The second factor was crustal factor, where the backtrajectories imply the source of the factor as the resuspension of local soil instead of African dust. The third factor was a clear marine factor and backtrajectories indicate that most of the trajectories touch to the Mediterranean Sea and transport sea salt elements. Factor 4 and 5 were anthropogenic factors of  $\text{NO}_3^-$  and  $\text{SO}_4^{2-}$  respectively. Western Mediterranean countries, North Africa and Russia were the potential sources of  $\text{NO}_3^-$  as concluded from the backtrajectories. In addition to the source regions of Russia, Ukraine and Western Mediterranean Countries, southeasterly trajectory components, including Israel and south east of Turkey, contributes to the  $\text{SO}_4^{2-}$  transportation to the region.

In a conclusion, in Eastern Mediterranean region although there is high amounts of acid forming compounds of  $\text{SO}_4^{2-}$  and  $\text{NO}_3^-$  mainly from long range transportation, the acidity of rain water is quite low. Neutralizing compounds of  $\text{CaCO}_3$  and  $\text{NH}_3$  which are loaded to the atmosphere through the resuspension of local soil and fertilizer applications respectively are responsible from the observed high average pH values. Therefore, in Eastern Mediterranean region acid deposition is not as detrimental as it is observed in other parts of the world due to the extensive and effective neutralization of the acidifying compounds, which is due to the calcareous content of Antalya soil.

### **5.1. Recommendations for Future Research**

This study represents the rain water composition, acidification and extends of neutralization, the possible sources of components and their source regions by investigating ion balance, short and long term variations, positive matrix factorization and potential source contributions in Eastern Mediterranean Region in terms of major ions and trace elements.

Investigation of the area 8 years is not long enough to answer all the questions about the acid rain, since atmosphere has extensive variations and rain water has dynamic nature. Furthermore, measuring the soil acidity at the station and over the Mediterranean region will be helpful to explain the acid deposition on soil.

To understand the ionic composition of rain water clearly, further assessment of bicarbonate ion and organic compounds should be added for the ion balance.

In the determination of trace elements, the solubility is significant since they have toxic effects on ecosystem. The dissolved form of trace elements is directly used up by the organisms, whereas the deposited fraction may or may not be solubilized in soil. Investigation of the solubility of the trace metals should be included in the study since to make clear the significant effects in rain water composition researches.

## REFERENCES

- Alagha, O., 2000. "Wet and dry deposition fluxes of pollutants over a black sea forest region", Ph.D. Thesis, Department of Chemistry, Middle East Technical University, Ankara.
- Alagha, O., Tuncel, G., 2003. "Evaluation of air quality over the black sea: Major ionic composition of rain water", *Water, Air, and Soil Pollution: Focus* 3, 87-96.
- Al-Momani, I.F., Tunçer, S., Eler, U., Örtel, E., Şirin, G., Tuncel, G., 1995a. "Major ion composition of wet and dry deposition in the eastern Mediterranean basin", *The Science of the Total Environment* 164, 75-85.
- Al-Momani, I.F., Ataman, O.Y., Anwari, M.A., Tuncel, S., Köse, C., Tuncel, G., 1995b. "Chemical composition of precipitation near an industrial area at İzmir, Turkey", *Atmospheric Environment* 29, 1131-1143.
- Al-Momani, I.F., 1995c. "Long range atmospheric transport of pollutants to the Eastern Mediterranean basin", Ph.D. Thesis, Department of Environmental Engineering, Middle East Technical University, Ankara.
- Al-Momani, I.F., Güllü, G., Ölmez, I., Eler, U., Örtel, E., Şirin, G., Tuncel, G., 1997. "Chemical composition of eastern Mediterranean aerosol and precipitation: Indications of long-range transport", *Pure and Applied Chemistry* 69, 41-46.
- Al-Momani, I.F., Aygun, S., Tuncel, G., 1998. "Wet deposition of major ions and trace elements in the eastern Mediterranean basin", *Journal of Geophysical Research* 103 – D7 8287- 8299.
- Al-Momani, I.F., Güllü, G., Eler, U., Örtel, E., Şirin, G., Tuncel, G., 1999. "Long range transport of pollutants from Europe to the eastern Mediterranean", *Fresenius Envir Bull* 8, 249-256.
- Al-Momani, I.F., Momani, K.A., Jaradat, Q.M., 2000. "Chemical composition of wet precipitation in Irbid, Jordan", *Journal of Atmospheric Chemistry* 35, 47-57.
- Al-Momani, I.F., 2003. "Trace elements in atmospheric precipitation at Northern Jordan measured by ICP-MS: acidity and possible sources", *Atmospheric Environment*, 37, 4507-4515.

- Anttila, P., Paatero, P., Tapper, U., Jarvinen, O., 1995. "Source identification of bulk wet deposition in Finland by positive matrix factorization", *Atmospheric Environment* 14, 1705-1718.
- Ashbaugh, L.L., Malm, W.C., Sadeh, W.Z., 1985. A residence time probability analysis of sulfur concentration at Grand Canyon national park. *Atmospheric Environment* 19, 1263–1270.
- Avila, A., 1996. "Time trends in the precipitation chemistry at a mountain site in Northeastern Spain for the period 1983-1994", *Atmospheric Environment* 30, 1363-1373.
- Avila, A., Alarcon, M., 1999. "Relationship between precipitation chemistry and meteorological situations at a rural site in NE Spain", *Atmospheric Environment* 33, 1663- 1677.
- Avila, A., Alarcon, M., 2003. "Precipitation chemistry at a rural Mediterranean site: Between anthropogenic pollution and natural emissions", *Journal of Geophysical Research* 108(D9), 4278, doi:10.1029/2002JD002565.
- Baez, A.P., Belmont, R.D., Padilla, H.G., 1997. "Chemical composition of precipitation at two sampling sites in Mexico: A 7-year study", *Atmospheric Environment* 31, 915-925.
- Beverland, I.J., Crowther, J.M., Srinivas, M.S.N., Heal, M.R., 1998. "The influence of meteorology and atmospheric transport patterns on the chemical composition of rainfall in South-east England", *Atmospheric Environment* 32, 1039-1048.
- Charron, A., Plaisance, H., Sauvage, S., Coddeville, P., Galloo, J.C., Guillermo, R., 2000. "A study of the source-receptor relationships influencing the acidity of precipitation collected at a rural site in France", *Atmospheric Environment* 34, 3665-3674.
- Cabon, J.Y., 1999. "Chemical characteristics of precipitation at an Atlantic Station", *Water, Air, and Soil Pollution* 111, 399-416.
- Chen, W.H., 2001. "Dynamics of sulfur dioxide absorption in a raindrop falling at terminal velocity", *Atmospheric Environment* 35, 4777–4790.
- Cheng, M.D., Hopke, P.K., Zeng, Y., 1993. "A Receptor oriented methodology for determining source regions of particulate observed at Dorset, Ontario", *Journal of Geophysical Research* 98, 16839-16849.
- Chueinta, W., Hopke, P.K., Paatero, P., 2000. "Investigation of sources of atmospheric aerosol at urban and suburban residential areas in Thailand by positive matrix factorization", *Atmospheric Environment* 34, 3319-3329.

- Colin, J.L., Jaffrezo, J.L., 1990. "Solubility of major species in precipitation: Factors of variation", *Atmospheric Environment* 24A, 537-544.
- Dasch, J.M., Wolff, G., 1989. "Trace inorganic species in precipitation and their potential use in source apportionment studies", *Water, Air and Soil Pollution* 43, 401-412.
- Deboudt, K., Flament, P., Bertho, M.L., 2004. "Cd, Cu, Pb and Zn Concentrations in Atmospheric wet deposition at a coastal station in Western Europe", *Water, Air and Soil Pollution* 151, 335-359.
- Delaney, A.C., Pollock, W.H., Shedlovsky, J.P., 1973. "Tropospheric aerosol: the relative contribution of marine and continental components", *J.Geophys.Res.*, 78, 6249-6268.
- Doğan, G., 2005. "Comparison of the rural atmosphere aerosol compositions at different parts of Turkey", MS Thesis, Department of Environmental Engineering, Middle East Technical University, Ankara.
- Draaijers, G. P. J., Van Leeuwen, P., De Jong, G.H., and Erisman, J.W., 1997. "Base cation deposition in Europe--part II. Acid neutralization capacity and contribution to Forest nutrition", *Atmospheric Environment* 31, 4159-4168.
- EMEP Manual for Sampling and Chemical Analysis, NILU CCC 1/95, 1996. Norwegian Institute for Air Research, Norway.
- Environmental Protection Agency, 2004. "Acid Rain Program 2003 Progress Report", EPA 430-R-04-009.
- Erisman, J.W., De Leeuw, F.A.A.M., Van Aalst, R.M., 1989. "Deposition of the most acidifying components in the Netherlands during the period 1980-1986", *Atmospheric Environment* 23, 1051-1062.
- Erisman et al., Potma, C., Draaijers, G., Leeuwen, E.V., Van Pul, A., 1995. "A generalized description of the deposition of acidifying pollutants on a small scale in Europe", *Water, Air and Soil Pollution* 85, 2101- 2106.
- European Environment Agency, 2003a. "Air pollution in Europe 1990–2000", Topic report 4/2003a.
- European Environment Agency, 2003b. "Europe's Environment: the third Assessment", Environmental Assessment Report 10/2003b.
- European Environment Agency, 2005. "The European Environment, State and Outlook 2005". State and Environment Report No: 1/2005.

Fuelberg, H.E., Loring, R.O., Watson, M.V., Sinha, M.C., Pickering, K.E., Thompson, A.M., Satche, G.W., Blake, D.R. and Schoelberl, M.R., 1996. "TRACE A trajectory intercomparison: 2. Isentropic and kinematic methods", *Journal of Geophysical Research* 101, 23927-23939.

Gao, N., Cheng, M.D., Hopke, P.K., 1994. "Receptor modeling of airborne ionic species collected in SCAQS", *Atmospheric Environment* 28, 1447-1470.

Goldberg, E.D., 1963. "The ocean as a chemical system, in the sea", Edited by M.N. Hill, Vol 2, Chapter 1, Interscience: New York.

Gorham, E., Martin, F.B., Litzau, J.T., 1984. "Acid rain: ionic correlation in the eastern United States", *Science*, 225, 407-409.

Granat, L., 1972. "On the relation between pH and the chemical composition in atmospheric precipitation", *Tellus* 6, 550-560.

Guerzoni, S., Cristini, A., Caboi, R., Le Bolloch, O., Marras, I., Rundeddu, L., 1995. "Ionic composition of rain water and atmospheric aerosols in Sardinia, Southern Mediterranean", *Water, Air and Soil Pollution* 85, 2077-2082.

Güllü, G., 1996a. "Long range transport of aerosols", Ph.D. Thesis, Department of Environmental Engineering, Middle East Technical University, Ankara.

Güllü, G.H., Ölmez, I., Tuncel, G., 1996b. "Chemical concentrations and elements size distributions of aerosols in the eastern Mediterranean during strong dust storms", *The impact of desert dust across the Mediterranean*, 339-347.

Güllü, G.H., Al-Momani, I., Eler, U., Örtel, E., Şirin, G., Ölmez, I., Tuncel, G., 1997. "Determinations of source regions of pollutants measured at a rural site, Antalya", IV th Combustion and Air Pollution Symposium.

Güllü, G.H., Ölmez, I., Aygun, S., Tuncel, G., 1998. "Atmospheric trace element concentrations over the eastern Mediterranean Sea: Factors affecting temporal variability", *Journal of Geophysical Research* 103 – D17 21,943-21,954.

Güllü, G.H., Ulutaş, F., Belli, D., Erduran, S., Keskin, S., Tuncel, G., 1998. "Black Sea aerosol a long range atmospheric transport", *Turk Journal of Engineering and Environmental Science* 22, 289-303.

Güllü, G.H., Günaydın, G., Tuncel, G., 2001. "Potential source regions of pollutants measured in the Mediterranean and Black Sea atmospheres", *Turk Journal of Engineering Environmental Science* 25, 471-485.

Güllü, G.H., Ölmez, I., Öztaş, N.B., Tuncel, G., 2003. "Atmospheric trace element concentrations over the Eastern Mediterranean Sea: Factors affecting temporal variability", Chamber of Environmental Engineers, Environment Science and Technology 1, 23-38.

Güllü, G.H., Ölmez, I., Tuncel, G., 2004. "Source apportionment of trace elements in the Eastern Mediterranean atmosphere", Journal of Radioanalytical and Nuclear Chemistry 259, 163-171.

Hayward, S.F., 2004. "Index of leading environmental indicators", Pacific Research Institute, Ninth Edition.

Heaton, R.W., Rahn, K.A., Lowenthal, D.H., 1990. "Determination of trace elements, including regional tracers, in Rhode Island precipitation", Atmospheric Environment 24A, 147-153.

Hedin, L.O., Granat, L., Likens, G.E., Buishand, T.A., Galloway, J.N., Butler, T.J., Rodhe, H., 1994. "Steep declines in atmospheric base cations in regions of Europe and North America", Nature 367, 351-354.

Henry, R.C., Lewis, C.W., Hopke, P.K., Williamson, H.J., 1984. "Review of receptor model fundamentals", Atmospheric Environment 18, 1507-1515.

Hopke, P.K., Li, C.L., Ciszek, W. and Landsberger, S., 1995. "The use of bootstrapping to estimate conditional probability fields for source locations of airborne pollutants" Chemometrics and Intelligent Laboratory Systems 30, 69-79.

Hou, H., Takamatsu, T., Koshikawa, M.K., Hosomi, M., 2005. "Trace metals in bulk precipitation and throughfall in a suburban area of Japan", Atmospheric Environment 39, 3583-3595.

Hu, G.P., Balasubramanian, R., 2003. "Wet deposition of trace metals in Singapore", Water, Air and Soil Pollution 144, 285-300.

Jaradat, Q.M., Momani, K.A., Jiries, A.G., El-Alali, A., Batarseh, M.I., Sabri, T.G., Al-Momani, I.F., 1999. "Chemical composition of urban wet deposition in Amman, Jordan", Water, Air and Soil Pollution 112, 55-65.

Kaya, G. and Tuncel, G., 1997. "Trace element and major ion composition of wet and dry deposition in Ankara, Turkey", Atmospheric Environment 31, 3985-3998.

Keene, W.C., Galloway et al., J.N. and Holden, J.D., 1983. "Measurement of weak organic acidity in precipitation from remote areas of the world", J.Geophys.Res., 88, 5122-5130.

Khwaja, H.A. and Husain, L., 1990. "Chemical characterization of acid precipitation on Albany, New York", Atmospheric Environment, 24A, 1869-1882.

- Kim, E., Hopke, P.K., Edgerton, E.S., 2004. "Improving source identification of Atlanta aerosol using temperature resolved carbon fractions in positive matrix factorization", *Atmospheric Environment* 38, 3349–3362.
- Kubilay, N., Saydam, A.C., 1995. "Trace elements in atmospheric particulates over the eastern Mediterranean; concentrations, sources and temporal variability", *Atmospheric Environment* 29, 2289- 2300.
- Kuloğlu, E. and Tuncel, G., 2005. "Size distribution of trace elements and major ions in the Eastern Mediterranean atmosphere", *Water, Air, and Soil Pollution*, 167: 221–241.
- Lacaux, J.P., Delmas, R., Kouddio, G., Cros, B., Andreae, M.O., 1992. "Precipitation chemistry in the Mayombe forest of equatorial Africa", *J.Geophys. Res.*, 97, 6195-6206.
- Lee, E., Chan, C.K., Paatero, P., 1999. "Application of positive matrix factorization in source apportionment of particulate pollutants in Hong Kong", *Atmospheric Environment* 33, 3201-3212.
- Lee, B.K., Hong, S.H. and Lee, D.S., 2000. "Chemical composition of precipitation and wet deposition of major ions on the Korean peninsula", *Atmospheric Environment* 34, 563- 575.
- Lehmann, C.M.B., Bowersox, V.C., Larson, S.M., 2005. "Spatial and temporal trends of precipitation chemistry in the United States, 1985–2002", *Environmental Pollution* 135, 347-361.
- Lindberg, S.E., 1982. "Factors influencing trace metal, sulfate and hydrogen ion concentrations in rain", *Atmospheric Environment*, 16, 1701-1709.
- Liu, W., Wang, Y., Russell, A., Edgerton, E.S., 2005. "Atmospheric aerosol over two urban–rural pairs in the southeastern United States: Chemical composition and possible sources", *Atmospheric Environment* 39, 4453-4470.
- Losno, R., Bergametti, G., Carlier, P., Mouvier, G., 1991. "Major ions in marine rain water with attention to sources of alkaline and acidic species", *Atmospheric Environment* 25, 763-770.
- Lupu, A. and Meanhaut, W., 2002. "Application and comparison of two statistical trajectory techniques for the identification of source regions of atmospheric aerosol species", *Atmospheric Environment* 36, 5607- 5618.
- Luria, M., Peleg, M., Sharf, G., Alper, D.S.T, Spitz, N., Ami, Y.B., Gawii, Z., Lifschitz, Yitzchaki, A., and Seter, I., 1996. "Atmospheric Sulfur over the East Mediterranean Region", *Journal of Geophysical Research* 101(D20), 25,917-25,930.

- Lynch, J.A., Grimm, J.W., Bowersox, V.C., 1995. "Trends in precipitation chemistry in the United States: A national perspective, 1980-1992", *Atmospheric Environment* 29, 1231-1246.
- Maherasa, P., Xoplakia, E., Davies, T., Martin-Vide, J., Bariendos, M., Alcoforado, M.J., 1999. "Warm and cold monthly anomalies across the Mediterranean basin and their relationship with circulation; 1860-1990", *International Journal of Climatology* 19, 1697-1715.
- Mason, B., 1966. "Principles of Geochemistry", 3<sup>rd</sup> Edition, John Wiley, New York.
- Mouli, P.C., Mohan, S.V., Reddy, S.J., 2005. "Rain water chemistry at a regional representative urban site: influence of terrestrial sources on ionic composition", *Atmospheric Environment* 39, 999-1008.
- Mihalopoulos, N., Sephanou, E., Kanakidoou, M., Pilitsidis, S., Bousquet, P., 1997. Tropospheric aerosol ionic composition in the Eastern Mediterranean region, *Tellus*, 49, 314-326.
- NRC (National Research Council), 1983. Acid deposition: Atmospheric Processes in Eastern North America, National Academy of Sciences, Washington, District of Columbia.
- Paatero, P., Hopke, P.K., 2003. "Discarding and downweighting high-noise variables in factor analytic models", *Analytica Chimica Acta* 490, 277- 289.
- Paatero, P., 2000. "User's guide for positive matrix factorization programs PMF2 and PMF3, Part 1: tutorial".
- Paatero, P., 1997. Least square formulation of robust nonnegative factor analysis. *Chemometrics and Intelligent Laboratory Systems* 37, 23-35.
- Paatero, P., Tapper, U., 1994. Positive Matrix Factorization: a non-negative factor model with optimal utilization of error estimates of data values. *Environmetrics* 5, 111-126.
- Pio, C. A., Salgueiro, M.L., Nunes, T.V., 1991. "Seasonal and air-mass trajectory effects on rain water quality at the southwestern European border", *Atmospheric Environment* 25, 2259-2266.
- Polissar, A.V., Hopke, P.K. and Poirot, R.L., 2001. "Atmospheric aerosol over Vermont: 1. Seasonal variability and sources", *Environmental Science and Technology* 35, 4604-4621.
- Prendes, P., Andrade, J.M., Lopez-Mahia, P., Prada, D., 1999. "Source apportionment of inorganic ions in airborne urban particles from Coruna city (N.W. of Spain) using positive matrix factorization", *Talanta* 49, 165-178.

Puxbaum, H., Simeonov, V., Kalina, M.F., 1998. "Ten years trends (1984-1993) in the precipitation chemistry in Central Austria", *Atmospheric Environment* 32, 193-202.

Qin, Y., Oduyemi, K., Chan, L.Y., 2002. "Comparative testing of PMF and CFA models", *Chemometrics and Intelligent Laboratory Systems* 61, 75– 87.

Ramadan, Z., Eickhout, B., Songa, X.H., Buydens, L.M.C., Hopke, P.K., 2003. "Comparison of Positive Matrix Factorization and Multilinear Engine for the source apportionment of particulate pollutants", *Chemometrics and Intelligent Laboratory Systems* 66, 15- 28.

Rodhe, H., Dentener, F., Schulz, M., 2002. "The global distribution of acidifying wet deposition", *Environmental Science Technology* 36, 4382-4388.

Sanusi, A., Wortham, H., Millet, M., Mirabel, P., 1996. "Chemical composition of rain water in Eastern France", *Atmospheric Environment* 30, 59-71.

Saxena, A., Kulshrestha, U.C., Kumar, N., Kumari, K.M., Srivastava, S.S., 1996. "Characterization of Precipitation at Agra", *Atmospheric Environment* 30, 3405-3412.

Seto, S., Oohara, M., Iwase, K., 1992. "Some statistical characteristics of concentration and wet deposition in relation to rainfall amount for sulfate and nitrate in rain water", *Atmospheric Environment*, 16, 3029-3038.

Seto, S., Oohara, M., Ikeda, Y., 2000. "Analysis of precipitation chemistry at a rural site in Hiroshima Prefecture, Japan", *Atmospheric Environment* 34,621- 628.

Seto, S., Hara, H., Sato, M., Noguchi, I., Tonooka, Y., 2004. "Annual and seasonal trends of wet deposition in Japan", *Atmospheric Environment* 38, 3543-3556.

Tolun, N. and Pamir, A.N., 1975. "Explanatory text of the geological map of Turkey, Hatay sheet" Publ. Min. Res. And Explor. Inst. Publ., Ankara, 99 pp and appendices.

Tuncel, S., Ungör, S., 1996. "Rain water chemistry in Ankara, Turkey", *Atmospheric Environment* 30, 2721-2727.

Tunçer, B., 2000. "Chemical composition of precipitation in Central Anatolia", MS Thesis, Department of Environmental Engineering, Middle East Technical University, Ankara.

Tunçer, B., Bayar, B., Yesilyurt, C., Tuncel, G., 2001. "Ionic composition of precipitation at the Central Anatolia (Turkey)", *Atmospheric Environment* 35, 5989-6002.

United Nations Economic Commission for Europe (UNECE), 2005. Convention on Long-range Transboundary Air Pollution. Protocols to the Convention. ([http://www.unece.org/env/lrtap/status/lrtap\\_s.htm](http://www.unece.org/env/lrtap/status/lrtap_s.htm) )

United Nations Environment Program, World Meteorological Organization (UNEP, WMO) (1989). Meteorological and climatological data from surface and upper air measurements for the assessment of atmospheric transport and deposition of pollutants in the Mediterranean Basin: A review. MAP Technical Reports Series No.30, Athens, UNEP, 137.

Van Leeuwen, E.P., Draaijers, G.P.J., Erisman, J.W., 1996. "Mapping wet deposition of acidifying components and base cations over Europe using measurements", *Atmospheric Environment* 30, 2495-2511.

Watson, J.G., Zhu, T., Chow, J.C., Engelbrecht, J., Fujita, E.M., Wilson, W.E., 2002. "Receptor modeling application framework for particle source apportionment", *Chemosphere*, 49, 1093–1136.

Wehrens, R., Putter, H., Buydens, L.M.C., 2000. "The bootstrap: a tutorial" *Chemometrics and Intelligent Laboratory Systems* 54, 35-52.

Yörük, E., 2004. "Composition of the atmosphere at the Central Anatolia", M.S. Thesis, Department of Environmental Engineering, Middle East Technical University, Ankara.

Zeng, Y., Hopke, P.K., 1989. "A study of the sources of acid precipitation in Ontario, Canada", *Atmospheric Environment*, 23, 1499-1509.

Zhang, D.D., Peart, M., Jim, C.Y., He, Y.Q., Li, B.S., Chen, J.A., 2003. "Precipitation chemistry of Lhasa and other remote towns, Tibet", *Atmospheric Environment* 37, 231-240.